2-2010

Analyses of Arabidopsis Yellow Stripe-Like (YSL) Family of Metal Transporters

Heng-Hsuan Chu
University of Massachusetts Amherst, marspig.chu@gmail.com

ANALYSES OF ARABIDOPSIS YELLOW STRIPE-LIKE (YSL) FAMILY OF METAL TRANSPORTERS

A Dissertation Presented

by

Heng-Hsuan Chu

Submitted to the Graduate School of the
University of Massachusetts Amherst in partial fulfillment
of the requirements for the degree of

DOCTOR OF PHILOSOPHY

February 2010

Plant Biology

ANALYSES OF ARABIDOPSIS YELLOW STRIPE-LIKE (YSL) FAMILY OF METAL TRANSPORTERS

A Dissertation Presented

by

Heng-Hsuan Chu

Approved as to style and content by:

_____
Elsbeth L. Walker, Chair

_____
Danny J. Schnell, Member

_____
Wei-Lih Lee, Member

_____
Elsbeth L. Walker, Director, Plant Biology

DEDICATION

To my supportive family, my parents and my wife

ACKNOLEDGMENTS

I would like to thank Elsbeth Walker, for her five years of patient guidance, calm nerve, and tireless support as an advisor, especially her patience for watching after this clumsy student. Here efforts are greatly appreciated. I want to thank my committee, Danny Schnell and Wei-Lih Lee, for their valuable comments and suggestion on my project. I want to thank Dr. Jennifer Normanly and Dr. Tobias Baskin for their advice and help. I want to thank Dr. Brian Waters for his guidance at the beginning of my Ph.D. life. The five years within the Walker lab and Morrill Science Center would not have been as enjoyable without the following people: Dr. Yun Kang, Dr. Nathan Nims, Kham Vongpaseuth, Jeff Chiecko, Burcu Kokturk, and Susan Capistran. I want to thank my parents, Ying-Chuan Chu and Jui-Mei Hung, for their understanding and support. I want to thank my patient wife, Ya-Ling Wang, for her sacrifice and support. Ph.D. belongs to her too.

ABSTRACT

ANALYSES OF ARABIDOPSIS YELLOW STRIPE-LIKE

(YSL) FAMILY OF METAL TRANSPORTERS

FEBRUARY, 2010

HENG-HSUAN CHU, B.A., CHUNGSHING UNIVERSITY

Ph.D., UNIVERSITY OF MASSACHUSETTS AMHERST

Directed by: Professor (Elsbeth L. Walker)

Iron is one of the most important micronutrients used by living organisms. Iron is frequently a limiting nutrient for plant growth, and plants are a major source of iron for human nutrition. The most prominent symptom of iron deficiency in plants is interveinal chlorosis, or yellowing between the veins, which appears first in the youngest leaves. Iron deficiency anemia (IDA) is the number one human nutritional deficiency worldwide. In order to solve the problem of iron deficiency, it is desirable to breed plants that have increased iron in those parts that are consumed by humans. To do this, we must first understand the molecular basis of Fe uptake, transport, and storage in plants. In soil, iron is quickly oxidized to Fe(III), and Fe(III) is relatively insoluble, thus difficult for plants to obtain. Our lab has been working on metal ion homeostasis mechanisms in plants and the ultimate goal of our research is to understand the mechanisms by which plants maintain the correct levels of iron,

zinc and copper in each cell and tissue.

The Yellow Stripe-like (YSL) family of proteins has been identified based on sequence similarity to maize Yellow stripe 1 (YS1). YS1 transports Fe(III) that is complexed by phytosiderophores (PS), strong Fe(III) chelators of the mugineic acid family of compounds. Non-grass species of plants neither make nor use PS, yet YSL family members are found in non-grass species including *Arabidopsis thaliana*. YSLs in non-grasses have been hypothesized to transport metals that are complexed by nicotianamine (NA), an iron chelator that is structurally similar to PS and which is found in all higher plants.

In this dissertation, Arabidopsis YSL1 and YSL3 are demonstrated to be important in iron transport and also responsible for loading Fe, Cu, and Zn from leaves into seeds. Arabidopsis YSL4 and YSL6 are demonstrated to be involved in iron transport and metal mobilization into seeds. The transport function of Arabidopsis YSL1 and YSL2 are shown be partially overlapping to the function of Arabidopsis YSL3 in vegetative structures, but distinct in reproductive organs. Arabidopsis YSL3 and YSL6 are shown to have distinct functions *in planta*.

TABLE OF CONTENTS

Page

LIST OF TABLES

Table Page

LIST OF FIGURES

Figure Page

CHAPTER 1

INTRODUCTION AND BACKGROUND

1.1 Significance of iron:

Iron (Fe) is an essential micronutrient used by living organisms. Because of iron's ability to accept and donate electrons, it is essential for many cellular functions in plants, including chlorophyll biosynthesis, photosynthesis, and respiration. The most widespread human nutritional problem in the world is iron deficiency anemia (World Health Organization), and plants are a major source of iron for human nutrition. Thus, increasing the ability of plants to take up iron could have a dramatic impact on human health (Clemens *et al*., 2002; Guerinot, 2001). However, iron is frequently a limiting nutrient for plant growth. Although iron is abundant in soils, it is often present in insoluble complexes, particularly in aerobic conditions and at neutral or alkaline pH (Guerinot, 1994). Plants need Fe in the concentration range of 10^{-4}M -10^{-9}M for optimal growth (Guerinot *et al*, 1994), but the concentration range of free Fe(II) and Fe(III) in well-aerated soil is less than 10^{-15}M (Marschner, 1995). Biofortification, a method of developing crops to increase their nutritional value through conventional selective breeding or genetic engineering, is considered

as a sustainable way to improve the iron deficiency anemia problem.

In addition to problems caused by iron deficiency, excess iron can cause damage to cells. During the reduction of molecular oxygen, superoxide and hydrogen peroxide can be generated in cells, and can react with Fe(II) and Fe(III) to form highly reactive hydroxyl radicals. The hydroxyl radicals can cause damage to cellular compartments such as lipids, DNA, and protein. In conclusion, too little iron affects plants' growth and too much iron causes damage to plant cells. Therefore, maintaining iron homeostasis is critical for plants and hence iron homeostasis is highly regulated in plants. In order to achieve the goal of biofortification, improving our understanding of iron homeostatic mechanisms is critical.

1.2 Iron acquisition:

To overcome the generally low supply of Fe in soil, higher plants have evolved two distinct strategies, Strategy I and Strategy II (Figure 1.1), to take up Fe from the rhizosphere, the zone that surrounds the roots (Marschner *et al*., 1986).

1.2.1 Reduction-based Strategy I:

All dicots, as well as the non-grass monocots, use Strategy I, which is composed of three steps: proton release, Fe(III) chelate reduction, and Fe(II)

Figure 1.1: A comparison of Strategy I and Strategy II iron uptake.

(A) Strategy I plants extrude protons into the rhizosphere to lower the soil pH and increase Fe(III) solubility. The solubilized Fe(III) is then reduced by FRO2 into Fe(II) and taken up by IRT1.

(B) Strategy II plants secrete PS into the soil to chelate Fe(III), and then the Fe(III)-PS chelates are taken up by YS1 into the roots.

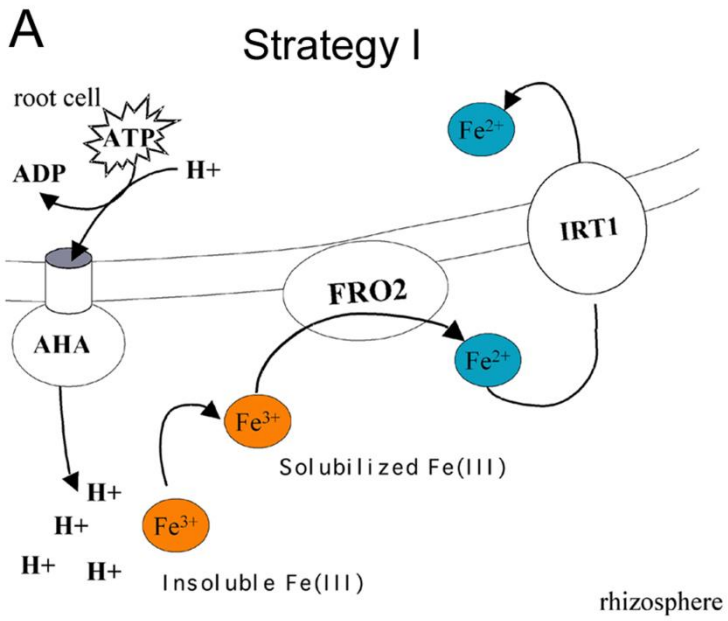
A
Strategy I
root cell
ATP
ADP
H+
Fe2+
IRT1
FRO2
AHA
Fe2+
Fe3+
Solubilized Fe(III)
H+
H+
H+
H+
Fe3+
Insoluble Fe(III)
rhizosphere

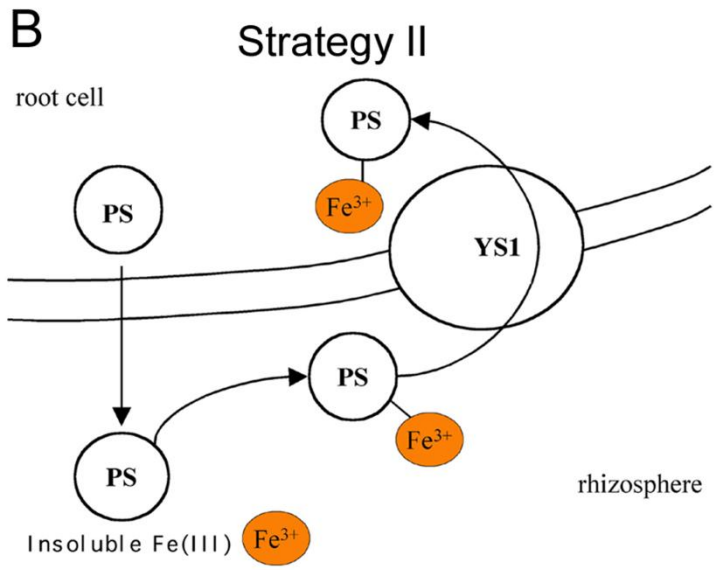
B
Strategy II
root cell
PS
PS
Fe3+
YS1
PS
Fe3+
PS
rhizosphere
Insoluble Fe(III)
Fe3+

transport (Eide *et al*., 1996; Robinson *et al*., 1999). At the proton release step, Strategy I plants use a proton ATPase to pump protons into the rhizosphere to lower the soil pH and increase the solubility of Fe(III). For every one unit drop in pH, Fe(III) becomes 1000 fold more soluble (Olsen *et al*., 1981). The recently identified cucumber CsHA1 proton ATPase was shown to contribute to the proton-pumping response of Strategy I plants (Santi *et al*., 2005; Santi *et al*., 2008). The *AHA7* (Arabidopsis H+ ATPase) gene was shown to be up-regulated during iron deficiency and its expression depends on FIT1 transcription factor 1 which has been reported to be involved in iron deficiency response (Colangelo and Guerinot, 2004). This result implies that AHA7 may be involved in iron deficiency induced proton release.

At the Fe(III) chelate reduction step, the solubilized Fe(III) is reduced at the cell surface by a plasma membrane-bound ferric reductase. The resulting ferrous iron, Fe (II), is more soluble than Fe(III), making it more bioavailable. In Arabidopsis, the gene for Fe(III)–chelate reduction, *FRO2*, has been cloned and characterized (Robinson *et al*., 1997, 1999; Connolly *et al*., 2003). The Arabidopsis mutant, *frd1* (ferric reductase defective 1), lacks iron-deficiency inducible Fe(III) chelate reductase activity and exhibits a severe chlorosis phenotype with iron limitation (Yi and Guerinot, 1996). The corresponding

gene, *FRO2*, was identified based on sequence similarity to the yeast ferric reductase, FRE1, and the human respiratory burst NADPH oxidase, gp91 phox. FRO2 was shown to be able to complement the *frd1* phenotype and is considered as the main Fe(III) chelate reductase in roots (Robinson *et al*., 1997). Plants overexpressing *FRO2* are tolerant to growth on low iron media (Connolly *et al*., 2003). Moreover, overexpression of Arabidopsis *FRO2* in soybean confers resistance to low iron growth condition and enhanced ferric reductase activity. Fe(III) chelate reductases have also been identified in pea (PsFRO1) (Waters *et al*., 2002) and tomato (LeFRO1) (Li *et al*., 2004). Just like Arabidopsis *FRO2*, expression of *PsFRO1* is induced by iron limitation whereas *PsFRO1* is expressed throughout the whole roots but not restricted to outer layer of roots, suggesting an additional role in iron mobilization within plants (Waters *et al*., 2002). *LeFRO1*, localized to the plasma membrane using transient transformation of onion epidermal cells, confers Fe(III) chelate reducatase activity when expressed in yeast and is expressed in both shoots and roots (Li *et al*., 2004).

At the Fe(II) transport step, the Fe(II) produced by ferric chelate reductase is transported from rhizosphere into the roots by the ferrous transporter, IRT1 and its orthologs, many of which have been cloned and characterized (Eide *et*

al., 1996; Connolly *et al*., 2002; Henriques *et al*., 2002; Varotto *et al*., 2002; Vert *et al*., 2002). IRT1 (iron-regulated transporter 1), a member of ZIP (ZRT, IRT–like proteins) family of metal transporters, is responsible for transport Fe(II) across the plasma membrane into the root cells. The Arabidopsis *IRT1* gene, identified by functional complementation of an iron uptake defective yeast (Eide *et al*., 1996), is localized to the plasma membrane and is highly expressed in the root's epidermal cells during iron deficiency. Yeast functional complementation assays showed that IRT1 is able to transport Fe, Mn, Zn, Cd, and probably Co (Eide *et al*., 1996; Korshunova *et al*., 1999; Rogers *et al*., 2000). Arabidopsis i*rt1* mutant plants exhibit chlorosis and display seedling lethality unless supplied with high levels of soluble iron (Vert *et al*., 2002), again suggesting that IRT1 is involved in Fe transport. Furthermore, although iron supplementation alone can rescue *irt1* mutants, *irt1* plants have reduced levels of Fe, Mn, Zn, and Co. Plants are known to accumulate zinc, manganese, cobalt, and cadmium in response to iron starvation (Welch et al., 1993; Cohen et al., 1998). However, the accumulation of these heavy metals under iron starvation was lost or greatly reduced in *irt1-1* plants, suggesting that the accumulation is mediated primarily by IRT1. Thus, IRT1 transports Fe, Zn, Mn, Cd, and Co in Arabidopsis roots.

In Arabidopsis, there are 16 members in the ZIP transporter family (Lasswell *et al*., 2000; Mäser *et al*., 2001). Arabidopsis IRT2, which is expressed in the outer layers of roots during iron deficiency, has the highest sequence similarity to IRT1 among all these members. Although IRT2 is able to rescue iron uptake defective yeast, *irt2* mutant plants exhibit no phenotype and overexpression of *IRT2* cannot rescue *irt1* mutant plants, suggesting that IRT2 plays a different role than IRT1 (Vert *et al*., 2001). IRT1 orthologs have been identified in tomato and pea. In tomato, just like *AtIRT1*, expression of *LeIRT1* and *LeIRT2* are specific to roots and are induced by iron limitation (Eckhardt *et al*., 2001). In pea, the related transporter *RIT1* (Root Iron Transporter 1) is expressed in iron deficient roots and showed Fe, Zn, and Cd transport when expressed in yeast (Cohen *et al*., 2004).

1.2.2 Chelation-based strategy II:

Graminaceous plants like rice, wheat and maize, which are the predominant agricultural crops, use Strategy II for primary iron uptake. The roots of strategy II plants do not acidify the rhizosphere, and they do not display increased root ferric reductase activity in response to iron starvation. Strategy II plants release phytosiderophores (PS): non-proteinogenic amino acid derivatives of the mugineic acid (MA) family that form stable Fe(III)

chelates (Takagi, 1976; Takagi *et al*., 1984). In the rhizosphere, PS solubilizes the Fe(III) in the soil. Specific uptake systems located at the root surface then take up the Fe(III)-PS chelates (Takagi *et al*., 1984). It is important to mention that non-graminaceous plants neither synthesize nor use PS (Romheld *et al*., 1986). Rice is a special case in graminaceous plants. In addition to Fe(III)-PS, rice plants can also take up Fe(II) via IRT-like transporters (Cheng *et al*., 2007; Ishimaru *et al*., 2006). Rice plants that are defective in synthesizing PS do not show an iron deficiency phenotype if Fe(II) is supplied. However, unlike Strategy I plants, both H-ATPase and Fe(III) chelate reductase activity are not induced by iron limitation, possibly because rice can compensate for the lack of effective Fe(III) chelate reductases due to its wetland culture. It is likely that the ability to take up Fe(II) may reflect an adaptation to growth in paddy soil, where Fe(II) is more available due to low oxygen.

1.3 Iron homeostasis in plants:

Iron homeostasis in plants requires regulation of many components. As described previously, the key components involved in iron uptake from soil into roots have already been characterized, but little is known about the mechanisms involved in moving iron from root epidermis into xylem, moving

iron from xylem into cells or subcellular compartments in leaves, or iron re-distribution from mature leaves into seeds. Several genes have been demonstrated to be significant for iron translocation in Arabidopsis. FRD3, a multidrug and toxin efflux (MATE) family member, is required for citrate efflux into the root vasculature (Durrett *et al*, 2007). Citrate is thought to be involved in long-distance iron transport from roots to shoots, and Fe was found to exist as Fe(III)-citrate chelates in xylem exudates (Tiffin, 1966, 1970). FRD3 was shown to be able to transport citrate by heterologous studies in *Xenopus oocytes*. Consistent with the role of FRD3 as a citrate transporter, the xylem exudates of *frd3* mutants contained less citrate and iron, and this phenotype can rescued by citrate supplementation. Recently, rice FRDL1 has also shown to be a citrate transporter required for efficient translocation of iron in rice (Yokosho *et al*, 2009).

The Arabidopsis vacuole membrane transporter, VIT1 (vacuole iron transporter 1), is necessary for iron localization in Arabidopsis seeds (Kim *et al*, 2006). In yeast, vacuoles are the main intercellular storage compartment for iron. The yeast CCC1 is a vacuole membrane transporter responsible for accumulation of Fe and Mn. Loss of function of CCC1 in yeast results in sensitivity to high extracellular iron because of high iron toxicity from failure to

move cytosolic iron into vacuole. VIT1 is the Arabidopsis ortholog of yeast CCC1, and has been shown to complement the high iron sensitivity of yeast *ccc1* mutants by increasing vacuolar iron content, implying that VIT1 is a vacuole membrane iron transporter. Although retaining normal iron content, seeds of *vit1* mutant plants exhibit abnormal iron distribution in developing embryos. Normally, iron is distributed to provascular strands of the hypocotyls, radicle, and cotyledons. However, in vit1-1 seeds, instead of staying in the provasculature, Fe is diffusely localized throughout the hypocotyl and radical, and in the epidermal cells of the cotyledons.

NRAMP3 and NRAMP4, two metal transporters of the natural resistance-associated macrophage protein (NRAMP) family, are important for seed germination on low iron (Lanquar *et al*, 2005). Iron in the vacuoles of *nramp3nramp4* double mutant seeds failed to be exported during germination, causing germination to be arrested under iron-limiting conditions.

OPT3, a member of Arabidopsis oligopeptide transporter (OPT) family, was shown to be involved in movement of iron into developing seeds (Stacey *et al*, 2008). *opt3-2* mutants, which have reduced levels of OPT3, exhibited constitutive expression of iron deficiency responses in roots regardless of iron supplementation, resulting in over-accumulation of iron in leaves, but

decreased levels of iron in seeds.

In addition to FRO2 which is involved in primary iron uptake via strategy I, the Arabidopsis FRO family contains seven other members and these members are expressed in various locations. For example, FRO2 and FRO3 are specific to roots and their expression is induced by iron limitation. However, *FRO2* is expressed primarily in the outer layer of roots, whereas *FRO3* is primarily expressed in the vascular cylinder (Dinneny *et al*., 2008; Mukherjee *et al*., 2006). *FRO6*, *FRO7*, and *FRO8* are expressed predominantly in green tissues (Mukherjee *et al*., 2006; Wu *et al*., 2005). FRO6 expression has been shown to be induced by light. FRO6 and FRO7 are predicted to localize to the chloroplast, while FRO8 is predicted to localize mitochondria. These results suggest either that these FRO proteins have functions other than Fe(III) reduction, or that reduction-based iron mobilization is also required in many location throughout the plant. Consistent with the latter view, Fe(III) chelate reductase activity can be detected in leaves sunflower (de la Guardia and Alcantara, 1996) and *Vigna unguiculata* (Brüggemann *et al*, 1993).

1.4 The role of nicotianamine (NA):

NA, a non-proteinogenic amino acid found in all plants, is the biochemical

precursor of PS in grasses and is structurally similar to PS (Figure 1.2). Nicotianamine is synthesized by a one-step condensation reaction of three molecules of *S*-adenosyl-methionine by the enzyme nicotianamine synthase (NAS; Shojima et al., 1989; Herbik et al., 1999; Higuchi et al., 1999). NA chelates metal cations, including Fe(II) and Fe(III), as well as Zn(II), Cu(II), Mn(II), Co(II), and Ni(II). Unlike PS, NA is not secreted to the external environment, and is thought to have a role in internal metal homeostasis in all plants (Stephan *et al*., 1996). NA is present in shoots and roots at concentrations from 20 to 500 nM/g fresh weight (Stephan *et al*, 1990). The concentration of NA in xylem and phloem are about 20 uM (Pich *et al*, 1996) and 130 uM (Schmidke *et al*, 1995) respectively, implying a role as a significant metal chelator in plants.

The NA synthesis-defective tomato mutant *chloronerva* (Higuchi *et al*., 1996; Rudolph *et al*., 1985) exhibits interveinal chlorosis and defects in metal accumulation and translocation (Stephan and Scholz, 1993). Transgenic tobacco plants constitutively expressing barley NAAT, an enzyme that consumes endogenous NA, were shown to have chlorotic young leaves and abnormally shaped flowers. These plants have abnormal Fe, Zn, and Mn distribution (Takahashi *et al*., 2003), suggesting that NA plays a role in internal

Figure 1.2: The structure and predicted complex conformation of NA and deoxymugineic acid (DMA), the predominant phytosiderophore synthesized by *Zea mays*.

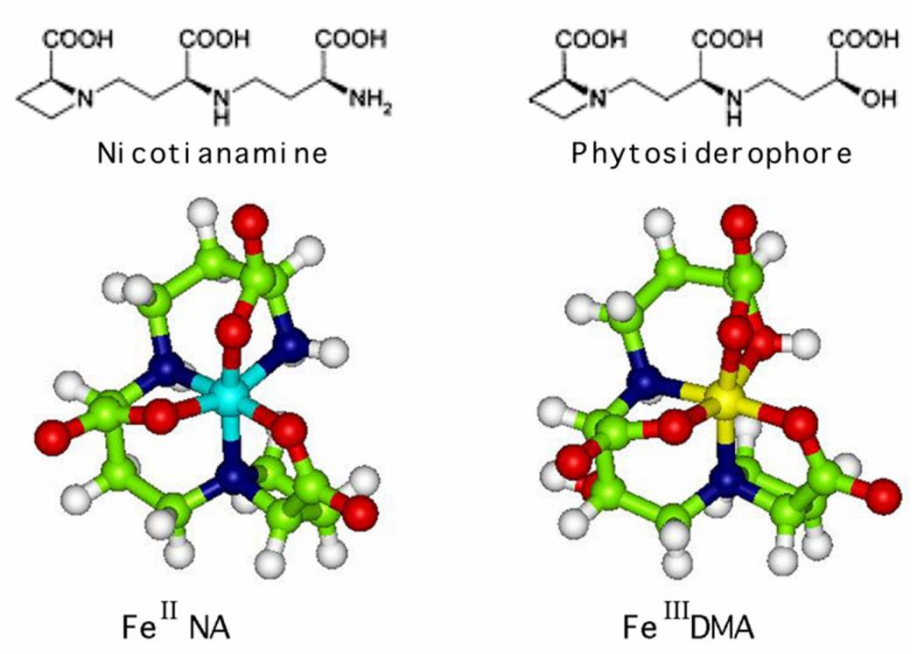
COOH
COOH
COOH
N
N
H
NH2
Nicotianamine
COOH
COOH
COOH
N
N
H
OH
Phytosiderophore
Fe II NA
Fe III DMA

metal transport. Recently, two Arabidopsis quadruple nicotianamine synthase mutants were generated, nas4x-1 and nas4x-2 (Klatte *et al*., 2009). nas4x-2, which had full loss of NAS function, was sterile. nas4x-1, although containing a T-TDNA insertion in the 5' untranslated region of the NAS2, showed partial *NAS2* expression. *NAS2* is normally expressed in roots, whereas in nas4x-1, *NAS2* expression was also observed in leaves. nas4x-1 exhibited chlorosis, which became severe under iron deficiency and during flowering. Nicotianamine was not detectable in rosette leaves of reproductive stage nas4x-1 plants but was detected in vegetative rosette leaves and seeds at a low level. Fe deficiency symptoms were exhibited in leaves, roots, and flowers. However, chlorotic leaves also showed signs of sufficient Fe supply, since expression of two marker genes, *FER1* and *FRO3*, which are induced by iron deficiency, was not up-regulated. This suggests that the mutant cannot sense iron deficiency signals normally. Fe accumulation was observed in rosette leaves, whereas decreased Fe levels were detected in flowers and seeds. The mutant was not able to normally mobilize Fe to flowers and seeds. These data suggest that nicotianamine is required for seed iron loading and iron deficiency responses.

1.5 Maize Yellow Stripe 1 (ZmYS1), the founder of the YSL family:

Fe(III)-phytosiderophore complexes are taken up by a specific transporter at the root surface in graminaceous plants. The membrane bound Fe(III)-PS transporter of maize is called Yellow Stripe 1 (YS1) (Curie *et al*., 2001; Roberts *et al*., 2004), a protein that is distantly related to the Oligopeptide Transporter (OPT) family of proteins. Expression of ZmYS1 is induced by iron deficiency. Mutant *ys1* plants, which exhibit yellow stripes between the veins, make normal amounts of PS (von Wiren *et al*., 1994), but lack the ability to efficiently use Fe(III)-PS as a source of iron (Jolley and Brown, 1991; Hopkins *et al*., 1992; von Wiren *et al*., 1994; von Wiren *et al*., 1995). The maize *Ys1* gene (*ZmYS1*) functionally complements a *fet3fet4* iron uptake defective yeast strain (Eide *et al*., 1996), but only on medium containing Fe(III)-PS complex, not on medium containing un-complexed sources of iron (Curie *et al*., 2001). Moreover, ZmYS1 was reported to transport Fe(III)–PS in experiments using two-electrode voltage clamp analysis in *Xenopus oocytes* (Schaaf *et al.*, 2004; Murata *et al*, 2006). These results suggest that ZmYS1 is a phytosiderophore-dependent iron transporter.

1.6 The Yellow Stripe-Like (YSL) family:

The YSL family was identified based sequence similarity to ZmYS1 and is well conserved. Despite the fact that non-grasses do not synthesize or

secrete PS, multiple YSL genes are found in many species including monocots, dicots, gymnosperms, ferns, and mosses. The whole YSL family can be divided into three distinct, well conserved groups based on their sequence similarity (Figure 1.3). It is becoming increasingly well established that YSL proteins are Fe(II)-NA transporters and /or Fe(III)-PS transporters (specifically in grasses) responsible for iron translocation throughout whole plants or iron uptake from soil into roots (specifically in grasses).

1.6.1 The Fe(III)-PS transporters:

Barley YS1 (HvYS1) is able to functionally complement iron uptake defective yeast grown on medium containing Fe(III)-PS, but not medium containing Fe(III) only or Fe(II)-NA complex (Murata *et al.*, 2006), suggesting its role as a Fe(III)-PS transporter. Just like ZmYS1, HvYS1 is up-regulated in iron deficient roots (Murata *et al*, 2006). The HvYS1 transporter is located on the plasma membrane of epidermal cells according to immuno-histological staining with an anti-HvYS1 antibody and transient expression of HvYS1::GFP fusion proteins (Murata *et al*, 2006). 18 members were identified in the rice (*Oryza sativa*) YSL family (Koike *et al,* 2004). Recently, rice YSL18 (OsYSL18) was shown to be a Fe(III)-PS transporter via two-electrode voltage clamp analysis in *Xenopus oocytes* (Aoyama *et al*, 2009). OsYSL18 is

Figure 1.3: Cladogram illustrating the relationships among YSL proteins. Three distinct sub-groups of YSLs are represented in both the rice and Arabidopsis, indicated in red, green, and blue. The more distinct related AtOPT clade is indicated in violet. Several fungal OPT members (indicated by their Genebank accession number) are also shown.

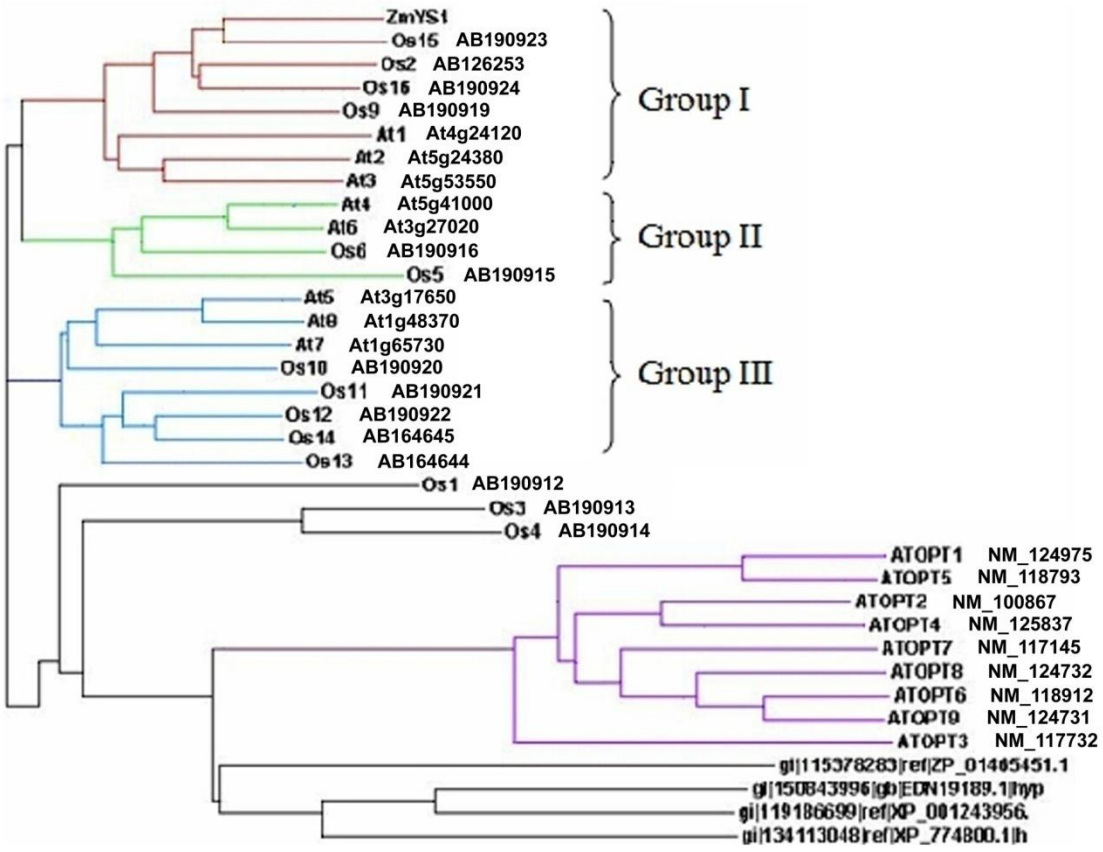
ZmYS1
Os15 AB190923
Os2 AB126253
Os16 AB190924
Os9 AB190919
At1 At4g24120
At2 At5g24380
At3 At5g53550
Group I
At4 At5g41000
At6 At3g27020
Os6 AB190916
Os5 AB190915
Group II
At5 At3g17650
At8 At1g48370
At7 At1g65730
Os10 AB190920
Os11 AB190921
Os12 AB190922
Os14 AB164645
Os13 AB164644
Group III
Os1 AB190912
Os3 AB190913
Os4 AB190914
ATOPT1 NM_124975
ATOPT5 NM_118793
ATOPT2 NM_100867
ATOPT4 NM_125837
ATOPT7 NM_117145
ATOPT8 NM_124732
ATOPT6 NM_118912
ATOPT9 NM_124731
ATOPT3 NM_117732
gi|115378283|ref|ZP_01465451.1
gi|150843996|gb|EDN19189.1|hyp
gi|119186699|ref|XP_001243956.
gi|134113048|ref|XP_774800.1|h

reported to be localized to the plasma membrane when transiently expressed in onion epidermal cells, and is expressed in reproductive organs and the phloem of lamina joints.

1.6.2 The Fe(III)-PS/Fe(II)-NA transporters:

ZmYS1 is able to rescue iron uptake defective yeast on medium containing Fe(II)-NA and Fe(III)-PS but not on medium containing an un-chelated source of iron, suggesting its role as an Fe(III)-PS and Fe(II)-NA transporter (Robert *et al*, 2004; Schaaf *et al*, 2004; Murata *et al*, 2006). Expression of ZmYS1 in leaves also implies a role in iron translocation within plants that is distinct from iron uptake from soil into roots. Among the 18 YSLs in rice, OsYSL15 has the highest similarity to ZmYSL1 and was thought to be the best candidate for an ortholog of rice YS1. Similar to ZmYSL1, OsYSL15 is up-regulated under iron deficiency, and was reported to transport Fe(III)-PS and Fe(II)-NA complex according to the results of yeast functional complementation assays (Lee *et al*, 2009). OsYSL15 was shown to be localized to the plasma membrane by subcelluar localization of OsYSL15::GFP in onion epidermal cells, and is expressed in shoots, roots and seeds (Lee *et al*., 2009; Inoue *et al*., 2009). *OsYSL15* knockout mutant plants exhibit a chlorotic phenotype when grown in iron limited conditions and have

reduced Fe in developing seeds. Furthermore, overexpression of *OsYSL15* resulted in an elevated level of iron in shoots and roots. Taken together, OsYSL15 is an iron transporter required for iron uptake from soil into roots and iron distribution in the plants and to seeds, and thus is functionally equivalent to ZmYS1 and HvYS1.

1.6.3 The Fe(II)-NA transporters:

Expression of rice *YSL2* (*OsYSL2*) was observed in the vascular bundles of leaves and flowers and in developing seeds during maturation, and this gene is strongly induced by iron deficiency (Koike *et al*, 2004). OsYSL2 is localized to the plasma membrane of vascular cells, and generates Fe(II)-NA dependent currents in *Xenopus* oocytes. The *Thalaspi caerulescens* YSL3 protein was demonstrated to transport both Fe(II)-NA and Ni-NA using both functional complementation and radioactive uptake assays, and is expressed in both shoots and roots, again suggesting a role in metal transport in the plants (Gendre *et al*, 2006).

There are eight members of the Arabidopsis YSL family (Figure 1.3). The Arabidopsis YSL family members share high sequence similarity. In yeast complementation assays conducted by Ray Didonato, all the AtYSLs tested were able to functionally complement the iron-uptake-defective yeast

strain, *fet3fet4*, in the presence of Fe(II) with NA but not Fe(III) only, Fe(II) only, or Fe(III) with MA (Figure 1.4). This indicates that AtYSLs are transporters of Fe(II)-NA complexes. AtYSL3 was not included in the experiment because we were not able to clone an At*YSL3* cDNA. At*YSL3* causes lethality in *E. coli*. Our lab has demonstrated that AtYSL2 can transport not only Fe(II)-NA but also Cu-NA and the expression of AtYSL2 is regulated by the level of Fe or Cu that is available to the plant (Didonato *et al*, 2004) . The AtYSL2 gene is expressed in root endodermis and pericycle and in xylem-associated cells of the leaf vasculature. AtYSL2 is localized to the plasma membrane, mostly in the lateral zone of vascular parenchyma cells, implying a role in moving metals laterally in the vascular tissue.

Single null mutations in the *AtYSL1* and *AtYSL3* genes, *ysl1-2* and *ysl3-1*, cause no morphological phenotype (Waters *et al*, 2006). Our group has identified an *ysl1ysl3* double mutant that exhibits interveinal chlorosis (Figure 1.5 A to E). The fact that this interveinal chlorosis phenotype can be rescued by application of Fe-EDDHA (Figure 1.5 H; Waters *et al*, 2006) suggests that YSL1 and YSL3 might be important for iron homeostasis in leaves. The *ysl1ysl3* double mutant also exhibits reproductive defects, such as stunting of inflorescence, (Figure 1.5 F) low pollen viability (Figure G), and defective

Figure 1.4: Yeast functional complementation assay (Conducted by Ray Didonato).

Growth tests of DEY1453 *(fet3fe4* double mutant) yeast transformed with negative (vector *pFL61*) control, positive control *IRT1* (a well characterized iron transporter), *ZmYS1*, and Arabidopsis *YSL* cDNA. Strains were spotted at two dilutions onto SD-URA (pH=5.5) containing 50 uM Fe-citrate growth permissive), 10 uM $FeCl_3$, 10 uM $FeCl_3$ supplemented with 10 uM mugineic acid (MA, a phytosiderophore), 4 uM $FeSO_4$, 4 uM $FeSO_4$ supplemented with 5 uM NA, and 4 uM $FeSO_4$ supplemented with 5 uM MA. Ascorbate was present in Fe(II)-containing plates.

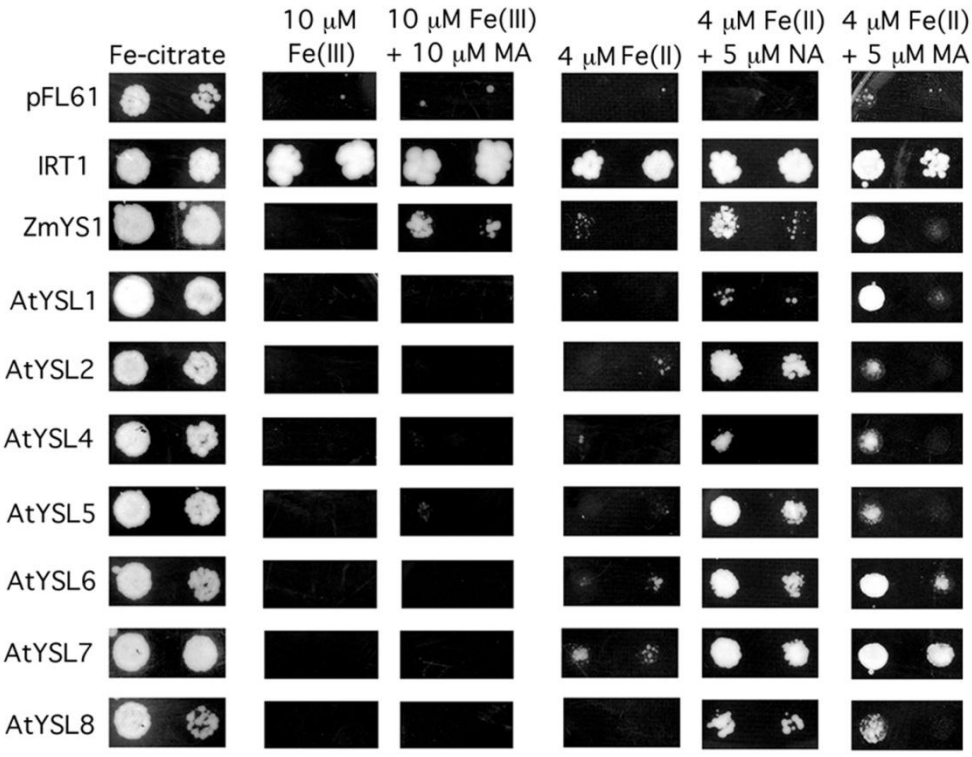
Fe-citrate
10 μM Fe(III)
10 μM Fe(III) + 10 μM MA
4 μM Fe(II)
4 μM Fe(II) + 5 μM NA
4 μM Fe(II) + 5 μM MA
pFL61
IRT1
ZmYS1
AtYSL1
AtYSL2
AtYSL4
AtYSL5
AtYSL6
AtYSL7
AtYSL8

Figure 1.5: *ysl1ysl3* double mutant phenotype (Waters *et al*, 2006).

(A) WT rosette. (B) *ysl1ysl3* double mutant rosette. (C) WT leaf. (D) Leaf of WT plant grown under iron deficiency conditions. (E) *ysl1ysl3* double mutant leaf. (F) Anther of a *ysl1ysl3* double mutant stained for viable pollen. Viable pollen stains purple, while inviable pollen is bluegreen. (G) Anther of a WT plant shown at the same magnification as in F. (H) Left : WT. Middle : *ysl1ysl3* double mutant exhibits chlorosis and stunted inflorescence. Right : *ysl1ysl3* double mutant + Fe-EDDHA .

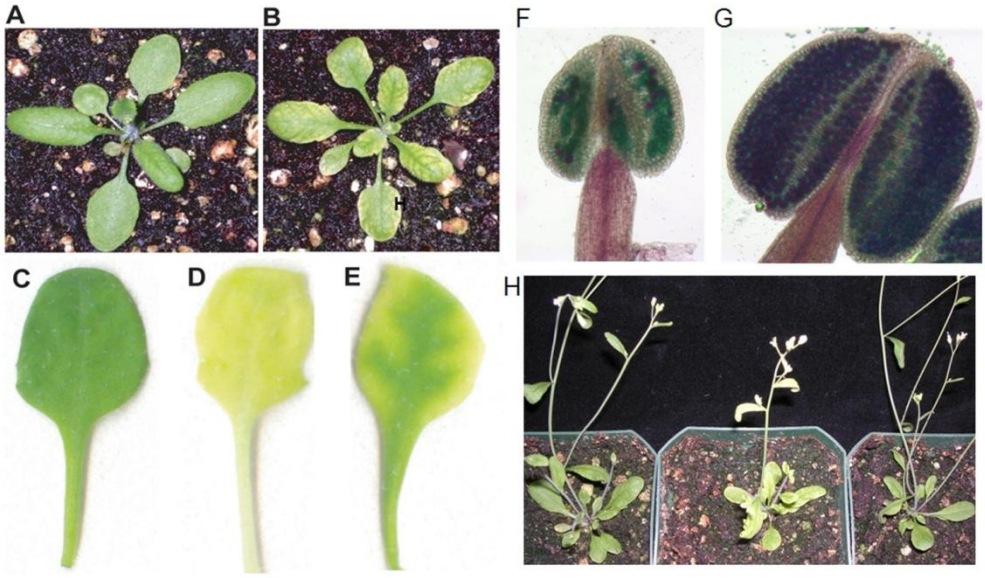
A
B
F
G
C
D
E
H

seeds with arrested embryos, implying that YSL1 and YSL3 are necessary for proper pollen and seed development.

Although the YSLs have been shown to play important roles in iron uptake from soil, translocation throughout whole plants, and loading into seeds, only very few of them have been well characterized. Using the model plant Arabidopsis to study the roles of YSL family transporters is an ideal way of understanding the functions of YSLs. We have hypothesize that YSL family has role in lateral movement of metals out of vasculature during vegetative growth and movement of metals towards phloem during senescence. I have put my effort on characterizing four members in the Arabidopsis family, YSL1, YSL3, YSL4, and YSL6 using reverse genetics, ICP-MS measurement of metals, GUS histochemical analysis, GFP fusion localization, and etc.. Here, I present results of experiments suggesting the roles of the AtYSLs as metal transporters, and experiments that elucidate the physiological function of these YSLs on the whole plant level. The information obtained during this project could eventually be applied to crop improvement, either to allow better growth on iron deficient soil, devise strategies for biofortification, or both.

CHAPTER 2

MATERIALS AND METHODS

2.1 Plant growth conditions:

2.1.1 Plate-grown plants:

Seeds were sterilized by being placed in an eppendorf tube (1.5mL) or a 15 mL falcon tube, depending on quantity, and suspected level of contamination of seeds. For eppendorf tubes and up to 0.05g of seeds, 1 mL-1.2 mL were used for each step. For 15 mL tubes, 2-3mL volumes were used for each step. Seeds were soaked in 70% ethanol, 0.05% Triton X-100 for 10 min with occasional vortexing. When seeds sank to the bottom of the tubes, the supernatant was removed with a pipette. All the following wash changes were performed in the sterile hood. The first wash was replaced with the same volume of 100% ethanol and left to stand for 5 min with occasional vortexing. The 100% ethanol wash was repeated once more and the ethanol was left on the seeds while preparing Whatman filter papers (VWR, West Chester, PA). Whatman filter papers were labeled with a marker pen, soaked in 100% ethanol, and then allowed to dry in a sterile hood. Seeds were drawn from the bottom using a 1 mL pipette, and then gently placed onto

the Whatman paper. When the seeds dried, they were imbibed in sterile distilled 0.1% agarose at 4C for 3-5 days. Plants were grown in sterile petri plates containing 1X MS medium with or without antibiotics. Plates were placed in an upright position so that the roots grew along the surface rather than inside the agar, which allowed for easy transfer. Incubator conditions for plate-grown plants were 16 hour light, 8 hour dark at 22C.

2.1.2 Soil-grown plants:

Seeds were imbibed in sterile distilled 0.1% agarose at 4C for 3-5 days. The seeds were then sown directly onto potting mix (Fafard Canadian Growing Mix 2) pre-treated with Gnatrol (Valent Bioscience Corporation, Libertyville, Illinois). Alternatively, plate-grown seedlings were transferred from plates 7 days after germination. Growth chamber conditions for soil-grown plants were 16 hour light, 8 hour dark at 22C.

2.1.3 Fe-EDDHA supplementation:

For Fe-EDDHA supplementation experiments, Col-0 and *ysl1ysl3* plants were subirrigated with tap water (as negative control) and were subirrigated with 0.5 mg/L Fe-EDDHA (Sprint 138; Becker-Underwood, Ames, Iowa) for 15 minutes once per week throughout the plant's life cycle. Plants were allowed to grow to maturity.

2.1.4 Foliar application of Fe:

Foliar application of Fe was performed by spraying a 2 mg/mL solution of ferric ammonium citrate (Sigma, St. Louis, MO) directly onto the aboveground portions of the plants. Control plants were sprayed with a 2 mg/mL solution of ammonium citrate. Spraying commenced when the first true leaves emerged from seedlings and continued every 3 to 4 d throughout the rest of the plant's life cycle.

2.1.5 Germination test:

Germination tests were performed by surface sterilizing seeds and allowing them to imbibe at 4°C for 48 to 72 h. One hundred seeds were then either plated onto standard MS agar or onto soil. Percentage viability of seeds was determined 7 d after sowing, at which time germination was scored as successful emergence of the hypocotyls and cotyledons.

2.2 Molecular techniques:

2.2.1 DNA isolation from *E. coli* by boiling lysis:

Single colonies were picked up by sterile toothpicks and grown in 2 mL LB plus appropriate antibiotic in sterile 14 mL test tubes for 16 hours. 1.5 mL of culture was transferred to 1.5 mL eppendorf tubes and centrifuged at 17000 xG. The resulting bacterial pellet was resuspended in 350 ul of STET buffer (0.1M

NaCL, 10mM Tris-HCLpH8.0, 1mM EDTA pH8.0, 5% Triton X-100). 25 ul of a freshly prepared solution of lysozyme (10 mg/mL in 10 mM Tris-HCL pH 8.0) was added and the tubes were vortexed for 3 seconds. The tubes were placed in a boiling –water bath for exactly 40 seconds, and then centrifuged at 17000 xG for 10 minutes at room temperature. The pellets of bacterial debris were removed using toothpicks. 40 ul of 2.6M sodium acetate (pH 5.2) and 420 ul of isopropanol were added to the supernatant, followed by mixing by vortexing, and the tubes were placed at room temperature for 5 minutes. The pellets of nucleic acids were recovered by centrifugation at 17000 xG for 5 minutes at room temperature. The supernatants were removed by aspiration and then 1 mL of 70% ethanol was added, followed by centrifugation at 17000 xG for 2 minutes at 4 C. Supernatants were removed and the tubes were allowed to dry. The pellets of nucleic acids were re-dissolved in 50 ul of TE (pH 8.0).

2.2.2 Large scale isolation of plasmid DNA from *E. coli*:

100 mL cultures were inoculated with 1 mL of overnight culture and allowed to grow overnight with appropriate selection. Cells were spun down at 24200 xG in two 50 mL falcon tubes. Pellets were re-suspended in 3.5 mL Solution I (50 mL glucose, 10 mM EDTA pH 8.0, 25 mM Tris-HCL pH 8.0),

followed by 7 mL of freshly made Solution II (1% SDS, 0.2 M NaOH). The tubes were mixed gently, and put on ice. 5.3 mL cold 3 M KOAc was added ,and tubes were kept on ice for 10 minutes, then at room temperature for 2 minutes, followed by centrifugation at 24200 xG for 10 minutes at 4 C. 13 mL supernatant was transferred to a fresh 50mL Falcon tube, and tubes were filled to top with 100% ethanol, kept at room temperature for 2 minutes, and centrifuged at 10000 for 10 minutes at 4 C. Pellets were re-suspended in 2 mL TE buffer and then transferred to 15 mL Falcon tubes. 2 mL of cold 5 M LiCl was added, and debris was spun down at 24200 xG for 10 minutes at 4 C. Supernatant was transferred to a fresh tube, and 2 volumes of room temperature ethanol was added and centrifuged at 24200 xG for 10 minutes at 4 C. Pellets were washed with 10 mL 70% ethanol, centrifuged at 24200 xG for 10 minutes at 4 C, and dried, then re-suspended in 400 ul sterile water and transferred to a 1.5 mL eppendorf tube. 2 ul 10 mg/mL RNase A was added and tube was incubated at 37 C for 30 minutes. Nucleic acids were extracted in Phenol/chloroform/isoamyl alcohol (25:24:1) equilibrated with TE and then chloroform/isoamyl alcohol (24:1). 1/10 volume of 3M NaOAc and 2 volumes of room temperature 100% ethanol were added, and tubes were incubated at room temperature for 5 minutes, spun at 17000 xG for 5 minutes at 4 C. The

pellet was washed with 70 % ethanol, dried, and re-suspended in 100 – 150 ul TE or water.

2.2.3 Plant genomic DNA extraction (small scale):

A single Arabidopsis leaf was ground using a drill with a pellet pestle (Kimble Chase, Vineland, NJ) in liquid nitrogen in a 1.5 mL eppendorf tube, and then 750 ul of extraction buffer (100 mM Tris, pH 8.0; 50 mM EDTA, pH 8.0; 500 mM NaCl) and 50 ul 20% SDS were added, mixed thoroughly, and incubated at 65 C for 10 minutes. 250 ul of KOAc solution (For 100 mL: 11.5 mL 5M KOAc, 11.5 mL acetic acid, 28.5 mL H_2O; filter sterilize) was added and tubes were placed on ice for 20 minutes, followed by centrifugation at 17000 xG for 10 minutes at room temperature. The supernatant was moved into fresh 1.5 mL tubes containing 500 ul isopropanol, mixed well, and placed at -20 C for 20 minutes. After centrifuging at 17000 xG for 10 minutes at room temperature, pellets were re-suspended in 40 ul water. 1 ul RNAse A (10 mg/mL) was then added and incubated at 37 C for 30 minutes. 100 ul of Phenol/chloroform/isoamyl alcohol (25:24:1) equilibrated with TE was added, mixed thoroughly, and spun at 17000 xG for 5 minutes at room temperature. The aqueous (upper) layer was transferred to a new tube, and then 10 ul of 3M NaOAc and 200 ul isopropanol were added, followed by centrifugation at

17000 xG for 5 minutes at room temperature. The supernatant was removed and pellets were washed with 80% ethanol, dried, and re-suspended in 50 ul TE or water.

2.2.4 RNA isolation:

Different organs of the plants were ground in 1.5 mL using RNase-free disposable pestles (VWR, Batavia, Illinois). Total RNA was isolated using the RNeasy plant mini kit (Qiagen, Valencia, CA), followed by DNase treatment with DNA-free kit (Ambion, Austin, Texas). Total RNA concentration was quantified using a spectrometer (260 nm; Beckman DU640B, Fullerton, CA), and confirmation of RNA quality was performed by visualizing on a 1X TBE gel stained with ethidium bromide.

2.2.5 RT-PCR:

One microgram of total RNA was reverse transcribed using Superscript III Reverse Transcriptase (Invitrogen, Carlsbad, CA). 50ng cDNA (based on the starting amount of RNA) from the RT reaction was used in a 25ul PCR reaction using Ex-Taq polymerase (Takara) under the following cycling conditions: an initial denaturation step of 94 C for 3 min, followed by cycles of 94 C for 15 sec, 60 C for 15 sec, 72 C for 1 min, with a final elongation step of 72 C for 7 min. The number of PCR cycles was varied for each primer set, to

ensure that amplification was in linear phase: for *Actin2* and *18S* rRNA, 20 cycles were used; for *YSL3*, 27 cycles was used; for YSL4 and YSL6, 25 cycles was used. Sequences of all primers used are in Table 2.1. Control primers for A*ctin2* were AtActin2 5' and AtActin2 3' and for 18S rRNA were 18S forward and 18S reverse. Primers used for *YSL3* amplification were oAtYSL3.2481..2595 and oAtYSL3.3567..3591. Primers used for *YSL4* amplification were oAtYSL4c.7..33 and oAtYSL4c.1296..1269. Primers used for *YSL4* amplification were oAtYSL6.3196..3221 and oAtYSL6.3995..3969.

2.2.6 Destination vector construction:

pDEST-CGFP: The name of this vector stands for destination vector for cDNA fusion GFP localization. A Gateway reading frame cassette B (Invitrogen, Carlsbad, CA) was inserted into vector psmGFP (CD3-326, ABRC) 3' to the CaMV35S promoter and 5' to the smGFP and NOS terminator using the SmaI restriction site.

pDEST-GGFP: The name of this vector stands for destination vector for genomic DNA fusion GFP localization. The fragment of smGFP with NOS terminator was dropped from psmGFP vector and inserted into pPZP222 (Hajdukiewicz *et al*, 1994) using BamHI and EcoRI sites, followed by insertion of a Gateway reading frame cassette B in front of smGFP using the SmaI site.

Table 2.1: Primers used in this study.

Primer name	Sequence (5'-3')
AtActin2..5'	GCAAGTTCATCACGATTGGTGC
AtActin2..3'	GAACCACCGATCCAGACACTGT
18S Forward	CGGCTACCACATCCAAGGAA
18S Reverse	GCTGGAATTACCGCGGCT
oAtYSL1.1526..1555	CAGTCTCCATGGAAATAGAGCAAAGAAGG
oAtYSL1.HA1	GTCGTACGGGTATGAAGCTAAGAACTTCATACATATCGGAGG
oAtYSL1.HA2	TCACGCGTAGTCCGGCACGTCGTACGGGTATGAAGCTAAGAACTT
oAtYSL1c.2..27	CAGTCTCCATGGAAATAGAGCAAAGA
oAtYSL1c.2033..2006	TCCTCTGAAGCTAAGAACTTCATACAT
oAtYSL2.1541..1567	CTTCAAATGGAAAACGAAAGGGTTGAG
oAtYSL2.HA1	GTCGTACGGGTAATGAGCCGCAGTGAAGTTCATACAGATA
oAtYSL2.HA2	TCACGCGTAGTCCGGCACGTCGTACGGGTAATGAGCCGCAGT
oAtYSL3.26..50	ACAGTCACATGAACCGGAATCTCGG
oAtYSL3.1521..1496	ACTCCTCAGTTTTTTCCAAGAACAGA
oAtYSL3.2481..2595	ATTGGCCAGGAAACAAGTGTTTGGGT
oAtYSL3.3567..3591	GACAAGTCCCGCGACTACACCATTT
oAtYSL3.4208..4179	GTAACTCGAATATTTACTCGGCATGAAGCC
oAtYSL3.4209..4175	TTAACTCGAATATTTACTCGGCATGAAGCCCATAC
oAtYSL3c.39..65y	ATCCACTAGTAACGGCCGAAATGAGGAGTATGATGATGGAGAGAG
oAtYSL3.4203..4198y	CCGCCACTGTGCTGGATATCTGTAACTCGAATATTTACTCGGCAT
oAtYSL4.96..120	AAAACATTTTCACCACTGCAAGGTG
oAtYSL4c.7..33	TCTGAGAGTGAGAGGAATCACTGAAAA
oAtYSL4c.1296..1269	AAACTCGAGGGGTATACGGTCCTTGAGA
oAtYSL4c.2145..2112	GTCTCGGATGGTCTAAAGTACATACAAATGGGTG
oAtYSL4.HA1	GTCGTACGGGTAGGATGGTCTAAAGTACATACAAAT
oAtYSL4.HA2	TCACGCGTAGTCCGGCACGTCGTACGGGTAGGATGGTCTAAAGTA
oAtYSL6.828..856	CCGAGTCTAAAGCTAAACCAGAATTAACC
oAtYSL6.1500..1524	GCTAAAACATGGGGACGGAGATCCC
oAtYSL6.3196..3221	AATCTTGTCAAGATCATCGCTGTCAC
oAtYSL6.3995..3969	TCAGCAAAGCCCTCAATTCCGAGAATC
oAtYSL6.4347..4324	CTATCTTGCTGAGGACGGTCCAAA
oAtYSL6c.2076..2051	CTCTCTCTTGCTGAGGACGGTCCAAA
oAtYSL6.HA1	GTCGTACGGGTACTATCTTGCTGAGGACGGTCCAAAGTA
oAtYSL6.HA2	TCACGCGTAGTCCGGCACGTCGTACGGGTACTATCTTGCTGA

pDEST-YSL3p: The name of this vector stands for destination vector with *YSL3* promoter. The *YSL3* promoter was amplified using Platinum *Taq* DNA Polymerase High Fidelity (Invitrogen) and the following primers: oAtYSL3.26..50 and oAtYSL3.1521..1496. The *YSL3* promoter was then cloned into the SmaI site of vector pPZP222 (Hajdukiewicz *et al*, 1994), followed by insertion of a NOS terminator sequence into the SacI/EcoRI sites. Then a Gateway reading frame cassette A was inserted *3'* to *YSL3* promoter using the SacI site blunted by T4 DNA polymerase (New England Biolabs, Waltham, MA).

pDEST-OX: The name of this vector stands for destination vector for overexpression. A Gateway reading frame cassette B was introduced into the vector pMN20 (http://www.addgene.org), which contains four copies of CaMV 35S enhancer, using the SmaI site. This vector does not contain a NOS terminator sequence.

pDEST-YES6/CT: The name of this vector stands for destination vector of pYES6/CT. A Gateway reading frame cassette A was introduced into the vector pYES6/CT using the NotI site.

2.3 Mineral analysis preparation, seed weight and seed number determination:

For soil-grown plants, leaf samples were collected 20 days after sowing

and dried in an oven at 60 C. ICP-MS was performed by the Lahner lab (Purdue University).

Seed weight was determined based on a sampling of weights of 100 seed batches. Weight per seed was calculated from the average of three seed batches.

Seed number was determined by dividing the total weight of seeds by the weight per seed.

2.4 Agrobacterium-mediated stable transformation:

Arabidopsis plants were grown to flowering, and the main bolts were clipped to encourage proliferation of secondary bolts. *Agrobacterium tumefaciens* strain GV3101 carrying the vector of interest was grown in 100 mL LB with antibiotics at 28 C for 24 hours. The Agrobacterium was spun down at 7260 xG for 10 minutes at room temperature, and re-suspended in 5% sucrose. Silwet L-77 was then added to a concentration of 0.04%. The above-ground parts of the plants were dipped in Agrobacterium solution for 2 to 3 seconds with gentle agitation. Plants were returned to trays and were covered with lids for 16 to 24 hours to maintain high humidity. For higher rates of transformation, plants were dipped again seven days after the first dipping. Plants were watered and grown normally until seeds were ready for

collecting. Seeds were germinated on 1X MS medium with antibiotics to select for transformants, and seedlings were transferred to soil 7 days after germination.

2.5 Perl's stain:

Seeds were cut in half vertically using a double-edged blade under a dissecting microscope and then put into Perl's stain solution (4% Potassium ferrocyanide and 4% HCL) under vacuum for a period of either 15min or 4 hours. Perl's stain solution was then removed and samples were rinsed with double distilled water three times. Samples were mounted in water for microscopic observation.

2.6 Cloning of YSLs for yeast complementation assays:

2.6.1 Cloning of YSL1, YSL4, and YSL6:

YSL1 cDNA was amplified by RT-PCR using Platinum *Taq* DNA Polymerase High Fidelity (Invitrogen) and the following primers: oAtYSL1c.2..27 and oAtYSL1c.2033..2006. *YSL4* cDNA was amplified by RT-PCR using Platinum *Taq* DNA Polymerase High Fidelity (Invitrogen) and the following primers: oAtYSL4c.7..33 and oAtYSL4c.2145..2112. *YSL6* cDNA was amplified by RT-PCR using Platinum *Taq* DNA Polymerase High Fidelity (Invitrogen) and the following primers: oAtYSL6.1500..1524 and

oAtYSL6c.2076..2051. *YSL1*, *YSL4* and *YSL6* cDNA were then cloned into gateway vector pCR8/GW/TOPO (Invitrogen, Carlsbad, CA), and then introduced into the vector pDEST-YES6/CT after sequencing to ensure no PCR errors.

2.6.2 Cloning of YSL3 cDNA directly in yeast:

YSL3 cDNA was amplified by RT-PCR using Platinum *Taq* DNA Polymerase High Fidelity (Invitrogen) and the following primers: oAtYSL3c.39..65y, and oAtYSL3.4203..4198y. Each primer contains an 18 nucleotide overlap with yeast expression vector pYES6/CT for *in vivo* homologous recombination. *YSL3* cDNA fragment and linearized pYES6/CT were co-transformed into the iron-uptake-defective yeast strain DEY1453 and recombinant plasmids were selected using blasticidin resistance. Sequencing was performed to ensure no PCR error had occured.

2.7 Grafting:

The inflorescences (3-7 cm long, and with similar diameters) of soil-grown Col0 and *ysl1ysl3* plants were cut using a double-sided blade and then placed in water to prevent drying prior to grafting. A short tube of appropriate diameter (~ 0.5 - 1 cm; Small Parts Inc., Part #: STT-20-10), was placed over the cut inflorescence of the stock, the tube was filled with distilled water. The scions

were then inserted into the other end of the tubing until they touched the stem of the scion. The plants were returned to trays covered with lids for 3-5 days to maintain moisture, allowing plants to recover (Rhee and Somerville, 1995).

2.8 GFP fusion and intercellular localization:

2.8.1 GFP fusion:

YSL1 cDNA was amplified by RT-PCR using Platinum *Taq* DNA Polymerase High Fidelity (Invitrogen) and the following primers: oAtYSL1c.2..27 and oAtYSL1c.2033..2006 which altered the stop codon from TAG to GAG. *YSL1* cDNA was then cloned into Gateway vector pCR8/GW/TOPO (Invitrogen, Carlsbad, CA), and introduced into the vector pDEST-CGFP via LR recombination, to generate a C-terminal translational fusion to smGFP under the control of CaMV 35S promoter. The 35S::YSL1::GFP fusion construct was then transiently expressed in onion epidermal cells by biolistic bombardment.

Full length *YSL3* genomic DNA was amplified using Expand High-Fidelity polymerase (Roche) and the following primers: oAtYSL3.26..50, and oAtYSL3.4208..4179 which altered the stop codon from TAA to TAC. *YSL3* genomic DNA was then cloned into pDEST-GRuB (pPZP212 backbone with smGFP inserted using *Bam*HI and *Eco*RI site) to generate a C-terminal

translational fusion to smGFP. The YSL3::GFP fusion construct was then stably expressed in *ys1ysl3* double mutant plants following Agrobacterium-mediated transformation.

Full length *YSL4* genomic DNA was amplified using Platinum *Taq* DNA Polymerase High Fidelity (Invitrogen) and the following primers: oAtYSL4.96..120 and oAtYSL4.2145..2112 which altered the stop codon from TAG to GAG. Full length *YSL6* genomic DNA was amplified using Platinum *Taq* DNA Polymerase High Fidelity (Invitrogen) and the following primers: oAtYSL6.828..856 and oAtYSL6.2076..2051 which altered the stop codon from TAG to GAG. *YSL4* and *YSL6* genomic DNA then cloned into gateway vector pCR8/GW/TOPO (Invitrogen), and introduced into the vector pDEST-GGFP to generate a C-terminal translational fusion to smGFP via LR recombination. The YSL4::GFP and YSL6::GFP fusion constructs were then stably expressed in *ysl4-2* and *ysl6-5* mutant plants, respectively, following Agrobacterium-mediated transformation.

2.8.2 Transient transformation:

For each onion bombardment experiment, six milligrams of 1.0µM gold particles (Bio-RAD) were weighed in a 1.5 mL eppendorf tube and prepared by the following steps: Sonication for 10 minutes in 1 mL of 70% EtOH, vortexing

for 15 minutes, settling for 15 minutes, centrifuging for a five second pulse at 12782 xG. 70% EtOH was removed from the gold particles, which were then washed twice with 100% ethanol, and three times with sterile double distilled water. Gold was re-suspended in 100µl of 50% glycerol, vortexed for five minutes, and then 30µl was aliquoted into three 1.5 mL eppendorf tubes. Four micrograms of plasmid DNA (1µg/µl) (35S::YSL1::GFP or psmGFP) was added and vortexed for five seconds. 30µl of freshly prepared 2.5M $CaCl_2$ was added to each tube, and then vortexed for five seconds. 12µl of 0.1M spermidine was added to each tube and vortexed for three minutes, followed by incubation at room temperature for 30 minutes, and then centrifugation for five seconds. Supernatants were removed, and the gold was washed with 84µl of 70% EtOH twice. The gold was then re-suspended in 24µl 100% EtOH by gentle flicking, and 8 µl was immediately disbursed into the center of microcarrier discs (Bio-RAD, Hercules, CA) that were placed in 6 well plates, and allowed to dry. While waiting for the gold to dry, onion tissues were prepared in a sterile hood. The outer paper layers of the onion were removed. Dry tips were cut off and the onion was split lengthwise into quarters. One or two innermost layers of leaves were discarded to expose the fleshy medium-sized leaves. Starting at the tip of the leaf, the outer epidermis was

hand-peeled from the underlying tissue. The strip of epidermis was put on MS medium with the outer surface of the epidermis facing down. Incisions were made so that the epidermis made good contact with the medium. Microcarriers were loaded into the PDS-1000/He instrument (Bio-Rad, Hercules, CA) and were released with 1100-PSI pressure onto onion epidermal cells at a stopping screen to target distance of 6 centimeters. Two bombardments per sample were delivered by this method, with the sample being turned 180 degrees before each shot to ensure equal transformation across the plate. Four replicates of each experiment were performed. The onion epidermal peels were then incubated in the dark at 30 C. After 48 hours, samples were mounted in water for microscopic observation.

2.8.3 Microscopic observation:

Roots of 5 day old seedlings (YSL3, YSL4, and YSL6) were mounted in water for microscopic observation. Green fluorescent cells were imaged by Zeiss 510 Meta Laser Scanning Confocal Microscope (Nikon) with excitation at 488 nm, and the fluorescence emission signal was recovered between 520 and 550 nm.

2.9 GUS histochemical staining:

2.9.1 Promoter GUS fusion:

The YSL4 promoter region containing 785 bps upstream of the YSL4 initiating ATG was cloned create a C-terminal translational fusion to GUS reporter gene. The YSL6 promoter region containing 601 bps upstream of the YSL6 initiating ATG was cloned to create a C-terminal translational fusion to GUS reporter gene. *YSL4p*::GUS and *YSL6p*::GUS construct were then stably introduced into Arabidopsis by Agrobacterium-mediated transformation.

2.9.2 GUS histochemical staining:

Tissues were pre-fixed in ice-cold 10% acetone for 10 minutes, and then were placed in 6 well polystyrene dishes with enough GUS buffer (0.1 M $NaPO_4$ pH=7.2, 0.5 mM $K_3Fe(CN_6)$, 10 mM EDTA, 0.01% Triton X-100, 0.5 mg/mL X-gluc) to cover. Tissues were stained at 37 C for 2-24 hours. For tissues containing chlorophyll, tissues were soaked in 70% ethanol, followed by several washes with 70% ethanol until the samples were clear.

2.10 Overexpression of YSLs:

YSL3 genomic DNA was amplified using Platinum *Taq* DNA Polymerase High Fidelity (Invitrogen) and the following primers: oAtYSL3.26..50 and oAtYSL3.4209..4175. *YSL6* genomic DNA was amplified using Platinum *Taq* DNA Polymerase High Fidelity (Invitrogen) and the following primers: oAtYSL6.828..856 and oAtYSL6.4347..4324. *YSL3* and *YSL6* genomic DNA

were cloned into gateway vector pCR8/ GW/TOPO (Invitrogen), and introduced into the vector pDEST-OX via LR recombination. The constructs were stably transformed into wild type Arabidopsis plants and homozygous transformants were obtained by kanamycin selection.

2.11 Chlorophyll content determination:

For iron starvation tests, *YSL3*-overexpression lines were grown on 1X MS medium for 10 days and then transferred to MS-Fe medium for a variable number of days prior to quantification of chlorophyll. Leaves of soil-grown *YSL3p::YSL1* and *YSL3p::YSL2* lines were collected at day 20. Shoots and leaves were placed in 3 mL of *N*,*N*'-dimethylformamide and chlorophyll was extracted overnight. Total chlorophyll was measured by spectrophotometer at absorbance 647nm and 664.5nm. Total chlorophyll content (ug/mL) was determined using the equation $17.9*A_{467}+8.08*A_{664.5}$ (Inskeep and Bloom, 1985).

2.12 Complementation of *ysl1ysl3* double mutants:

The *YSL3* promoter was amplified using Platinum *Taq* DNA Polymerase High Fidelity (Invitrogen) and the following primers: oAtYSL3.26..50 and oAtYSL3.1521..1496. The *YSL3* promoter was then cloned into vector pPZP222. For Cloning of *YSL1*, *YSL2*, and *YSL6* cDNA, an HA tag

(YPYDVPDYA) was added to the C terminus of each cDNA in a two step strategy. *YSL1* cDNA was amplified by RT-PCR using Platinum *Taq* DNA Polymerase High Fidelity (Invitrogen) and the following primers: oAtYSL1.1526..1555 and oAtYSL1.HA1 which altered the stop codon from TAG to TAC and added the first twelve nucleotides of the HA tag to the 3' end of the *YSL1* cDNA. A secondary PCR reaction was then performed using primary PCR product as template and the following primers: oAtYSL1.1526.. 1555 and oAtYSL1.HA2 which adds the entire HA tag sequence to the 3' end of the *YSL1* cDNA. *YSL2* and *YSL6* cDNA were amplified using the same method as for *YSL1* cDNA. Primers for *YSL2* primary PCR were oAtYSL2.1541..1567 and oAtYSL2.HA1. Primers for *YSL2* secondary PCR were oAtYSL2.1541..1567 and oAtYSL2.HA2. Primers for *YSL6* primary PCR were oAtYSL6.1500..1524 and oAtYSL6.HA1. Primers for *YSL6* secondary PCR were oAtYSL2.1500..1524 and oAtYSL6.HA2. *YSL1*, *YSL2* and *YSL6* cDNA were cloned into the vector pDEST-YSL3p under the control of the *YSL3* promoter. *YSL3p*::*YSL1*, *YSL3p*::*YSL2* and *YSL3p*::*YSL6* constructs were then stably transformed into *ysl1ysl3* double mutant and selected using gentamycin resistance.

CHAPTER 3

CHARACTERIZATION AND COMPARISON OF ARABIDOPSIS YSL1, YSL2, AND YSL3

3.1 Introduction:

The Arabidopsis YSL family contains eight members (Figure 3.1), and was identified based on sequence similarity to ZmYS1. The AtYSL proteins share strong full-length sequence similarity to each other (over 50%) and to ZmYS1 (over 67%). The YSL proteins are extremely hydrophobic, which is consistent with their being membrane bound transporters. According to predicted topology by TMAP (Persson and Argos, 1994, 1996), YSL proteins contain 15 putative transmembrane domains. Two regions were found to be poorly conserved. One is a poorly conserved (variable) predicted extracellular loop that occurs between putative transmembrane domains 7 and 8. The other variable region is the N-terminal portion of the YSLs, but in spite of the poor sequence similarity, these regions share a striking similarity of amino acid composition. These N-terminal regions precede the first transmembrane domain, and are predicted in all cases to be intracellular. They are extremely acidic, containing large numbers of glutamic and aspartic acid residues.

Figure 3.1: Phylogenetic analysis of AtYSL family and ZmYS1 proteins.

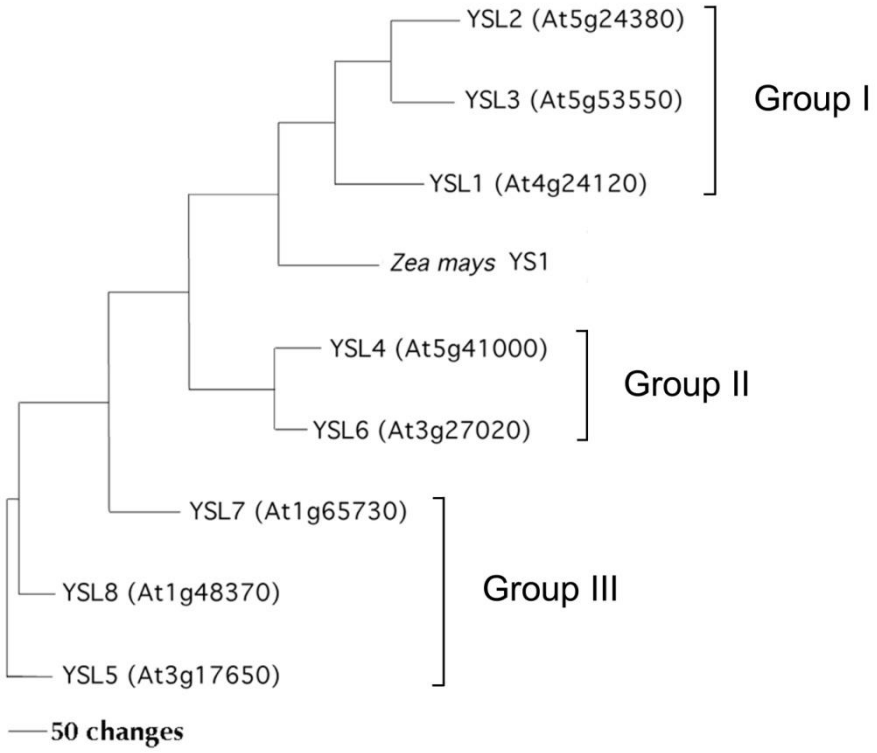
YSL2 (At5g24380)
YSL3 (At5g53550)
YSL1 (At4g24120)
Zea mays YS1
YSL4 (At5g41000)
YSL6 (At3g27020)
YSL7 (At1g65730)
YSL8 (At1g48370)
YSL5 (At3g17650)
50 changes
Group I
Group II
Group III

Aside from this glutamic acid rich region, there are no obvious potential metal ligands that are strongly conserved within the YSL family.

The whole AtYSL family can be divided into three groups based on sequence similarity (Figure 3.1). YSL1, YSL2, and YSL3 fall into the same group. These three YSLs have the highest similarity to ZmYS1 (73%, 77%, and 76% respectively) and share over 60 percent sequence identity (YSL1 and YSL2 are 79% similar; YSL2 and YSL3 are 83% similar). Moreover, their expression patterns are quite similar to each other. These three genes are expressed strongly in the xylem parenchyma of leaves, and are down-regulated during iron deficiency (DiDonato *et al*., 2004; Waters *et al*., 2006). Taken together, the protein sequence similarity and the similar expression patterns lead us to hypothesize that YSL1, YSL2, and YSL3 perform similar functions.

Characterization of mutants of *YSL1*, *YSL2*, and YSL3 revealed no morphological phenotypes in the single mutants. *YSL1* single mutant plants exhibit subtle phenotypes- decreased NA and Fe contents in seeds, and excess NA in leaves with normal Fe content (Le Jean et al., 2005). Our group identified a *ysl1ysl3* double mutant that exhibits strong interveinal chlorosis (Figure 1.5 A to E; Waters *et al*, 2006). The fact that this interveinal chlorosis

phenotype can be rescued by application of Fe-EDDHA (Figure 1.5 H; Waters *et al*, 2006) suggests that YSL1 and YSL3 may be important for iron utilization in leaves. In addition, leaves of the double mutants have decreased levels of Fe and elevated levels of Mn, Zn, and Cu. Thus, we have proposed that the role of YSL1 and YSL3 is to transport metal-NA complexes into vascular parenchyma cells (Figure 3.2A). Lower mRNA levels of YSL1 and YSL3 in Fe-limiting conditions would decrease Fe removal from the xylem into adjacent tissues (Figure 3.2B). This would facilitate direct Fe exchange from xylem into phloem, which we hypothesize can occur without YSL1 and YSL3 (Figure 3.2C). In this way, during periods of iron deficiency, the increased phloem Fe would be delivered to the young leaves, which are primarily supplied with nutrients from phloem. The *ysl1ysl3* double mutants also exhibited reproductive defects, implies that YSL1 and YSL3 are involved in metal transport during reproduction. Studies addressing reproduction in the double mutant will be discussed in Chapter 4.

Our lab has demonstrated that ZmYS1 and AtYSL2 can transport Fe(II)-NA (Curie *et al*., 2001; DiDonato *et al*., 2004; Roberts *et al*., 2004). In this chapter, I examined that YSL1 and YSL3 are Fe-NA transporters by yeast functional complementation assay. Furthermore, I examined that YSL1 and YSL3 are

Figure 3.2: Working model of YSL1 and YSL3 in vegetative tissues of Col0 and *ysl1ysl3* double mutant plants.

(A) Model in Col0 plants during period of iron sufficiency. YSL1 and YSL3 take up metal ions that arrive via xylem. This uptake occurs mostly in the xylem parenchyma. Once inside the cells, iron moves through the symplast or is effluxed elsewhere.

(B) Model in Col0 plants during period of iron sufficiency. When iron is limited for growth, YSL1 and YSL3 expression is low, causing iron to remain in the vein, and allowing them to be exchanged readily into the phloem. The phloem iron can then move to the growing parts of the plant such as young leaves, thus allowing their continuous development at the expense of storage by mature leaves.

(C) Model in *ysl1ysl3* mutant plants. Loss of function of YSL1 and YSL3 results in decreased Fe removal from the xylem into adjacent tissues, and thus facilitates direct Fe exchange from xylem into phloem. If metal sensing mechanisms are located in the phloem, then high levels of metals in the phloem may send an inappropriate signal of metal sufficiency in spite of actual low levels of metals in most leaf cells.

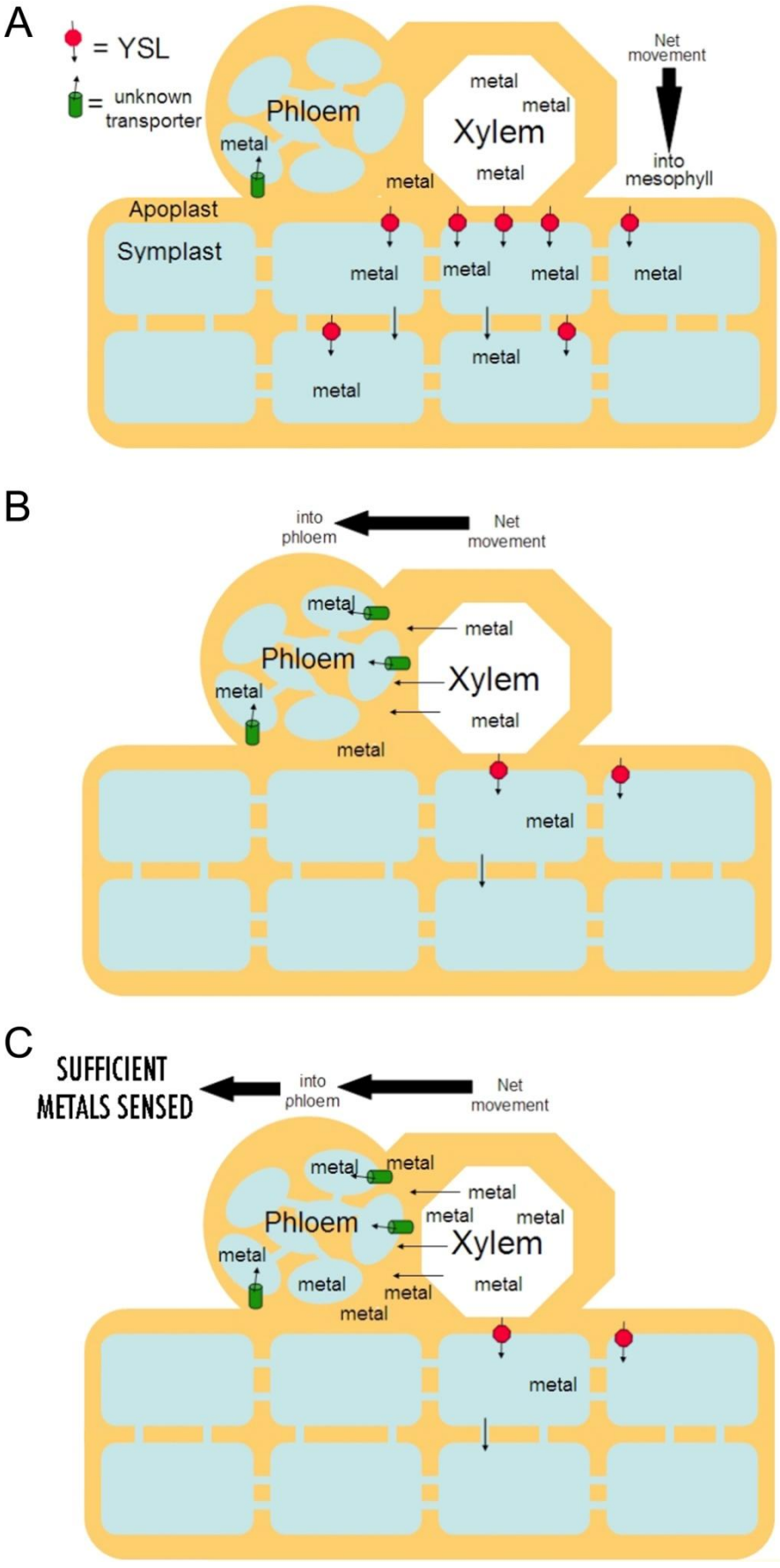
A
= YSL
= unknown transporter
Phloem
Xylem
Net movement
into mesophyll
Apoplast
Symplast
metal
B
into phloem
Net movement
C
SUFFICIENT METALS SENSED

localized to the plasma membrane, consistent with their roles as Fe-NA transporters that allow cells to take up iron from apoplast. Over-expressing AtYSL3 resulted in a small increase in copper in shoots and mildly increased Fe deficiency resistance, suggesting that YSL3 is involved in Fe utilization in Arabidopsis. The biochemical functions of YSL1, YSL2, and YSL3, the three members that fall into the same subgroup as YS1, were compared. I have demonstrated that the YSL1 or YSL2 proteins, when placed under the control of the AtYSL3 promoter, can only partially rescue the phenotypes of the *ysl1ysl3* double mutant, suggesting that although these three YSL transporters are closely related, they have distinct activities *in planta*.

3.2 Materials and methods:

The detailed materials and methods are described in Chapter 2. Sections Plant growth conditions (2.1), Molecular techniques (2.2), Mineral analysis by ICP-MS (2.3), Agrobacterium mediated stable transformation (2.4), Perl's stain (2.5), GFP fusion and intercellular localization (2.8), Overexpression of YSLs (2.10), Chlorophyll content determination (2.11), and Complementation of *ysl1ysl3* double mutants (2.12) are relevant to the work presented in this chapter.

3.3 Results:

3.3.1 Functional complementation of iron growth defects using *AtYSL1* and *AtYSL3*:

Previous lab members have attempted to clone AtYSL3 cDNA for use in yeast functional complementation assays. However, when attempting to clone AtYSL3 cDNA, both by RT-PCR and by screening cDNA libraries, every cDNA we obtained was either only a partial clone or was a mutated version. Two types of full length cDNA were obtained by RT-PCR; PCR errors caused frame shifts or retained introns were observed. These products are present in very low levels in our RT-PCR reactions—the vast majority of RT-PCR product is the correct size, and direct sequencing of PCR products confirms the presence of a large excess of the fully spliced, expected cDNA product. We conclude that even low levels of expression of YSL3 in *E. coli* are causing lethality, and thus the only clones we obtained were ones that do not encode YSL3 protein. We have made use of strains of *E. coli* that maintain plasmids at very low copy number (Copycutter™, Epicenter), hoping that the expression would be low enough to allow growth. However, this approach failed too. Recently, I successfully cloned YSL3 by direct cloning of YSL3 in yeast through homologous recombination (Oldenburg et al., 1997). The YSL3 cDNA from RT-PCR contains eighteen nucleotides homologous to the yeast

expression vector pYES6/CT. When the RT-PCR product and the vector were co-transformed into yeast, homologous recombination occurred allowing recovery of the desired plasmid. Sequencing was then performed to confirm correct splicing and no mutation. Sequencing results of YSL3::pYES6/CT clone reveal one mutation, which changed lysine to arginine in a conserved region but at a poorly conserved amino acid residue (Figure 3.3). Notably, both lysine and arginine are basic, indicating that they are similar to each other.

Using a yeast functional complementation assay, the abilities of YSL1 and YSL3 to transport Fe-NA and Fe-PS complexes were examined (Figure 3.4). This assay was performed by a colleague, Jeff Chiecko, in the lab. In this assay, *fet3fet4* yeast was transformed with the *YSL* -expressing plasmids, and with the empty *pYES6/CT* vector, which serves as a negative control. We made use of the beta-estradiol (BE) regulated expression system developed by Gao and Pinkham (Gao and Pinkham, 2000) to allow us to control the level of *YSL* expression in yeast). This system is used to achieve dose-dependent gene expression levels and further confers a tightly regulated off state, so that strains can be grown without expression of the target proteins (negative control). As a positive control to demonstrate viability of the strains, all strains

Figure 3.3: Protein alignment of ZmYS1, Arabidopsis YSLs (AtYSL),and rice YSLs (OsYSL) using Clustal W2. The arrow indicates the mutation, which changed lysine (K) to arginine (R) in the YSL3 clone.

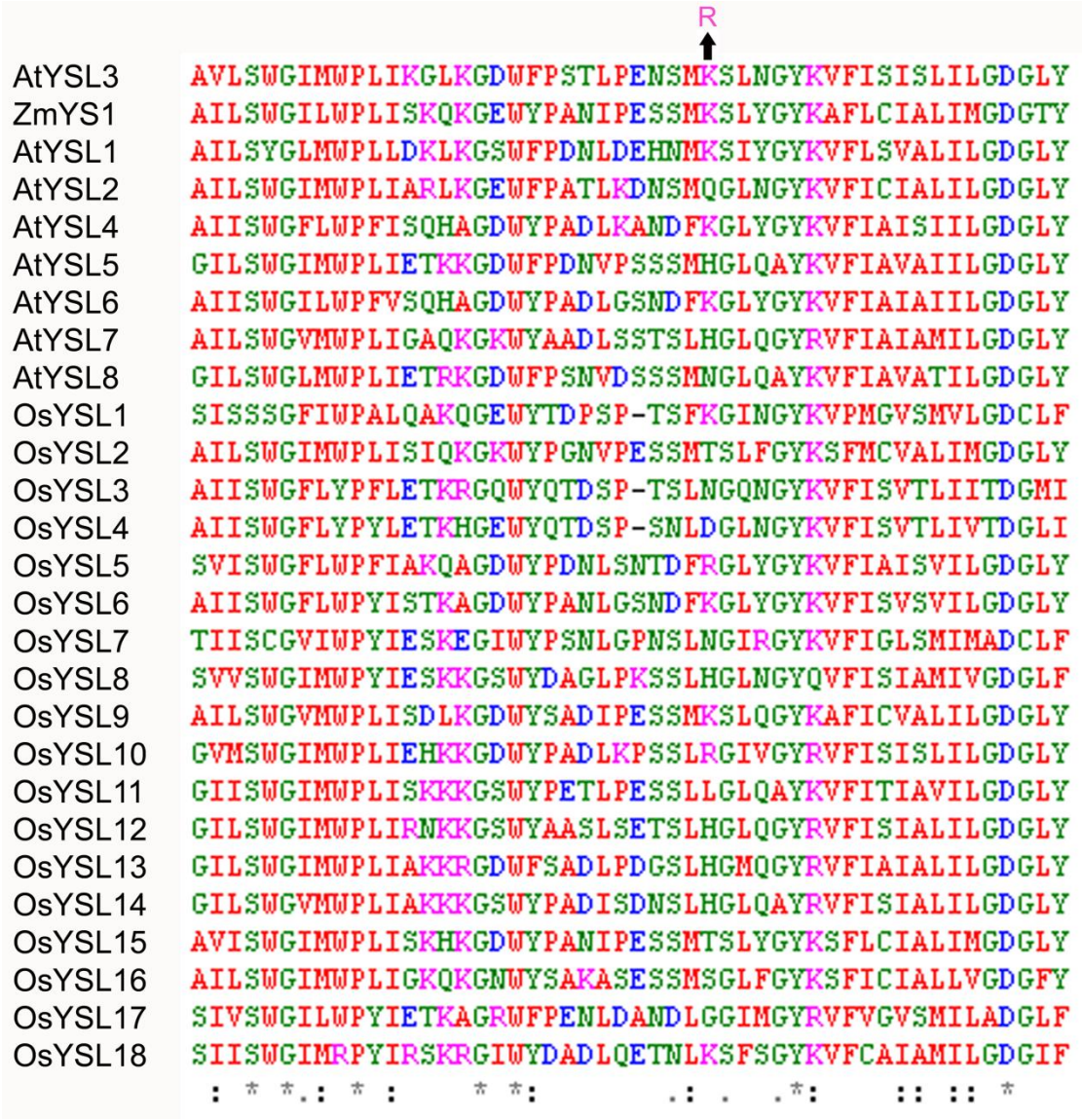
R
AtYSL3 AVLSWGIMWPLIKGLKGDWFPSTLPENSMKSLNGYKVFISISLILGDGLY
ZmYS1 AILSWGILWPLISKQKGEWYPANIPESSMKSLYGYKAFLCIALIMGDGTY
AtYSL1 AILSYGLMWPLLDKLKGSWFPDNLDEHNMKSIYGYKVFLSVALILGDGLY
AtYSL2 AILSWGIMWPLIARLKGEWFPATLKDNSMQGLNGYKVFICIALILGDGLY
AtYSL4 AIISWGFLWPFISQHAGDWYPADLKANDFKGLYGYKVFIAISIILGDGLY
AtYSL5 GILSWGIMWPLIETKKGDWFPDNVPSSSMHGLQAYKVFIAVAIILGDGLY
AtYSL6 AIISWGILWPFVSQHAGDWYPADLGSNDFKGLYGYKVFIAIAIILGDGLY
AtYSL7 AILSWGVMWPLIGAQKGKWYAADLSSTSLHGLQGYRVFIAIAMILGDGLY
AtYSL8 GILSWGLMWPLIETRKGDWFPSNVDSSSMNGLQAYKVFIAVATILGDGLY
OsYSL1 SISSSGFIWPALQAKQGEWYTDPSP-TSFKGINGYKVPMGVSMVLGDCLF
OsYSL2 AILSWGIMWPLISIQKGKWYPGNVPESSMTSLFGYKSFMCVALIMGDGLY
OsYSL3 AIISWGFLYPFLETKRGQWYQTDSP-TSLNGQNGYKVFISVTLIITDGMI
OsYSL4 AIISWGFLYPYLETKHGEWYQTDSP-SNLDGLNGYKVFISVTLIVTDGLI
OsYSL5 SVISWGFLWPFIAKQAGDWYPDNLSNTDFRGLYGYKVFIAISVILGDGLY
OsYSL6 AIISWGFLWPYISTKAGDWYPANLGSNDFKGLYGYKVFISVSVILGDGLY
OsYSL7 TIISCGVIWPYIESKEGIWYPSNLGPNSLNGIRGYKVFIGLSMIMADCLF
OsYSL8 SVVSWGIMWPYIESKKGSWYDAGLPKSSLHGLNGYQVFISIAMIVGDGLF
OsYSL9 AILSWGVMWPLISDLKGDWYSADIPESSMKSLQGYKAFICVALILGDGLY
OsYSL10 GVMSWGIMWPLIEHKKGDWYPADLKPSSLRGIVGYRVFISISLILGDGLY
OsYSL11 GIISWGIMWPLISKKKGSWYPETLPESSLLGLQAYKVFITIAVILGDGLY
OsYSL12 GILSWGIMWPLIRNKKGSWYAASLSETSLHGLQGYRVFISIALILGDGLY
OsYSL13 GILSWGIMWPLIAKKRGDWFSADLPDGSLHGMQGYRVFIAIALILGDGLY
OsYSL14 GILSWGVMWPLIAKKKGSWYPADISDNSLHGLQAYRVFISIALILGDGLY
OsYSL15 AVISWGIMWPLISKHKGDWYPANIPESSMTSLYGYKSFLCIALIMGDGLY
OsYSL16 AILSWGIMWPLIGKQKGNWYSAKASESSMSGLFGYKSFICIALLVGDGFY
OsYSL17 SIVSWGILWPYIETKAGRWFPENLDANDLGGIMGYRVFVGVSMILADGLF
OsYSL18 SIISWGIMRPYIRSKRGIWYDADLQETNLKSFSGYKVFCAIAMILGDGIF

were grown under permissive conditions (50 µM iron citrate; Figure 3.4A, B and C). When Fe(II) was provided in unchelated form (as 3 µM $FeSO_4$; Figure 3.4A), both AtYSL1 and AtYSL3 failed to restore growth, whereas both AtYSL1 and AtYSL3 were able to restore growth when NA was provided along with Fe(II) (3 µM $FeSO_4$ with 8 µM NA; Figure 3.4A). BE was withheld from the medium to demonstrate that growth is dependent on YSL expression, and no growth was observed (Figure 3.4A). This result showed that AtYSL1 and AtYSL3 are transporters of Fe(II)-NA complexes.

To examine whether AtYSL1 and AtYSL3 can transport Fe(III)-PS, the strains were grown on 10 µM $FeCl_3$ with or without 10 µM 2'-deoxymugineic acid (DMA; a phytosiderophore; Figure 3.4B) in the presence of the inducer BE. Both *AtYSL1* and *AtYLS3* were not expected to restore growth on Fe(III)-PS medium since Arabidopsis neither makes nor uses PS. As expected, *AtYSL1* failed to complement on medium containing Fe(III)-PS. Strikingly, *AtYSL3* was able to complement growth on the medium containing DMA but not on medium with $FeCl_3$ alone, suggesting that AtYSL3 is able to transport Fe-PS complexes. To demonstrate that growth is dependent on *AtYSL3* expression, BE was withheld from the medium, and no growth was observed (Figure 3.4B).

To confirm that the growth on Fe(III)-Ps medium was not from the residual

Figure 3.4: Functional complementation of *fet3fet4* yeast. DEY1453-derived yeast strains transformed with pGEV-TRP and constructs expressing YSL1, YSL3, or the empty pYES6/CT vector were grown on synthetic defined medium containing variable conditions for iron (Fe(II) or Fe(III)), chelator (DMA or NA), and beta-estradiol (BE). Pairs of spots correspond to 10-fold and 100-fold dilutions of the original cultures. This yeast complementation assay was performed by Jeff Chiecko.

(A) Results using Fe(II) and NA. Each plate contained the constituents indicated, as the following concentrations: 50 µM iron citrate, 3uM Fe(II)SO_4, 8 µM NA, 10 nM BE.

(B) Results using Fe(III) and PS. Each plate contained the constituents indicated, as the following concentrations: 50 µM iron citrate, 10uM Fe(III)Cl_3, 10uM DMA, 40nM BE. In addition, the Fe(II) chelator, BPDS, was added to some plates, as indicated.

(C) Results using Fe(III) and NA. Each plate contained the constituents indicated, as the following concentrations: 50 µM iron citrate, 10 µM Fe(III)Cl_3, 15 µM NA, 40nM BE.

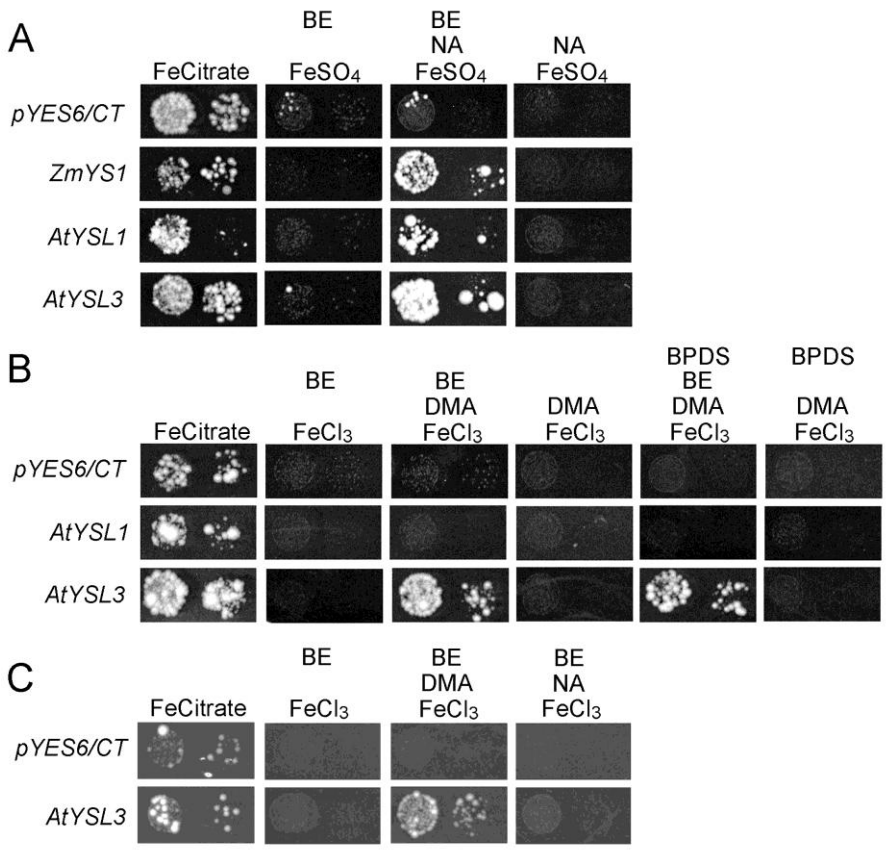
A
FeCitrate
BE
FeSO4
BE
NA
FeSO4
NA
FeSO4
pYES6/CT
ZmYS1
AtYSL1
AtYSL3
B
FeCitrate
BE
FeCl3
BE
DMA
FeCl3
DMA
FeCl3
BPDS
BE
DMA
FeCl3
BPDS
DMA
FeCl3
pYES6/CT
AtYSL1
AtYSL3
C
FeCitrate
BE
FeCl3
BE
DMA
FeCl3
BE
NA
FeCl3
pYES6/CT
AtYSL3

Fe(II) in the medium, the strong Fe(II) chelator 4,7-biphenyl-1,10-phenanthroline-disulfonic acid (BPDS) was used to remove any Fe(II). Functional complementation on Fe(III)-PS still occurred in the presence of BPDS, indicating that YSL3 transports Fe(III) (Figure 3.4B). The ability of AtYSL3 to use Fe(III)-PS as a substrate could imply that the substrate of AtYSL3 *in vivo* is Fe(III)-NA, since PS and NA share very high structural similarity. To test this, strains were grown on medium that contained 10 µM $FeCl_3$ with or without 15 µM NA (Figure 3.4C) in the presence of the inducer BE, and *AtYSL3* did not restore growth on Fe(III)-NA medium.

3.3.2 Localization of YSL1 and YSL3 proteins:

We have hypothesized that YSL1 and YSL3 are plasma membrane bound proteins responsible for distribution of Fe-NA complexes in Arabidopsis. To localize the expression of YSL1 and YSL3 protein precisely, the *YSL1* and *YSL3* genes were fused to GFP for sub-cellular localization. Both YSL1 and YSL3 are predicted to be plasma membrane proteins, and their activity in yeast (Figure 3.4) also reveals their role as plasma membrane transporters. For *YSL1*, *YSL1* cDNA was fused to GFP at the carboxyl terminus under the control of 35S promoter (*35S::YSL1::GFP*), and then transiently transformed into onion epidermal cells using microprojectile bombardment. A construct

containing soluble GFP under a 35S promoter was also included as a control (*35S-smGFP*; Figure 3.5D-F). The fluorescence signal of the *YSL1-GFP* fusion protein was observed at the periphery of the cell (Figure 3.5A-C), and no signal deviation around the nucleus was observed, indicating that YSL1 is localized to plasma membrane. For YSL3 localization, the whole gene was fused to GFP at the C-terminus (*YSL3-GFP*), and then stably transformed into *ys1ysl3* double mutants. Transgenic plants were screened by their green, rescued phenotype. The tonoplast localized protein TIP1 (Tonoplast Intrinsic Protein 1) was also included as a control to visualize tonoplast localization. The fluorescence signal from YSL3::GFP protein was observed in the periphery of cells of the vascular tissue of roots (Figure 3.5G-I). By contrast, the TIP1::GFP signal deviates around the nucleus (Figure 3.5J-L, yellow arrow) as expected and such deviation away from the cell periphery was never observed in plants transformed with YSL3::GFP. Thus, the *YSL3* gene is located in the plasma membrane. The GFP signal for YSL3 was observed almost exclusively in the lateral plasma membrane of the root but rarely at the apical or basal ends. This pattern is similar to that of YSL2 (Didonato *et al*, 2004) and is consistent with a role in the lateral movement of metals within vascular tissues.

Figure 3.5: Localization of YSL1 and YSL3 using GFP. (A-F) Localization in onion epidermal cells using microprojectile bombardment. (G-L) Localization in stably transformed Arabidopsis.

(A) Fluorescence image of an onion cell bombarded with *35S-YSL1-GFP* construct. (B) DIC image of the onion cell shown in (A). (C) Overlay of images shown in (A) and (B). (D) Fluorescence image of an onion cell bombarded with *35S-smGFP* construct. (E) DIC image of the onion cell shown in (D). (F) Overlay of images shown in (D) and (E). (G) Fluorescence image of the root of a plant stably transformed with the*YSL3-GFP* construct. (H) DIC image of the root shown in (G). (I) Overlay of images shown in (G) and (H). (J) Fluorescence image of the root of a plant stably transformed with a *35S-TIP* construct. Arrows indicate positions where the fluorescence signal deviates around nuclei. (K) DIC image of the root shown in (J). (L) Overlay of images shown in (J) and (K).

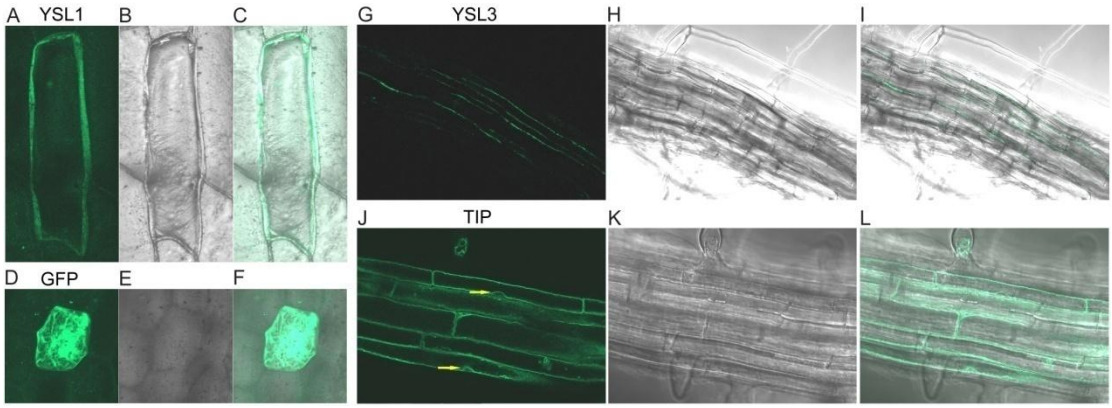
A YSL1
B
C
G YSL3
H
I
D GFP
E
F
J TIP
K
L

3.3.3 Over-expression of YSL3:

Over-expression has been an important tool for determination of the function of a gene. I attempted to increase the expression of *YSL3* to observe the direct impact to plants. For overexpression, the *YSL3* gene was cloned into pMN20, vector with 4 copies of the CaMV 35S enhancer. This construct is expected to enhance expression of *YSL3* without inducing ectopic expression (Weigel *et al*.,2000; Tian *et al*, 2004; Mora-García et al, 2004). The construct was stably transformed into wild type Arabidopsis plants and homozygous transformants were obtained by gentamycin selection. Three lines of homozygous transformants, YSL3 OX 5.8, 7.1, and 13.2, were generated, and RT-PCR results demonstrated that the mRNA level of *YSL3* was increased by 2.7, 1.6, and 2.4 fold respectively in the leaves of transgenic lines (Figure 3.6A). Line YSL3 OX 5.8 also showed increased expression of *YSL3* in the flowers and flower buds, whereas the other two lines had normal mRNA levels (Figure 3.6B and C). In the cauline leaves, normal mRNA levels were detected in all three lines (Figure 3.6D).

No morphological phenotype was observed for any line, so ICP-MS determination of metal content was performed on leaves and seeds of these plants. In the leaves, Cu levels were increased in all three lines

Figure 3.6: *YSL3* enhanced expression lines YSL3 OX L5.8, YSL3 OX L7.1, and YSL3 OX L13.2. Each line contains a 4X35S enhancer sequence upstream of a YSL3 genomic clone containing 1487 bp of native sequence upstream of the initiating ATG.

(A)-(D) Expression of *YSL3* by semi-quantitative (relative quantification) RT-PCR. *Actin2* was included as a control for template quantity. Lane1: Col0. Lane2: YSL3 OX L5.8. Lane3: YSL3 OX L7.1. Lane4: YSL3 OX L13.2. (A) In leaves. (B) In flowers. (C) In flower buds. (D) In cauline leaves. (E) ICP-MS determination of Mn, Fe, Cu, and Zn concentrations of leaves from 20 day old soil-grown plants. Results are given as ppm. Error bars represent standard error. Each sample contains 10 replicates. Asterisks indicate $P < 0.05$ by T-test. (F) ICP-MS determination of Mn, Fe, Cu, and Zn concentrations of seeds. Results are given as ppm. Error bars represent standard error. Each sample contains 10 replicates. Asterisks indicate $P < 0.05$ by T-test.

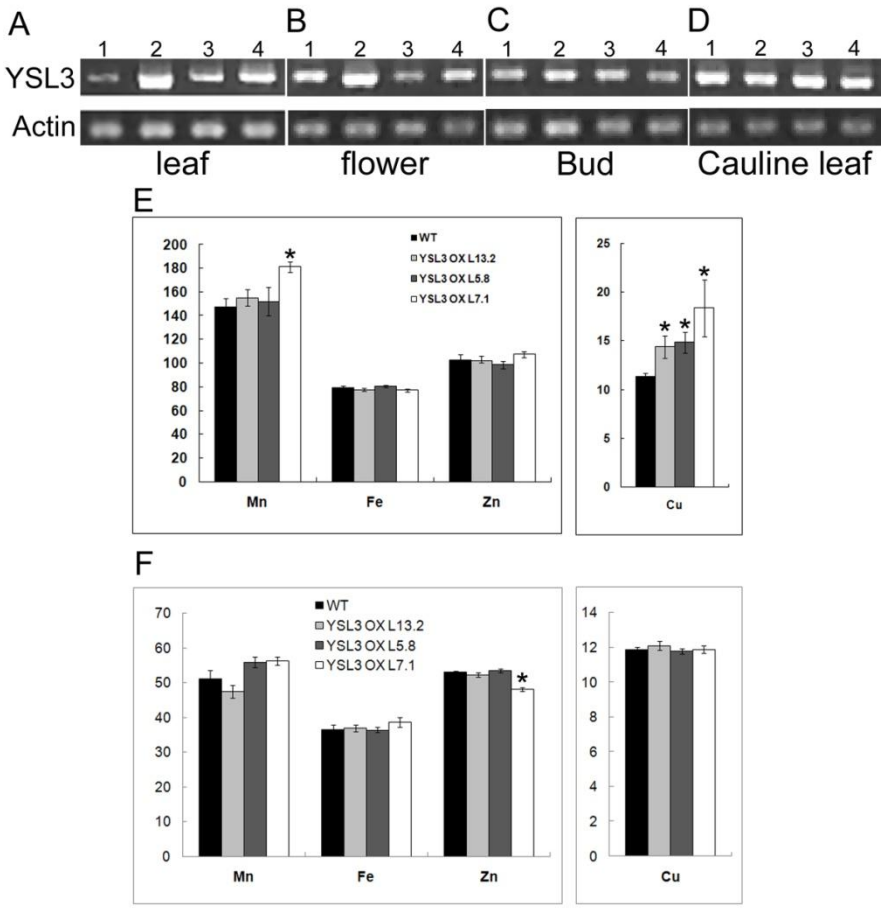
A
B
C
D
1 2 3 4 1 2 3 4 1 2 3 4 1 2 3 4
YSL3
Actin
leaf
flower
Bud
Cauline leaf
E
WT
YSL3 OX L13.2
YSL3 OX L5.8
YSL3 OX L7.1
Mn
Fe
Zn
Cu
F
WT
YSL3 OX L13.2
YSL3 OX L5.8
YSL3 OX L7.1
Mn
Fe
Zn
Cu

(Figure 3.6E). The Fe and Zn levels were not changed in the over-expression lines. Increased levels of Mn were only observed in line 7.1. In the seeds, no metal levels were changed except for a decreased level of Zn in line 7.1 (Figure 3.6F). However, since the changes of Mn and Zn were only observed in a single line, and did not correlate with mRNA levels, their significance is not clear. The weak or non-existent over-expression demonstrated by RT-PCR for flowers, buds, and especially cauline leaves may explain the lack of clear changes in metal content in seeds.

Since over-expression of YSL3 appears to be strongest in vegetative tissues in these lines, I examined whether this strong expression contributes to resistance or sensitivity to iron deficiency stress. Seeds of Col-0 plants and the three transgenic lines were germinated on MS medium for 10 days and then transferred to MS medium that lacked Fe. The total chlorophyll level of the seedlings, which reflects the level of iron deficiency chlorosis, was measured at various time points. Line 5.8, which had the highest expression relative to control plants level for *YSL3* mRNA (Figure 3.6A), had significantly increased chlorophyll content from 18 to 24 days of iron starvation (Figure 3.7), thus demonstrating resistance to prolonged iron deficiency. The two other lines with weaker expression showed no significant differences from wild type

Col0 plants.

3.3.4 Complementation of *ysl1ysl3* double mutants by *YSL1* or *YSL2*:

The Arabidopsis YSL family members share high sequence similarity, and the whole YSL family can be divided into three well-conserved groups based on their sequence similarity. YSL1, YSL2, and YSL3 fall into the same group. These three YSLs share over 60 percent sequence identity and their expression patterns are quite similar to each other. *ysl1* single mutants exhibit only subtle phenotypes and both *ysl2* and *ysl3* single mutant exhibit no phenotype, whereas *ysl1ysl3* double mutant showed a severe phenotype. Lack of clear phenotypes in the single mutants suggests that these closely related members of the family may share overlapping biochemical functions and differ only in their expression patterns. The overt phenotype of the *ysl1ysl3* double mutant is an ideal tool to define the biochemical function of YSL1, YSL2, and YSL3. In the experiment, *YSL1* and *YSL2* cDNA were driven by the *YSL3* promoter and stably transformed into *ysl1ysl3* double mutants. If using *YSL1* or *YSL2* promoter, function of YSL3 could not be compared since we could not clone a YSL3 cDNA because of toxicity in *E. coli*. If YSL1 and YSL2 have highly similar or identical biochemical functions to YSL3, then the severe phenotypes of double mutant should be alleviated or

Figure 3.7: Iron starvation response in wild-type and *YSL3* enhanced expression lines YSL3 OX L5.8, YSL3 OX L7.1, and YSL3 OX L13.2. Plants were grown on MS plates for 10 days, then transferred to MS without iron for a period of 0-24 days. The total chlorophyll content of the shoot system was measured every two days. Error bars represent standard error. Each sample contains 4 replicates.

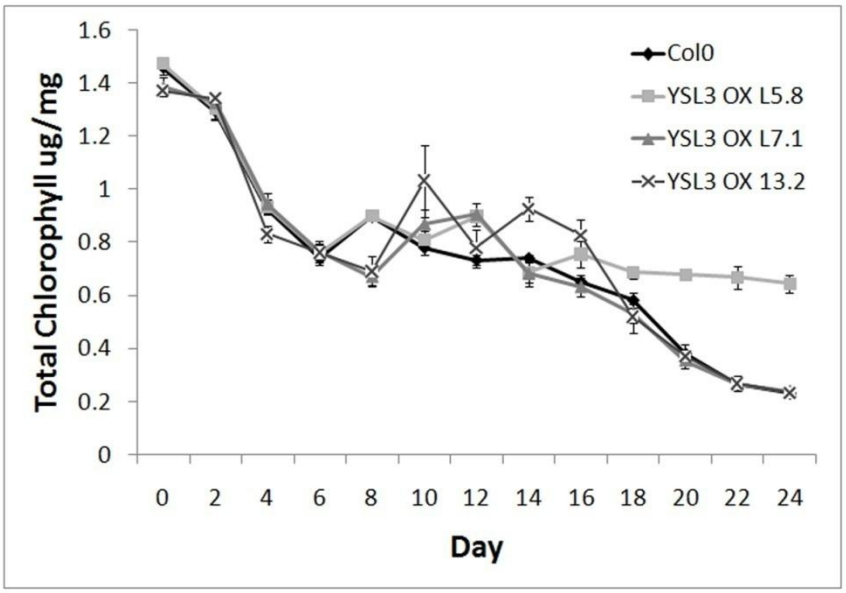
Total Chlorophyll ug/mg
1.6
1.4
1.2
1
0.8
0.6
0.4
0.2
0
0 2 4 6 8 10 12 14 16 18 20 22 24
Day
Col0
YSL3 OX L5.8
YSL3 OX L7.1
YSL3 OX 13.2

recovered. A *YSL3* whole gene fusion to GFP for localization studies was included as a positive control since this construct contains the same promoter as used in this experiment. Plants transformed with *YSL3p::YSL1* exhibited only a partially rescued phenotype. Chlorophyll levels of four transgenic lines (YSL3p::YSL1 L2, L3, L4, and L5) were significantly lower than those of WT, but significantly higher than those of the un-complemented double mutant (Figure 3.8A and B). The positive control, YSL3::GFP, did completely complement the chlorotic double mutant phenotype (Figure 3.8C). The seed number (as an indication of fertility) and seed weight (as an indication of seed development) of the four transgenic lines were similar to those of *ysl1ysl3* double mutant (Figure 3.8D and F), while both seed amount and seed weight are normal in *YSL3::GFP* complemented lines (Figure 3.8E and G). Thus, *YSL1* can only partially complement *YSL3* transport function *in planta*, suggesting that YSL1 and YSL3 are partially redundant at the level of protein function. In conclusion, *YSL1* and *YSL3* appear to have related but distinct functions *in planta*.

Similar to *YSL3p::YSL1* transgenic plants, plants transformed with *YSL3p::YSL2* also exhibited only a partially rescued phenotype. Chlorophyll levels of three transgenic lines (YSL3p::YSL2 L4, L7, and L9) were

Figure 3.8: Complementation of *ysl1ysl3* double mutants with *YSL1* and *YSL2*. *ysl1ysl3* double mutant plants were transformed with *YSL1* and *YSL2* cDNA driven by *YSL3* promoter (*YSL3p::YSL1* and *YSL3p::YSL2*). Four lines of *YSL3p::YSL1* (L2, L3, L4, and L5) and three lines of *YSL3::YSL2* were included (L4, L7, and L9). * indicates $P < 0.05$ by T-test. ** indicates $P < 0.01$ by T-test.

(A) 20 day old soil-grown Col0, *YSL3p::YSL1*, *YSL3p::YSL2*, and *ysl1ysl3* plants.

(B) Total chlorophyll concentration of leaves of *Col0*, *YSL3p::YSL1*, *YSL3p::YSL2*, and *ysl1ysl3* grown on soil for 20 days. Each sample represents 10 replicates.

(C) Total chlorophyll concentration of leaves of Col0, *YSL3-GFP*, and *ysl1ysl3* grown on soil for 20 days. Each sample contains 10 replicates.

(D) Average weight of an individual seed.

(E) Average weight of an individual seed.

(F) Average seed number per plant.

(G) Average seed number per plant.

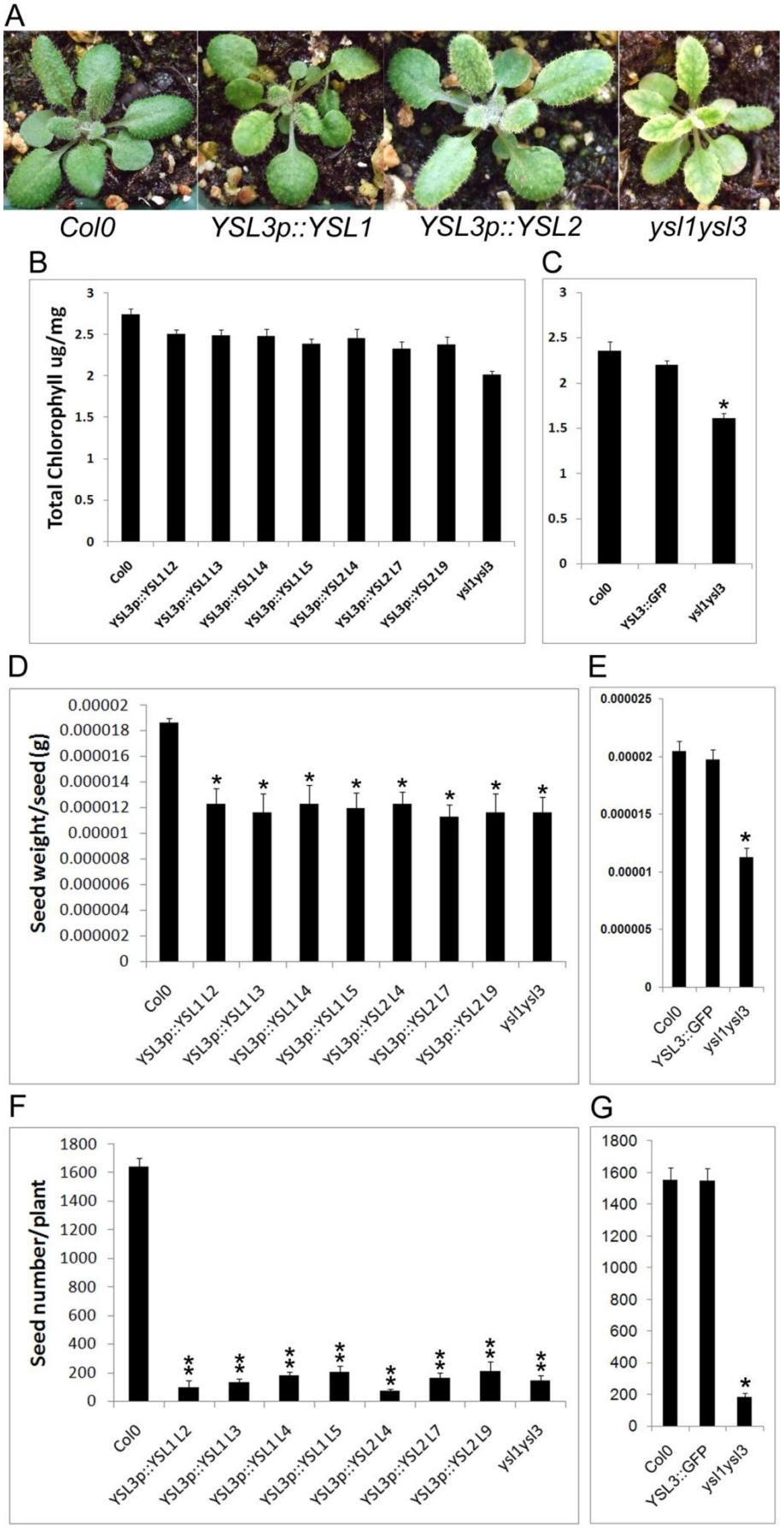
A
Col0
YSL3p::YSL1
YSL3p::YSL2
ysl1ysl3
B
Total Chlorophyll ug/mg
Col0
YSL3p::YSL1 L2
YSL3p::YSL1 L3
YSL3p::YSL1 L4
YSL3p::YSL1 L5
YSL3p::YSL2 L4
YSL3p::YSL2 L7
YSL3p::YSL2 L9
ysl1ysl3
C
Col0
YSL3::GFP
ysl1ysl3
D
Seed weight/seed (g)
E
F
Seed number/plant
G

significantly lower than those of WT, but significantly higher than those of the un-complemented *ysl1ysl3* double mutant (Figure 3.8A and B). The seed number and seed weight of the three transgenic lines were similar to those of *ysl1ysl3* double mutant (Figure 3.8D and F). Thus, *YSL2* can only partially complement *YSL3* transport function *in planta*, suggesting that YSL2 and YSL3 are partially redundant at the level of protein function. In conclusion, *YSL2* and *YSL3* appear to have related but distinct functions *in planta*.

3.4 Discussion:

Using the YSL3 construct I prepared, we showed the ability of AtYSL1 and AtYSL3 to take up iron using a yeast functional complementation assay (Figure 3.4). In this assay, by carefully controlling expression from a BE-inducible promoter, growth is dependent on expression of YSL protein. In addition, we showed that rescue of growth only occurs when both iron and chelator (NA or PS) are present in the growth medium. No complementation occurs when only an equal amount of iron but no chelator is present in the medium. This suggests that, in order to rescue growth, Fe-NA or Fe-PS complexes are required as substrates for the YSLs. As expected, AtYSL1 and AtYSL3 exhibited Fe(II)-NA transporter activity as AtYSL2. Strikingly, AtYSL3 can use Fe(III)-PS as substrates for transport (Figure 3.4C), since PS,

including DMA used in the assay, are not produced by Arabidopsis (Mori, S., 1999). Only grass species (*e.g.*, rice, maize, wheat, etc) produce PS, and so only these species would be expected to have YSLs that transport PS. One explanation is that AtYSL3 may possess the ability to transport Fe(III) bound to NA, since Fe(III)-NA complexes are expected to occur in all plants (von Wiren *et al*., 1999), including Arabidopsis. Because DMA shares high structural similarity to NA, it could substitute for NA to form a transportable complex. However, no complementation was observed when the assay was performed in medium containing Fe(III) and NA. This negative result can be attributed to a lack of Fe(III)-NA transport activity for AtYSL3, or to a problem with the assay conditions. For example, either unsuccessful Fe(III)-NA complexes formation, or unstable Fe(III)-NA complexes under the conditions in the medium could cause the assay to fail. Another explanation of the ability of YSL3 to transport Fe(III)-PS could be the amino acid substitution in the YSL3 construct used for this assay. The amino acid change from lysine to arginine may have altered the transport activity of the protein (Figure 3.3). However, this is unlikely to be the case since the altered amino acid not strongly conserved among YSL proteins, and known Fe(III)-PS transporters, ZmYS1, OsYSL15 (Figure 3.3), and HvYS1 (not shown) do not contain the R residue at this position. This

negative result of Fe(III)-NA transport assay leaves the question of Fe(III)-NA transport via AtYSL3 open. Thus, whether AtYSL3 can transport Fe(III)-NA in plants remains unclear.

Subcellular localization results showed that YSL1 and YSL3 are localized to the plasma membrane (Figure 3.5), consistent with their roles as Fe-NA transporters that allow cells to take up iron from apoplast. This is in agreement with our hypothesis that the role of YSL1 and YSL3 is to transport metal-NA complexes through vascular parenchyma cells into adjacent cells.

Over-expression of YSL3 increases the iron deficiency tolerance of plants (Figure 3.7), but does not cause any change in metal levels of seeds. The unaltered metal levels may be due to unchanged mRNA levels in the reproductive tissue (Figure 3.6B-D). The increased iron deficiency tolerance with unchanged levels of iron in leaves implies that elevated expression of YSL3 results in better iron utilization, rather than an increased capacity to take up or store iron.

Examination of the functional equivalency of Arabidopsis YSL1, YSL2, and YSL3 showed that YSL1 and YSL2, although they share high sequence similarity to YSL3, do not share completely redundant transport functions *in planta*. *ysl1ysl3* double mutant plants expressing YSL1 and YSL2 under

control of *YSL3* promoter only exhibited partial complementation in vegetative tissues, and exhibited no complementation in reproductive tissues (Figure 3.8). This result implies that the function of YSL3 is partially overlapping to the function YSL1 and YSL2 in vegetative structures, but distinct in reproductive organs.

CHAPTER 4

ROLES OF ARABIDOPSIS YSL1 AND YSL3 IN REPRODUCTION

4.1 Introduction:

In chapter 3, the functions of AtYSL1 and AtYSL3 in vegetative tissues were discussed, but AtYSL1 and AtYSL3 seem also to be important in reproductive tissues. In addition to vegetative defects, *ysl1ysl3* double mutant plants also exhibit reproductive defects such as low pollen viability (Figure 1.5 F and G), and defective seeds with arrested embryos (Waters *et al*, 2006), implying that YSL1 and YSL3 are necessary for proper pollen and seed development. Expression of AtYSL1 and AtYSL3 increases markedly during leaf senescence, a period in which many minerals are remobilized from leaves, presumably for delivery into developing inflorescences and seeds (Himelblau and Amasino, 2001). Direct measurements of metals in senescing and younger leaves demonstrated that *ysl1ysl3* double mutants failed to mobilize Cu and Zn from leaves, indicating that YSL1 and YSL3 are important for metal remobilization from senescing leaves (Waters *et al*, 2006).

Hence, we propose that, in addition to transporting metals into vascular

parenchyma cells for distribution away from veins into interveinal regions, YSL1 and YSL3 have an additional role in transport of metals away from interveinal regions toward the phloem in senescing leaves (Figure 4.1). Because YSL1 and YSL3 seem to play important roles in metal transport, we are particularly interested in understanding their physiological function in loading of metals into seeds.

In this chapter, the effect of Fe-EDDHA treatment of Col-0 and *ysl1ysl3* plants was examined, and foliar application of Fe was included to confirm that defects revealed in *ysl1ysl3* double mutant plants was due primarily to lack of iron. Perl's stain was performed to determine whether iron localization is normal in seeds of double mutants. Finally, grafting experiments were performed to determine whether YSL1 and YSL3 activity in leaves is necessary for successful reproduction of seeds.

4.2 Materials and methods:

The detailed materials and methods are described in Chapter 2. Sections Plant growth conditions (2.1), Mineral analysis by ICP-MS (2.3), Grafting (2.7), and Chlorophyll content determination (2.11) are relevant.

Figure 4.1: Working model of YSL1 and YSL3 in vegetative leaf and during leaf senescence.

(A) Vegetative growth: YSL1 and YSL3 take up metal ions that arrive via xylem. This uptake occurs mostly in the xylem parenchyma. Once inside the cells, iron moves through the symplast or is effluxed elsewhere.

(B) YSL1 and YSL3 take up metal ions that have been released from leaf cells. This uptake occurs mostly in the vascular parenchyma. Once inside the cells, iron moves through the symplast or is effluxed elsewhere prior to loading into phloem.

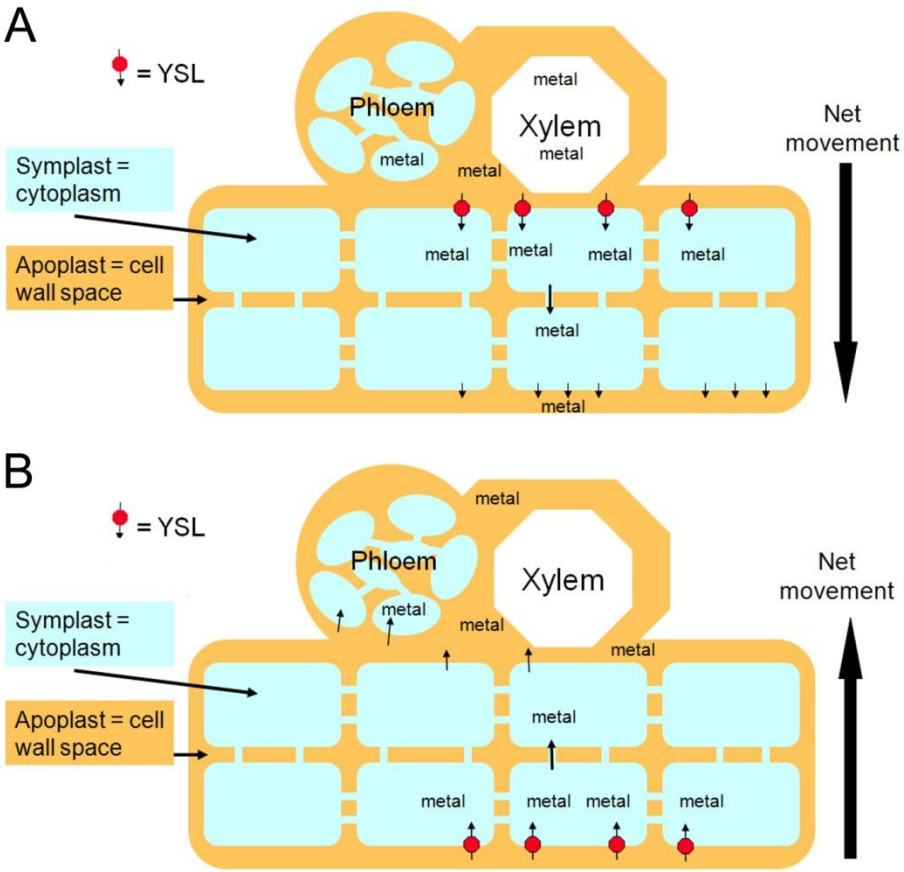
A
= YSL
Phloem
Xylem
metal
Net movement
Symplast = cytoplasm
Apoplast = cell wall space
B
= YSL
Phloem
Xylem
Net movement
Symplast = cytoplasm
Apoplast = cell wall space

4.3 Results:

4.3.1 Mineral homeostasis and fertility are partially rescued by Fe-EDDHA treatment:

In a previous study, *ysl1ysl3* double mutants exhibited altered levels of Mn, Fe, Zn, and Cu, yet Fe-EDDHA treatment reversed the chlorotic phenotype. Could Fe-EDDHA treatment cause metals other than Fe to change in the plants? In order to determine how Fe-EDDHA treatment affects the metal content of leaves and seeds, the metal concentrations in these organs were measured by ICP-MS. Double mutant plants had high leaf concentrations of Mn, Zn, and especially Cu (Figure 4.2). In this experiment, the concentration of iron was not significantly different from normal in leaves, but all experiments have shown consistent small (~10%) decreases in Fe concentration in leaves, which is often statistically significant. Subirrigation with Fe-EDDHA caused the concentration of Mn and Zn to decrease, while the concentration of Cu and Fe increased. With Fe(III)-EDDHA treatment, *ysl1ysl3* and Col-0 leaves had similar Mn, Fe, and Zn concentrations. Fe(III)-EDDHA treatment had no effect on the Cu levels of Col-0 shoots, but resulted in even greater Cu concentrations in *ysl1ysl3* leaves. Thus, treatment with this chelated form of iron caused unanticipated changes in the levels of several metals.

Figure 4.2: ICP-MS determination of Mn, Fe, Cu, and Zn concentrations in *ysl1ysl3* and Col0 leaves receiving treatment with Fe-EDDHA or water. Results are given as ppm. Error bar represents standard deviation. Each sample contains 10 replicates.

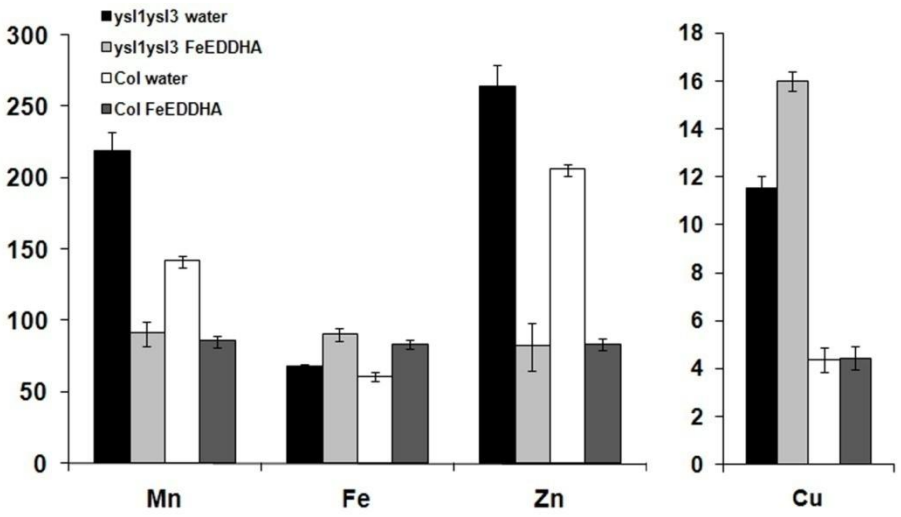
ysl1ysl3 water
ysl1ysl3 FeEDDHA
Col water
Col FeEDDHA
300
250
200
150
100
50
0
18
16
14
12
10
8
6
4
2
0
Mn
Fe
Zn
Cu

Use of the strong iron chelate solution, Fe-EDDHA, results in changes in 3/4 of the affected metals, calling into question whether the chlorotic phenotype of the double mutant is simply the result of iron deficiency, or instead is caused by a more complex imbalance in the levels of transition metals. Thus, we sprayed the plants with ferric ammonium citrate, an un-chelated form of iron. The *irt1* mutant, defective in primary iron uptake from soil, can be rescued by soil amendment (Vert et al, 2002). *irt1* mutant plants were included as a control to ensure that foliar application is effective in treating iron deficiency in Arabidopsis. The chlorophyll content of *irt1-1* mutants and *ysl1ysl3* double mutants increased significantly after application of iron ammonium citrate to the leaves. Control plants that were treated with ammonium-citrate (Figure 4.3) remained chlorotic, indicating that the chlorosis was caused by Fe deficiency. The effect of iron application on seed set in the double mutant plants was also examined. While both foliar application of iron (Figure 4.4 A) and subirrigation with Fe-EDDHA (Figure 4.4 B) resulted in increased seed production by the double mutants, the Fe-EDDHA treatment was much more effective: the number of seeds from the double mutant plants was only 13% that of WT after foliar spraying, while the number of seeds from double mutants treated with Fe-EDDHA was 57% of the normal seed number.

Figure 4.3: Total chlorophyll concentration of shoot system of wild-type, *irt1-1*, and *ysl1ysl3* plants receiving foliar application of ferric ammonium citrate or ammonium citrate (negative control). Plants homozygous for a mutation in *IRT1* (the main site of root iron uptake) were used as a control to ensure that Arabidopsis plants can use foliar applied iron. Error bar represents standard deviation. Each sample contains 3 replicates.

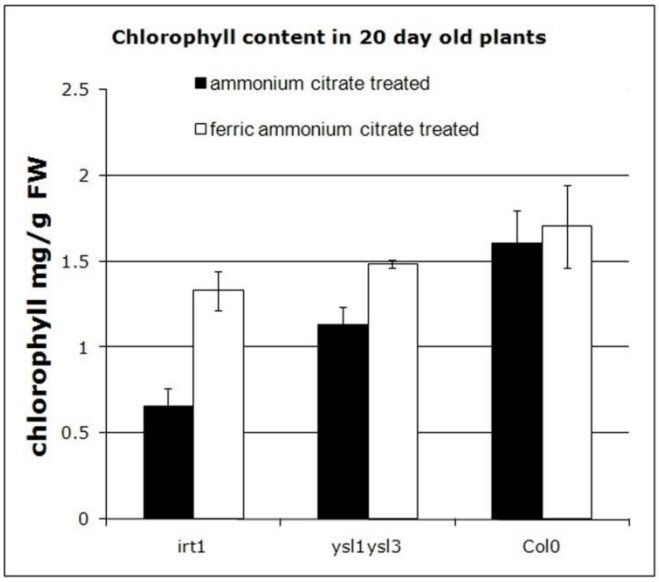
Chlorophyll content in 20 day old plants
ammonium citrate treated
ferric ammonium citrate treated
chlorophyll mg/g FW
2.5
2
1.5
1
0.5
0
irt1
ysl1ysl3
Col0

Figure 4.4: Response of seed production of wild-type, *irt1-1*, and *ysl1ysl3* plants to alternative methods of iron supplement. Error bars represent standard deviation.

(A) Seed production by plants receiving foliar treatment of ferric ammonium citrate or ammonium citrate (negative control).

(B) Seed production by plants receiving subirrigation treatment of Fe-EDDHA or water.

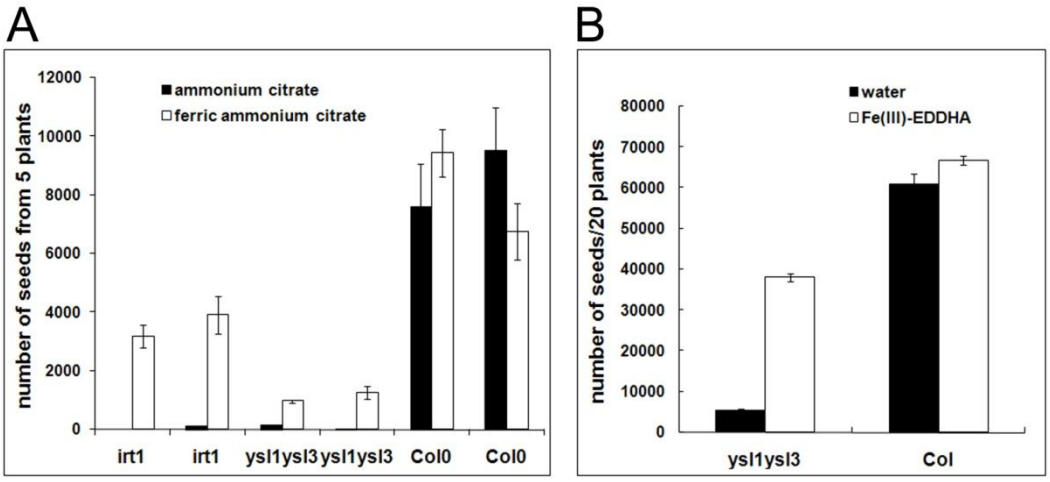
A
number of seeds from 5 plants
12000
10000
8000
6000
4000
2000
0
ammonium citrate
ferric ammonium citrate
irt1
irt1
ysl1ysl3
ysl1ysl3
Col0
Col0
B
number of seeds/20 plants
80000
70000
60000
50000
40000
30000
20000
10000
0
water
Fe(III)-EDDHA
ysl1ysl3
Col

Thus, treatment with both Fe-EDDHA and Fe-Citrate was able to at least partially restore the seed development defect, but Fe-EDDHA was much more effective. I also examined whether Fe-EDDHA treatment affects seed viability. Seeds from treated *ysl1ysl3* plants had much higher germination rates, both on soil (89% percent germination) and MS agar plates (92% percent germination), than the seeds from untreated plants (33% on soil; 74% on MS agar plates) (Table 4.1). In conclusion, treatment with Fe-EDDHA restored the seed viability defect of *ysl1ysl3* double mutant (Figure 4.4 and Table 4.1).

To understand the underlying cause of the change in seed viability, I measured the metal levels of seeds (Figure 4.5). Seeds of the double mutants had diminished levels of Fe, Zn, and Cu, suggesting that *YSL1* and *YSL3* are necessary for proper loading of these minerals into seeds. Treatment with Fe-EDDHA increased both Fe and Cu levels but decreased levels of Mn and Zn in seeds of both *ysl1ysl3* double mutants and WT. Notably, the Fe(III)-EDDHA treatment caused the level of seed Fe to rise to the same level as contained in Col-0 plants but did not raise Zn and Cu levels, yet the Fe(III)-EDDHA treatment did recover seed viability (Figure 4.5 and Table 4.1). Thus, we conclude that the seed defects resulted mainly from lack of Fe, not the lack of Cu, Zn, or Mn.

Table 4.1: Germination rate of Fe-EDDHA and water treated *ysl1ysl3* double mutant. Germination was scored as successful emergence of the hypocotyls and cotyledons. For each sample, three sets of 100 seeds were included in the experiment.

	Fe-EDDHA	water
Soil	89%±4.36	33%±7.00
MS agar	92%±5.29	74%±7.81

Figure 4.5: ICP-MS determination of Mn, Fe, Cu, and Zn concentrations in *ysl1ysl3* and Col0 seeds receiving treatment with Fe-EDDHA or water. Results are given as ppm. Error bar represents standard deviation. Each sample contains 4 replicates.

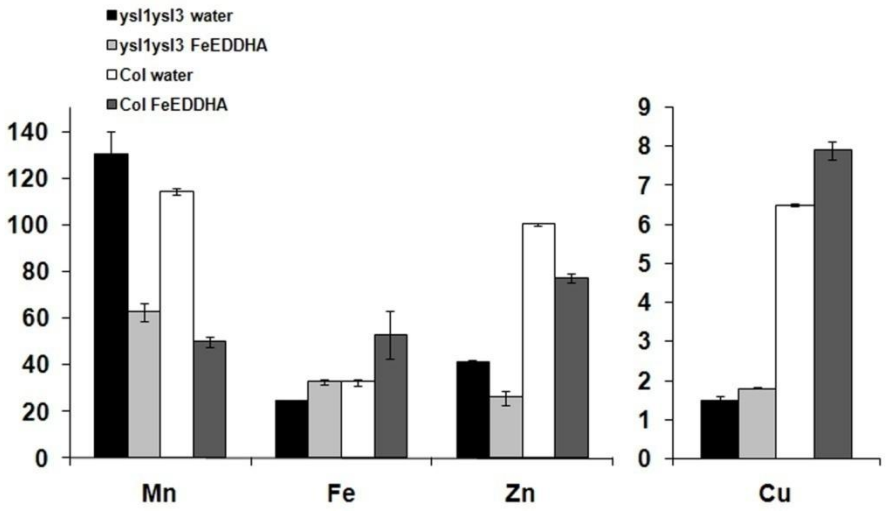
ysl1ysl3 water
ysl1ysl3 FeEDDHA
Col water
Col FeEDDHA
140
120
100
80
60
40
20
0
9
8
7
6
5
4
3
2
1
0
Mn
Fe
Zn
Cu

4.3.2 *ysl1ysl3* double mutant seeds retain correct iron localization:

We have previously shown that the seeds produced by *ysl1ysl3* double mutants are low in Fe, Zn, and Cu (Waters et al., 2006). To determine whether iron is localized normally in these seeds, I further examined the iron content in *ysl1-2*, *ysl3-1*, and *ysl1ysl3* mutant seeds by Perl's stain for Fe(III) (Figure 4.6). Using this method, Fe(III) is released from tissue deposits by treatment with dilute hydrochloric acid, and then reacts with potassium ferrocyanide to produce an insoluble blue compound, potassium ferric ferrocyanide (Prussian blue). Ferrous ions do not participate in the reaction, but since measures are not taken to prevent oxidation of Fe(II) to Fe(III) during the staining, both Fe(III) and Fe(II) may ultimately contribute to staining. In Arabidopsis seeds, iron is most concentrated in the vasculature of the embryo's cotyledons (Kim et al., 2006), and Perl's stain reveals this pattern (Figure 4.6A). *ysl1-2* and *ysl3-1* have a staining intensity similar to WT seeds, which indicated normal levels of iron, and are consistent with our previous metal measurement results. These single mutants also have correct iron localization (Figure 4.6B and C). Seeds of *ysl1ysl3* double mutants showed no staining at all even after four hours of staining, while seeds of *ysl1ysl3* double mutants treated with Fe-EDDHA do show staining, albeit after longer

Figure 4.6: Perl's staining of seeds. Seeds were cut in half and then stained with Perl's stain solution for 15 min except (D) and (F).

(A) Wild-type. (B) *ysl1-2*. (C) *ysl3-1*. (D) *ysl1ysl3* stained for 4 hours. (E) Seed from a *ysl1ysl3* plant that was supplemented with Fe-EDDHA. (F) Seed from a *ysl1ysl3* plant that was supplemented with Fe-EDDHA stained for 4 hours.

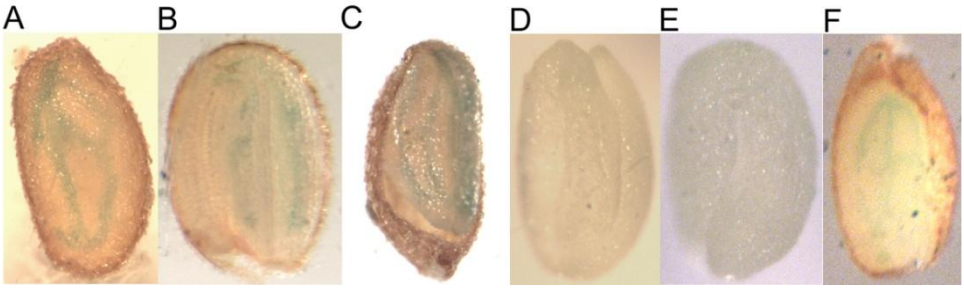
A
B
C
D
E
F

times (Figure 4.6D-F). The staining pattern of the double mutant seeds indicates that iron levels are reduced but iron localization is correct: iron is located in the vascular bundles of the cotyledons. Thus, loss of function of YSL1 and YSL3 results in low iron levels but does not affect iron localization in seeds.

4.3.3 *YSL1* and *YSL3* are necessary for loading metals into seeds:

Since previous data suggested that *YSL1* and *YSL3* are necessary for proper loading of Fe, Zn, and Cu into seeds, I sought to determine where *YSL1* and *YSL3* act to affect this process. To accomplish this, I performed inflorescence-grafting experiments. In these experiments, I grafted young (~3-7 cm) primary inflorescence stems (scion) of *ysl1ysl3* double mutant plants onto WT rosettes (stock), and then allowed flowering and seed set to proceed. If *YSL1* and *YSL3* are required in the vegetative tissues for proper metal levels in the seeds, the reproductive defects of *ysl1ysl3* double mutants should be rescued by grafting so that the seed development would be normal. On the other hand, if *YSL1* and *YSL3* are important in flowers or developing seeds, the *ysl1ysl3* scion would still produce defective pollen and/or seeds. As a control, self-grafts of WT plants were also made. I attempted to perform self-grafts of the *ysl1ysl3* double mutants, but was not able to obtain viable

grafts. Therefore, comparative data obtained from un-grafted *ysl1ysl3* double mutant plants is presented.

Using reciprocal crossing, failure of seed set in ysl1ysl3 double mutants has been demonstrated to be causing by defective pollen. Thus, in this experiment, seed set was used as an indication of pollen function. Seed set, seed weight, and metal content of the seeds were measured. The seed number and observation of anthers showed that grafting rescued the pollen defect of the scion (Figure 4.7A). Moreover, seed weight was also corrected by grafting (Figure 4.7B), suggesting that *YSL1* and *YSL3* function are necessary in the rosettes (stems/leaves/roots) for normal development of pollen and seeds. Furthermore, metal content measurement was performed to examine whether the grafting also recovered metal balance in seeds. As a control, un-grafted WT was also included in the measurement to observe whether metal levels were affected by grafting.

Measurements of the concentrations of Fe, Zn and Cu (Figure 4.7C) showed no significant difference between *ysl1ysl3* scion-grafted WT and un-grafted *ysl1ysl3* double mutant seeds. The Fe, Cu, and Zn levels of seeds produced by *ysl1ysl3* grafts were all significantly lower than the levels in WT self-graft. These results indicate that YSL1 and YSL3 are required in the

Figure 4.7: Inflorescence grafting experiment. *ysl1ysl3* double mutant scions (inflorescences) grafted onto WT stocks are labeled as *ysl1ysl3*+WT. WT+WT indicates wild type plants that were self-grafted as positive controls. *ysl1ysl3* double mutant was used as negative control since it was not possible to generate self-grafted *ysl1ysl3* plants. Un-grafted WT was included in metal measurement experiments as a positive control. Error bars represent standard deviation. Asterisks indicate $P < 0.05$ by T-test. WT+WT and *ysl1ysl3* contain 4 replicates. *ysl1ysl3*+WT contains 6 replicates. WT contains 10 replicates.

(A) Average seed number per silique. Each silique on the grafted inflorescences was opened and the seed number was counted.

(B) Average weight of an individual seed produced by the grafted inflorescences.

(C) Metal concentration of seeds of grafted plants. Metal content of the seeds produced by grafted inflorescences was determined using ICP-MS.

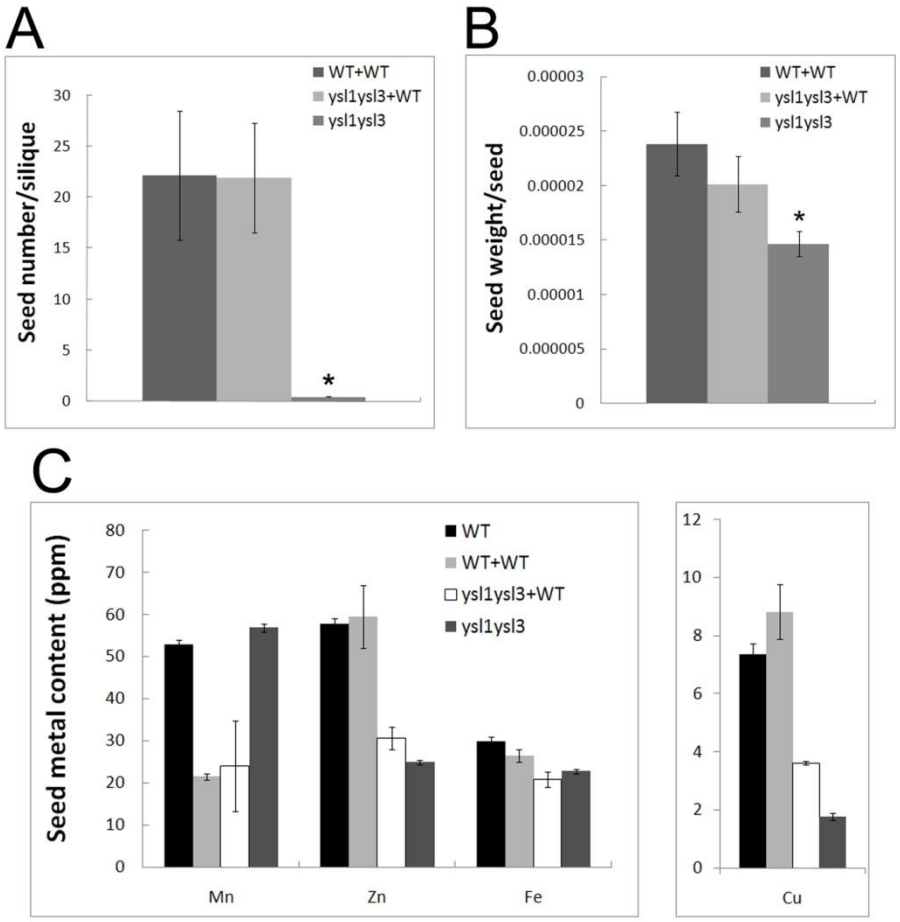
A
WT+WT
ysl1ysl3+WT
ysl1ysl3
Seed number/silique
30
25
20
15
10
5
0
*
B
WT+WT
ysl1ysl3+WT
ysl1ysl3
Seed weight/seed
0.00003
0.000025
0.00002
0.000015
0.00001
0.000005
0
*
C
WT
WT+WT
ysl1ysl3+WT
ysl1ysl3
Seed metal content (ppm)
80
70
60
50
40
30
20
10
0
Mn
Zn
Fe
12
10
8
6
4
2
0
Cu

grafted portion (inflorescence stems, flowers, or developing fruits and seeds) in order for the seeds to accumulate correct metal levels at maturity. The Fe, Cu, and Zn levels of seeds produced by double mutants were significantly different from un-grafted WT levels, consistent with previous results (Figure 4.5; Waters *et al*, 2006). The Mn levels of seeds produced by un-grafted WT were significantly higher than that of WT self-grafts indicating that grafting itself alters loading of Mn into seeds. The Mn levels in the seeds of *ysl1ysl3* grafts and WT self-grafts were similar, but are both significantly lower than that of both un-grafted WT and double mutants. Thus, grafting caused substantially diminished levels Mn in the seeds.

4.4 Discussion:

Together, the Fe-EDDHA and ferric ammonium citrate experiment show that, even though treatment with Fe-EDDHA causes changes in multiple metals, the reversal of chlorosis results only from increased iron, not from changes in the levels of other metals (Figure 4.2 and 4.3). Two reasons may be able to explain why Fe-EDDHA treatment decreased the levels of Zn and Mn in leaves. The first is that uptake or translocation of Zn and Mn was affected by EDDHA. Treatment with EDDHA only can address this issue. However, this experiment is currently not possible because Na-EDDHA has

not been commercially available for several years. The second is that the IRT1 Fe transporter, which takes up not only Fe but also Zn and Mn, is down-regulated when plants are treated with high levels of bioavailable iron. Thus, Fe abundant plants reduced uptake of Zn and Mn. This is consistent with a previous report that plants experiencing Fe deficiency typically contain high levels of Zn and Mn (Lahner et al., 2003).

Treatment with Fe-EDDHA restored the seed viability defect of *ysl1ysl3* double mutant (Figure 4.4 and Table 4.1). Furthermore, the metal levels of seeds are the cause of the change in seed viability. Treatment with Fe-EDDHA increased both Fe and Cu levels but decreased levels of Mn and Zn in seeds of both *ysl1ysl3* double mutants and WT. Notably, the Fe(III)-EDDHA treatment caused the level of seed Fe to raise to the same level as contained in Col-0 plants (Figure 4.5). Because Fe-EDDHA treatment did not raise Zn and Cu levels, yet did improve seed viability (Figure 4.4 and Table 4.1), we hypothesize that the seed viability defect of the double mutant is due primarily to a lack of iron.

We have shown that the seeds produced by *ysl1ysl3* double mutants are low in Fe, Zn, and Cu (Waters et al., 2006). Here, I further show that seeds of *ysl1ysl3* double mutant retain correct iron localization using Perl's stain. Thus,

loss of function of YSL1 and YSL3 results in low iron levels but does not affect iron localization in seeds.

Previous results suggested that *YSL1* and *YSL3* are important in senescing leaves for proper loading of Fe, Zn, and Cu from leaves into seeds. To determine where *YSL1* and *YSL3* act to affect this process, inflorescence grafting was used to show that *YSL1* and *YSL3* function are necessary in the rosettes (stems/leaves/roots) for normal development of pollen and seeds (Figure 4.7A and B). However, the fact that metal levels of *ysl1ysl3* grafts remained uncorrected showed that *YSL1* and *YSL3* are not only required in the rosettes. Instead, the metal measurement results suggested that YSL1 and YSL3 are also required in inflorescences for proper accumulation of metals in seeds (Figure 4.7C). Since YSL1 and YSL3 are poorly expressed in siliques and seeds, the presence of YSL1 and YSL3 in flowers, stems or cauline leaves is likely necessary for proper loading of metals into developing seeds. In conclusion, *YSL1* and *YSL3* do not only play a role in moving iron or other metals from leaves directly to seeds but also are needed within the flowers, stems or cauline leaves for correct metal accumulation in seeds.

The grafting experiment showed that recovery of expression of YSL1 and YSL3 in leaves restored seed weight and seed number defects of *ysl1ysl3*

double mutants, indicating that normal leaf expression of YSL1 and YSL3 is the key for normal seed weight and seed number. In chapter 3, *ysl1ysl3* double mutants complemented by *YSL1* and *YSL2* under control of *YSL3* promoter have partially restored chlorophyll level, indicating that function of *YSL3* in leaves was partially recovered. Thus, since normal expression of *YSL3* results in normal seed weight and seed number, these two traits were expected to be at least partially restored in the *ysl1ysl3* double mutants complemented by *YSL1* and *YSL2*. However, seed weight and seed number remain low in the complemented double mutant lines, implying two distinct YSL3 activities in leaves- one is needed during vegetative growth, and the other one is needed during reproduction/senescence.

CHAPTER 5

ROLES OF THE ARABIDOPSIS YSL4 AND YSL6 METAL TRANSPORTERS

5.1 Introduction:

The YSL family was identified based on sequence similarity to ZmYS1 and eight members were found in the Arabidopsis YSL family. The functions the three Arabidopsis family members most closely related to ZmYS1 (YSL1, YSL2, and YSL3) have been demonstrated previously (DiDonato *et al*., 2004; Le Jean et al., 2005; Waters *et al*., 2006; Chapter 3 and 4). The whole YSL family can be divided into three groups based on sequence similarity (Figure 1.3) and YSL4 and YSL6 belong to a distinct, well conserved group. AtYSL4 and AtYSL6 share 84 percent sequence identity and 92 percent similarity to each other. OsYSL6, belongs to the same sub-group (Figure 1.3), share 88 percent similarity to AtYSL4 and AtYSL6, suggesting that this is a really well conserved sub-group. The AtGenExpress microarray data available at www.arabidopsis.org was used to visualize the expression pattern of the AtYSL family in roots, rosettes, senescent leaves, flowers, and seeds. Based on these available microarray data, we conclude that *YSL1*, *YSL3*, and *YSL6*

are the most abundantly expressed members of the *AtYSL* family. Thus, *YSL6* is also of particular interest for functional analysis. However, YSL4 is not represented on the array, so its abundance cannot be determined. Since YSL4 has the highest similarity to YSL6, YSL4 is also particularly interesting.

Using yeast functional complementation, our lab has demonstrated that YSL4 and YSL6 can transport Fe(II)-NA (Figure1.4), implying that they have roles in the translocation of iron in Arabidopsis. In this chapter, *YSL4* and *YSL6* were shown to be highly expressed in both vegetative and reproductive tissues using RT-PCR and *YSL* promoter::GUS reporter constructs, implying that they may play an important role in Arabidopsis. YSL4 and YSL6 are localized to the plasma membrane, consistent with their roles as Fe-NA transporters. Loss of function of YSL4 and/or YSL6 resulted in altered metal levels. Over-expressing AtYSL6 resulted in a small increase in Zn in seeds. Moreover, YSL6 proteins under the control of the AtYSL3 promoter do not rescue the phenotypes of the *ysl1ysl3* double mutant, indicating a transport activity that is distinct from that of AtYSL1, AtYSL2, and AtYSL3.

5.2 Materials and methods:

The detailed materials and methods are described in Chapter 2. Sections Plant growth conditions (2.1), Molecular techniques (2.2), Mineral analysis by

ICP-MS (2.3), Agrobacterium mediated stable transformation (2.4), Perl's stain (2.5), GFP fusion and intercellular localization (2.8), Gus histochemical staining (2.9), Overexpression of YSLs (2.10), Chlorophyll content determination (2.11), and Complementation of *ysl1ysl3* double mutants (2.12) are of particular interest.

5.3 Results:

5.3.1 YSL4 and YSL6 are not iron regulated:

We have previously described that expression of *YSL1*, *YSL2*, and *YSL3* are stronger in above ground tissues than underground tissues and that expression of these genes is reduced in response to iron deficiency. To determine whether *YSL4* and *YLS6* are expressed in aboveground or underground parts and whether their mRNA levels change in response to iron deficiency, plants were grown on MS medium for 10 days and then transferred to MS and MS lacking iron for 5 days. RNA was extracted from shoots and roots and the expression levels of *YSL4* and *YSL6* were determined by semi-quantitative RT-PCR. Figure 5.1A and B shows that *YSL4* and *YSL6* are strongly expressed in both shoots and roots. Based on AtGenExpress microarray data available at www.arabidopsis.org, YSL4 mRNA was not detectable, indicating its presence at a low level, which is in conflict with the

Figure 5.1: Expression of *YSL4* and *YSL6* by semi-quantitative RT-PCR (A-D), and profile of *AtYSL* gene expression from AtGenExpress microarray in rosette leaves and senescing leaves of soil-grown plants (E and F). *AtYSL* genes not represented on the graphs were not detected. For (A) and (B), Col0 plants were grown on MS medium for 10 days and then transferred to MS or MS-Fe medium for 5 days. Actin was included as control. For (C) and (D), leaves were collected from Col0 plants grown on soil for 20 and 38 days. 18S rRNA was included as control.

(A) RT-PCR using RNA from shoots.

(B) RT-PCR using RNA from roots.

(C) RT-PCR using RNA from shoots.

(D) RT-PCR using RNA from shoots.

(E) Expression of *AtYSL*s in rosette leaves of mature soil-grown plants.

(F) Expression of *AtYSL*s in leaves of senescing soil-grown plants.

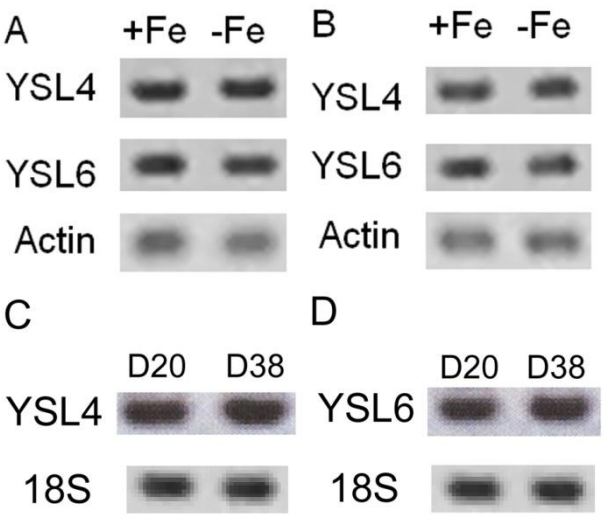
A
+Fe
-Fe
YSL4
YSL6
Actin
B
+Fe
-Fe
YSL4
YSL6
Actin
C
D20
D38
YSL4
18S
D
D20
D38
YSL6
18S

E

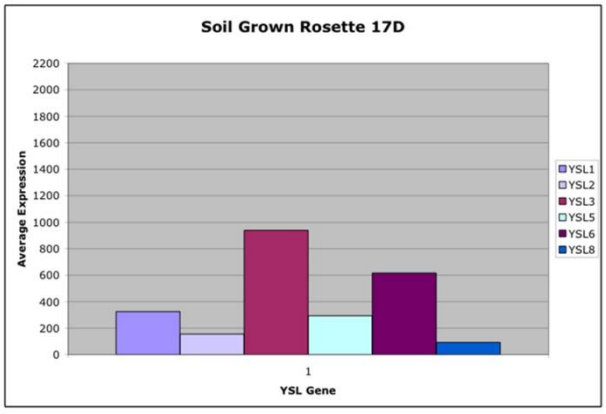
Soil Grown Rosette 17D
Average Expression
2200
2000
1800
1600
1400
1200
1000
800
600
400
200
0
1
YSL Gene
YSL1
YSL2
YSL3
YSL5
YSL6
YSL8

F

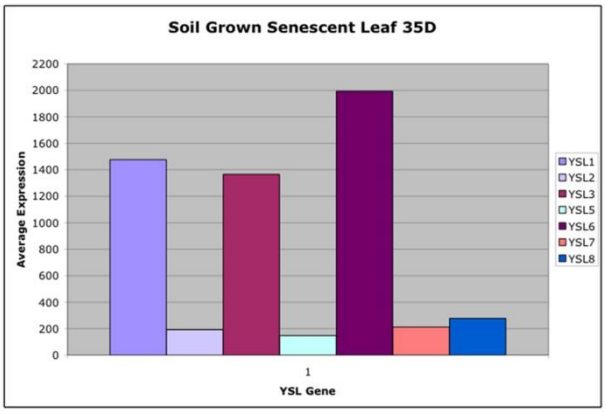
Soil Grown Senescent Leaf 35D
Average Expression
2200
2000
1800
1600
1400
1200
1000
800
600
400
200
0
1
YSL Gene
YSL1
YSL2
YSL3
YSL5
YSL6
YSL7
YSL8

RT-PCR results. The RT-PCR has been repeated for more than three times and the GUS histochemical analysis in section 5.3.2 also confirms that YSL4 is highly expressed in shoots and roots. Moreover, the expression levels of YSL4 and YSL6 are not regulated by iron deficiency (Figure 5.1A and B). This pattern of expression is markedly different from that of *YSL1*, *YSL2*, and *YSL3*, which are down-regulated under iron deficiency. Based on the AtGenExpress microarray data, expression of *YSL1*, *YSL3*, and *YSL6* all increase during leaf senescence (Figure 5.1E and F), and mRNA levels of *YSL1* and *YSL3* have been confirmed to increase during leaf senescence by RT-PCR and GUS histochemical staining (Waters *et al*, 2006). Thus, RT-PCR was performed to observe the expression of YSL4 and YSL6 during senescence. Figure 5.1C and D show that expression of both YSL4 and YSL6 are not increased during leaf senescence. This RT-PCR result of YSL6 is inconsistent with the microarray data, but again, the RT-PCR has been repeated three times. Thus, expression of *YSL6* is not increased during leaf senescence. Again, this pattern of expression is markedly different from that of *YSL1* and *YSL3*.

5.3.2 Expression pattern of YSL4 and YSL6:

To determine the tissue expression patterns of *YSL4* and *YSL6*, the promoter of each gene was fused to GUS and transformed into Col-0 plants. Plants were grown on MS medium or soil, and GUS activity was observed by histochemical staining in various tissues at different stages of the plant's life cycle. The expression patterns of *YSL4p::GUS* and *YSL6p::GUS* are quite similar to each other. *YSL4p::GUS* was strongly expressed in seeds, during germination, and in young seedlings (Figure 5.2A). In leaves, *YSL4p::GUS* was expressed generally in the whole leaf area in mature leaves (Figure 5.2E). This pattern is distinct from most of the *AtYSL* genes, which are most strongly expressed in the vasculature. In floral tissues, GUS staining was observed in the sepals (Figure 5.2C), pollen (Figure 5.2B), and siliques (Figure 5.2F). When siliques were opened, GUS staining was only observed in the valves but not in the vascular tissues inside (Figure 5.2G). In roots, GUS staining was observed mainly in vascular tissue, although staining can also be seen in other parts of the roots (Figure 5.2F).

YSL6p::GUS was also strongly expressed in seeds, during germination, and in young seedlings (Figure 5.3A and F). In leaves, *YSL6p::GUS* was strongly expressed in mature leaves (Figure 5.3B) in both vascular and intercostal regions. In floral tissues, GUS staining was observed in the

Figure 5.2: Histochemical staining of YSL4 promoter-GUS reporter plants. (A) Day 1 to day 7 of germination on MS medium. (B) Anther. (C) Flower. (D) Root and cross-section of root. (E) Mature leaf. (F) Silique. (G) An open silique.

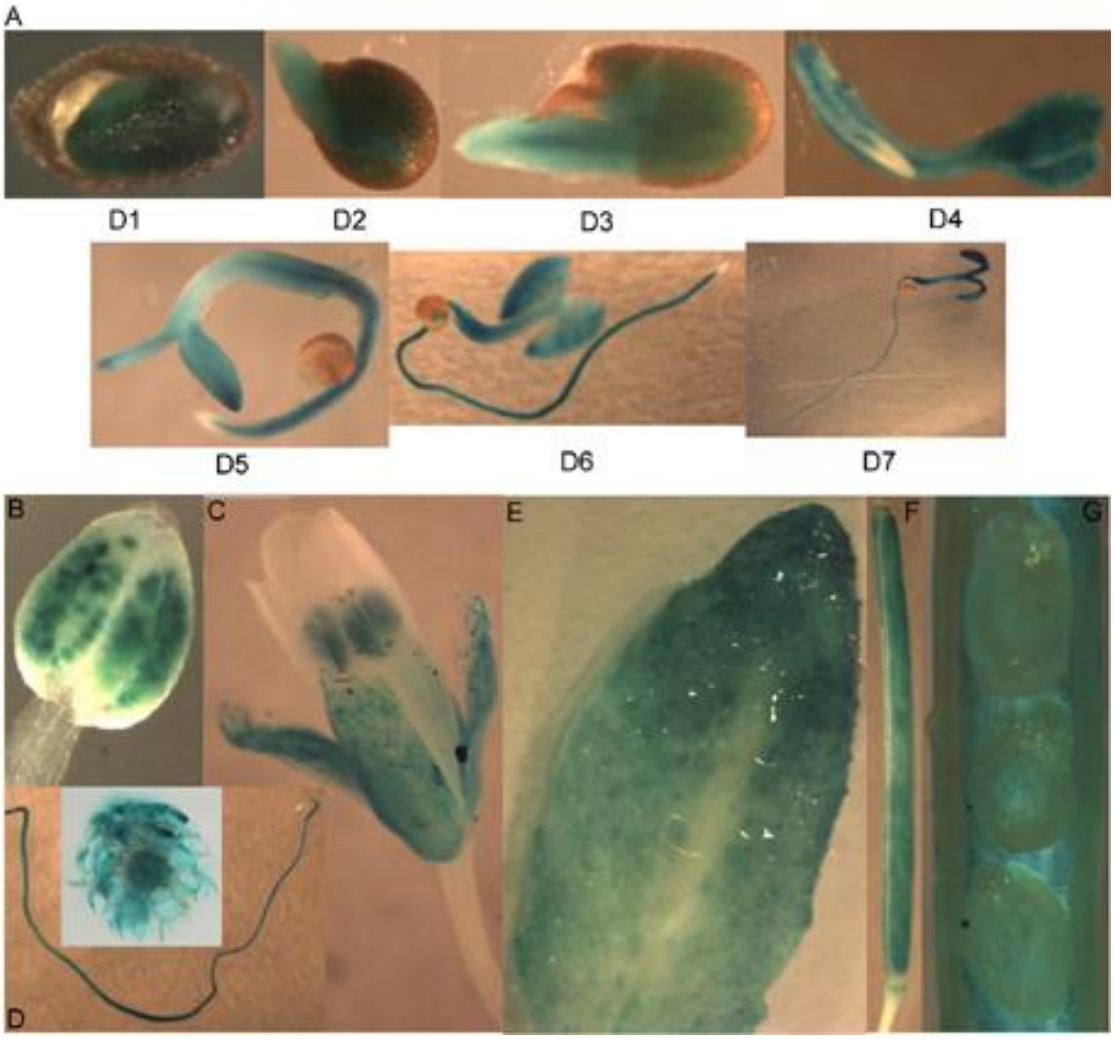
A
D1
D2
D3
D4
D5
D6
D7
B
C
D
E
F
G

Figure 5.3: Histochemical staining of YSL6 promoter-GUS reporter plants. (A) Day 1 to day 7 of germination on MS medium. (B) Root and crossection of root. (C) Rosette leaf. (D) Seeds and funiculi of an open silique. (E) Flower. (F) Young seedling.

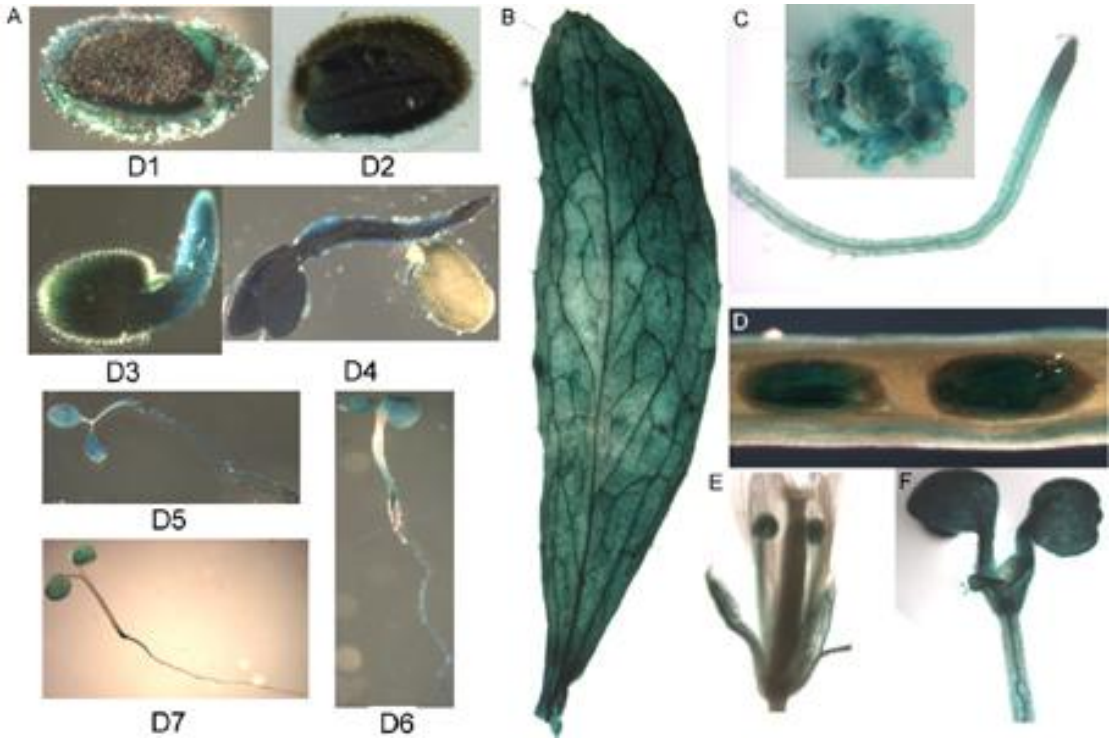
A
D1
D2
D3
D4
D5
D6
D7
B
C
D
E
F

sepals, anthers (Figure 5.3E), and siliques. When siliques were opened, GUS staining was not only observed in the valves but also in the funiculi (Figure 5.3D), implying a role in loading of iron from maternal tissues into seeds. In roots, GUS staining was observed mainly in the vascular tissues (Figure 5.3C). These expression patterns support the idea that *YSL4* and *YSL6* are active during the whole plant life cycle, and especially during germination. These results, together with strong sequence similarity of the two proteins, also suggest that YSL4 and YSL6 may perform overlapping functions in plants.

5.3.3 Localization of YSL4 and YSL6 protein:

To more precisely localize the expression of the YSL4 and YSL6 proteins, the whole *YSL4* and *YSL6* genes were fused to GFP and then stably transformed in to *ysl4-2 and ysl6-5* mutant plants, respectively, for sub-cellular localization. GFP fluorescence of the roots was observed by Zeiss confocal microscopy. Since a proteomics analysis had suggested that YSL4 and YSL6 were localized to the vacuole membrane (Jaquinod *et al*, 2007), Tonoplast Intrinsic Protein 1 (TIP1) was included for demonstration of the pattern associated with tonoplast localization (Figure 5.4D-F). GFP signal from TIP-GFP frequently deviates around the nucleus (Figure 5.4D, yellow arrow).

Figure 5.4: Subcellular localization of AtYSL6 in Arabidopsis roots.

(A)-(C) Confocal microscope images of a plant transformed with AtYSL6-GFP. (A) GFP image. (B) DIC image (C) Overlay image of (A) and (B). (D)-(F) As a control for tonoplast localization, confocal microscope image of the root of a plant transformed with GFP fused to AtTIP (Tonoplast Intrisic Protein). (D) GFP image. Note deviation of the GFP signal around nucleus (yellow arrow). (E) DIC image. (F) Overlay image of (D) and (E).

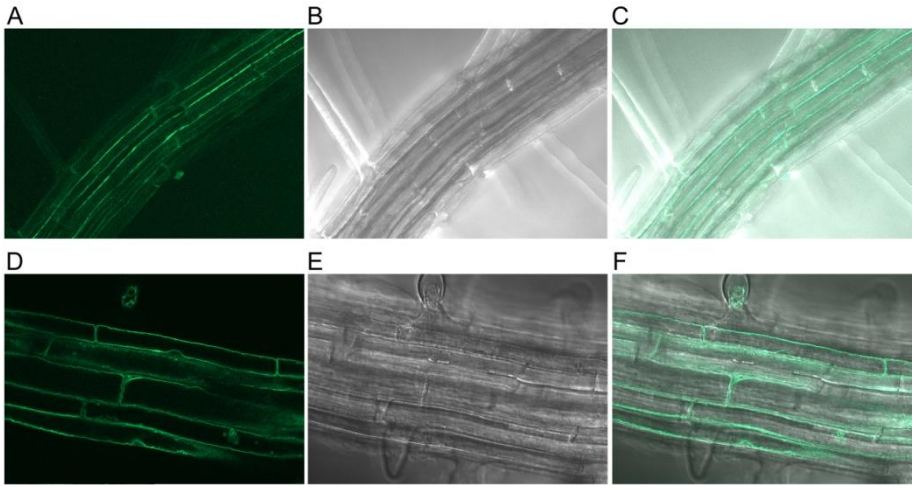
A
B
C
D
E
F

The fluorescence signal of YSL6 was observed at the periphery of the cell (Figure 5.4A-C), and signal deviation around the nucleus was never observed, indicating YSL6 is localized to plasma membrane. The fluorescence signal of *YSL4-GFP* fusion protein was also observed at the periphery of the cell (Figure 5.5A-C), and signal deviation around the nucleus was never visualized, suggesting that YSL4 is also localized to the plasma membrane.

5.3.4 Characterization of *ysl4* and *ysl6* knockout plants:

Among all the AtYSL family members, AtYSL4 and AtYSL6 belong to the same group (Figure 1.3), and share highest sequence similarity. The gene structure of AtYSL4 and AtYSL6 is similar (Figure 5.6A), with six exons in each gene. Furthermore, the length of each exon is also similar, suggesting that they may perform similar functions.

We have identified one T-DNA knock out allele for *ysl4* (SALK_025447; *ysl4-2*) and two T-DNA knock out alleles for *ysl6* (SALK_119560; *ysl6-4* and SALK_093392; *ysl6-5*). T-DNA insertion occurred in exon 5 in *ysl4-2*, in intron1 in *ysl6-4*, and in exon7 in *ysl6-5* (Figure 5.6A). In each case, no corresponding mRNA is detected in homozygous mutant individuals (Figure 5.6B, Lane 2, 5, and 6). Amplification of *YSL6* genomic DNA using gene specific primers (Figure 5.6B, Lane 4) was included to demonstrate that the

Figure 5.5: Subcellular localization of AtYSL4 in Arabidopsis root.

(A)-(C) Confocal microscope image of plant transformed with AtYSL6-GFP.

(A) GFP image. (B) DIC image. (C) Overlayed image of (A) and (B).

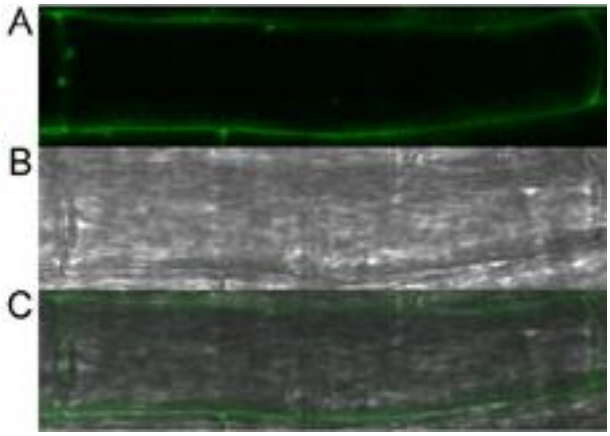
A
B
C

Figure 5.6: Characterization of *ysl4* and *ysl6* T-DNA knockout mutants.

(A) Schematic representation of the structure of *YSL4* and *YSL6.* Grey bars represent promter regions. Blue bars represent exons. Black lines represent introns (not to scale). Red triangles represent T-DNA insertions.

(B) Detection of *YSL4* and*YSL6* mRNA. RT-PCR was performed using RNA extracted from the leaves of wild type (WT), *ysl4-2*, *ysl6-4*, *ysl6-5,* and *ysl4ysl6* plants. WT genomic DNA (gDNA) was also included as control. Lane 1: WT cDNA with *YSL4* specific primers. Lane2: *ysl4-2* cDNA with *YSL4* specific primers. Lane 3: WT gDNA with *YSL6* specific primers. Lane 4: WT cDNA with *YSL6* specific primers. Lane 5: *ysl6-4* cDNA with *YSL6* specific primers. Lane 6: *ysl6-5* cDNA with *YSL6* specific primers.

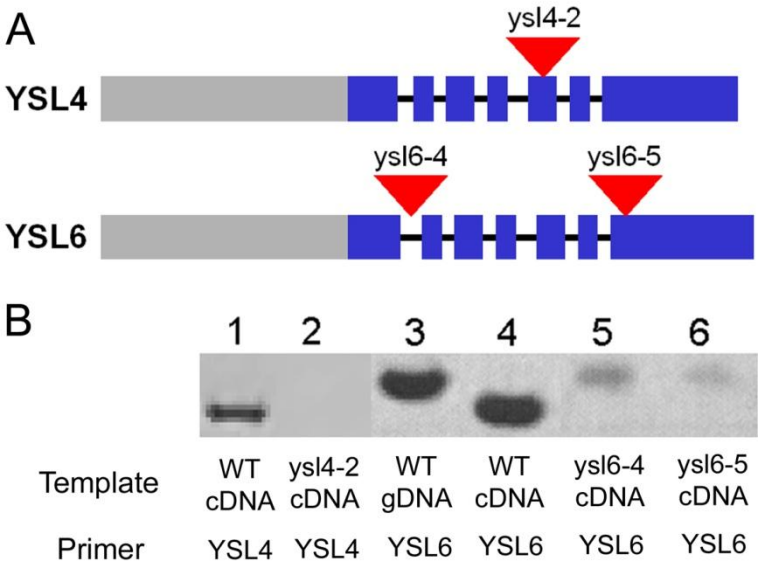
A
ysl4-2
YSL4
ysl6-4
ysl6-5
YSL6
B
1 2 3 4 5 6
Template
WT cDNA
ysl4-2 cDNA
WT gDNA
WT cDNA
ysl6-4 cDNA
ysl6-5 cDNA
Primer
YSL4 YSL4 YSL6 YSL6 YSL6 YSL6

bands seen in Figure 5.6B, Lane 5 and 6 results from genomic DNA contamination of the cDNA.

Since no obvious phenotype was observed in either *ysl4* or *ysl6* single mutants, I generated *ysl4ysl6* double mutant plants by crossing *ysl4-2* and *ysl6-5*. F2 plants were used for genotyping to identify double mutants. In homozygous *ysl4ysl6* double mutants, no PCR products of *YSL4* (Figure 5.7A) or *YSL6* (Figure 5.7C) is detected and T-DNA insertions in both *YSL4* (Figure 5.7B) and *YSL6* (Figure 5.7D) were detected. No overt phenotypes were observed in the *ysl4ysl6* double mutants.

5.3.5 Mutant plants have altered metal levels:

Because no obvious phenotypes could be discerned from single or double mutant plants, ICP-MS determination of metal content was performed (Figure 5.7) to see whether metal homeostasis is altered. Metals were measured in the leaves and seeds, because *YSL4* and *YSL6* showed strong expression in both vegetative and reproductive organs. The results of leaf metal content measurement showed that Mn is significantly high in *ysl4-2* and *ysl6-4*, and although not significant, there is a trend that Mn is high in *ysl6-5* (Figure 5.8A). Interestingly, Mn level is normal in the double mutants. Zn is also significantly high in *ysl4-2* and *ysl6-4*, but normal in *ysl6-5* and *ysl4ysl6*.

Figure 5.7: Characterization of *ysl4ysl6* double mutants. PCR was performed using genomic DNA as template to identify *YSL4*, *YSL6*, and T-DNA insertion. In (A) and (C), Col0 was included as a positive control of genomic DNA quality. In (B) and (D), Col0 was included as a negative control to confirm no PCR product can be generated without a T-DNA insertion.

(A) *YSL4* gene specific primers, which span through T-DNA insertion site, were used to show no wilt type *YSL4* present.

(B) Primers, which associate with *YSL4* T-DNA insertion, were used to show the presence of the T-DNA insertion.

(C) *YSL6* gene specific primers, which span through T-DNA insertion site, were used to show no wilt type *YSL6* present.

(D) Primers, which associate *YSL6* T-DNA insertion, were used to show the presence of the T-DNA insertion.

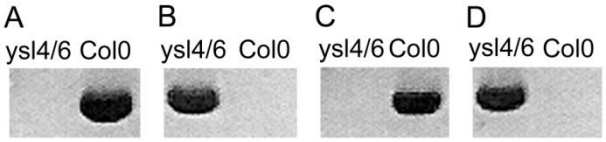
A
ysl4/6 Col0
B
ysl4/6 Col0
C
ysl4/6 Col0
D
ysl4/6 Col0

Figure 5.8: ICP-MS determination of metal concentrations of Col0, *ysl4-2*, *ysl6-4*, *ysl6-5*, and *ysl4ysl6*. Results are given as ppm. Error bars represent standard error. Each sample contains 10 replicates. Asterisks indicate $P < 0.05$ by T-test. (A) Metal concentrations of leaves. (B) Metal concentrations of seeds.

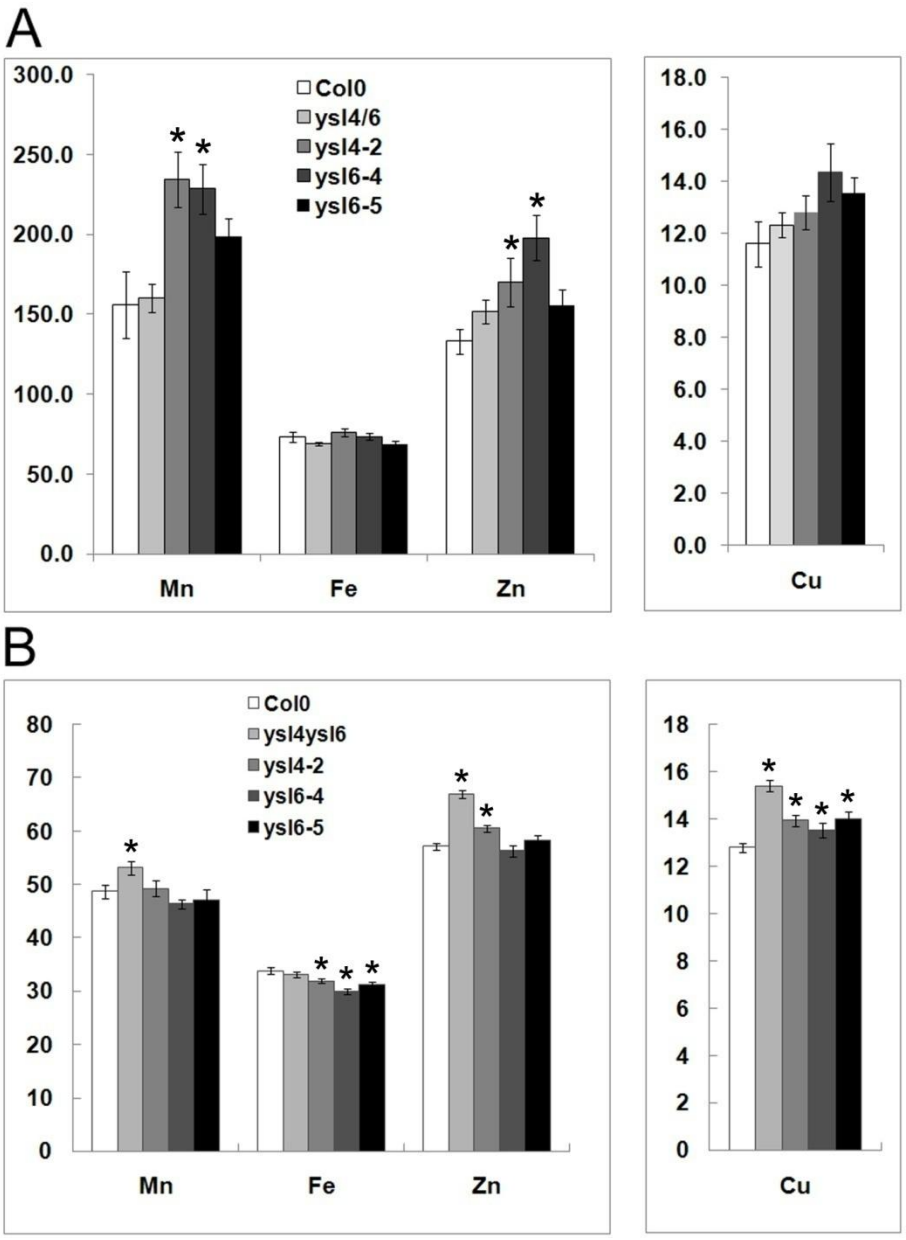
A
300.0
250.0
200.0
150.0
100.0
50.0
0.0
Col0
ysl4/6
ysl4-2
ysl6-4
ysl6-5
Mn
Fe
Zn
18.0
16.0
14.0
12.0
10.0
8.0
6.0
4.0
2.0
0.0
Cu
B
80
70
60
50
40
30
20
10
0
Col0
ysl4ysl6
ysl4-2
ysl6-4
ysl6-5
Mn
Fe
Zn
18
16
14
12
10
8
6
4
2
0
Cu

For the seeds, *ysl4-2* mutant seeds have decreased levels of Fe and increased levels of Zn and Cu (Figure 5.8B). Both *ysl6-4* and *ysl6-5* mutant seeds have decreased levels of Fe and increased levels of Cu (Figure 5.8B). Since both *ysl4* and *ysl6* single mutant seeds have altered Fe, Cu, and/or Zn levels, altered Fe, Zn, and Cu levels were expected to be observed in *ysl4ysl6* mutant seeds. As expected, *ysl4ysl6* double mutant seeds have increased levels of Zn and Cu (Figure 5.8B). Interestingly, decreased iron level was not observed in seeds of *ysl4ysl6* mutants. Moreover, seeds of *ysl4ysl6* mutants have increased levels of Mn.

5.3.6 Examination of growth of mutant lines:

Since YSL4 and YSL6 are highly expressed in seeds, and seeds of mutant lines (single and double mutants) exhibit altered metal levels, YSL4 and YSL6 may play important role in seeds. Thus, germination tests were performed test whether these mutants have germination defects. In this experiment, three sets of 100 seeds each of every line were germinated on normal MS medium plates and MS medium without added Fe, Zn, Cu, or Mn. Germination was defined as emergence of the radical, and was scored every 24 hours after plating. Germination rate and germination time of the seeds of

these mutants were normal when grown on MS medium and MS medium without Fe, Zn, Cu, or Mn (Figure 5.9).

Total chlorophyll level of 5 day old seedlings germinated on MS medium was measured to confirm whether mobilization and utilization of Fe was affected in the seeds of the mutants. Four sets of 20 seeds of each mutant line were placed on MS medium lacking Fe in a line parallel to a line of seeds from Col0 plants, allowing better visual comparison of greenness. Since Fe levels were decreased in seeds of the *ysl4* and *ysl6* single mutants, the mutants were expected to be more susceptible to Fe limiting conditions than Col0 plants. However, the chlorophyll level was statistically indistinguishable from Col0 in the seeds of each mutant (Figure 5.10). Furthermore, to test whether iron mobilization or utilization was affected by losing function of YSL4 or YSL6, or both, seeds were germinated on MS medium for 10 days and then transferred to MS medium without Fe, Zn, Cu, or Mn for 14 day, followed by total chlorophyll level measurements. The chlorophyll level of all the mutants showed no difference from that of Col0 (Figure 5.11), indicating that loss of function of YSL4 and/or YSL6 does not affect tolerance to metal deficiency. All mutants were also examined to observe whether they are more sensitive or tolerant to metal excess. Plants were grown on MS medium for 10 days and

Figure 5.9: Germination test of seeds of Col0, *ysl4-2*, *ysl6-4*, *ysl6-5*, *ysl4ysl6* plants. Three sets of 100 seeds each of every line were germinated on normal MS medium plates and MS medium without added Fe, Zn, Cu, or Mn (Marked as –Fe, -Zn, -Cu, and –Mn in the charts). Germination was defined as emergence of the radical, and was scored every 24 hours after plating.

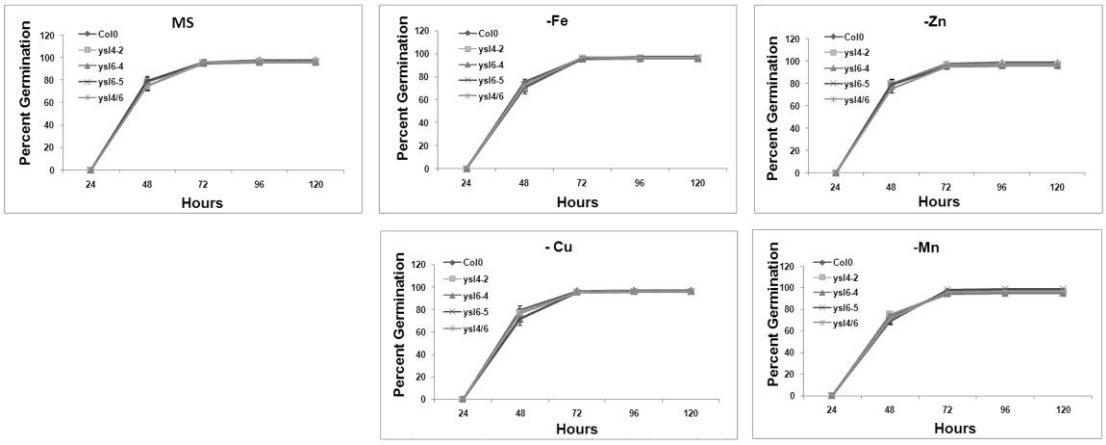
MS
-Fe
-Zn
- Cu
-Mn
Percent Germination
Hours
Col0
ysl4-2
ysl6-4
ysl6-5
ysl4/6
0
20
40
60
80
100
120
24
48
72
96
120

Figure 5.10: Metal starvation response in seedlings of Col0, *ysl4-2*, *ysl6-4*, *ysl6-5*, and *ysl4ysl6*. Seedlings were grown on MS medium lacking Fe for 5 days and then chlorophyll levels were measured.

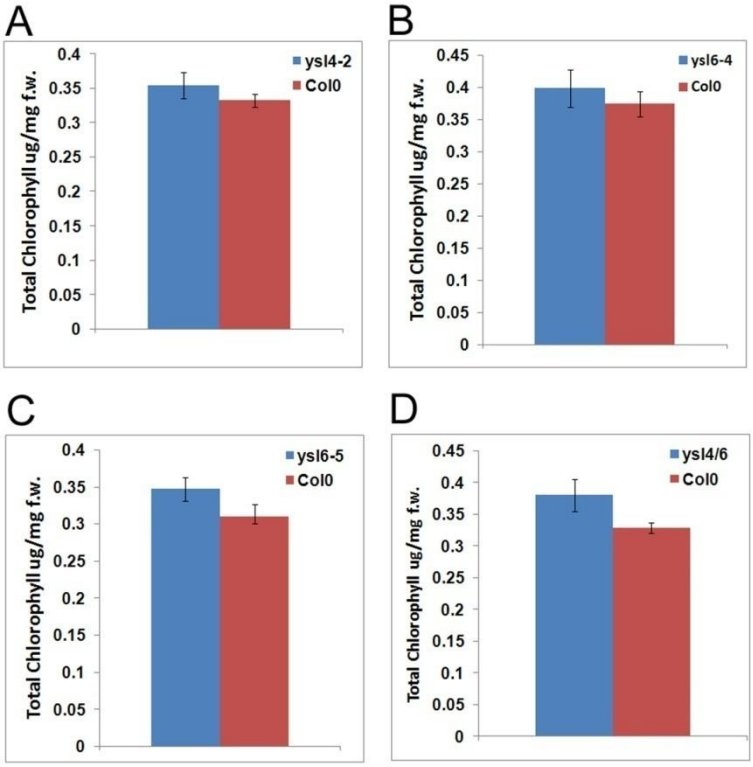
A
Total Chlorophyll ug/mg f.w.
0.4
0.35
0.3
0.25
0.2
0.15
0.1
0.05
0
ysl4-2
Col0
B
Total Chlorophyll ug/mg f.w.
0.45
0.4
0.35
0.3
0.25
0.2
0.15
0.1
0.05
0
ysl6-4
Col0
C
Total Chlorophyll ug/mg f.w.
0.4
0.35
0.3
0.25
0.2
0.15
0.1
0.05
0
ysl6-5
Col0
D
Total Chlorophyll ug/mg f.w.
0.45
0.4
0.35
0.3
0.25
0.2
0.15
0.1
0.05
0
ysl4/6
Col0

Figure 5.11: Metal starvation response in Col0, *ysl4-2*, *ysl6-4*, *ysl6-5*, and *ysl4ysl6* plants. Plants were grown on MS plates for 10 days, and then transferred to MS without Fe, Zn, Cu, or Mn for 14 days. The total chlorophyll content of the shoot system was measured.

(A) Chlorophyll levels of plants grown on MS medium lacking Fe.

(B) Chlorophyll levels of plants grown on MS medium lacking Zn.

(C) Chlorophyll levels of plants grown on MS medium lacking Cu.

(D) Chlorophyll levels of plants grown on MS medium lacking Mn.

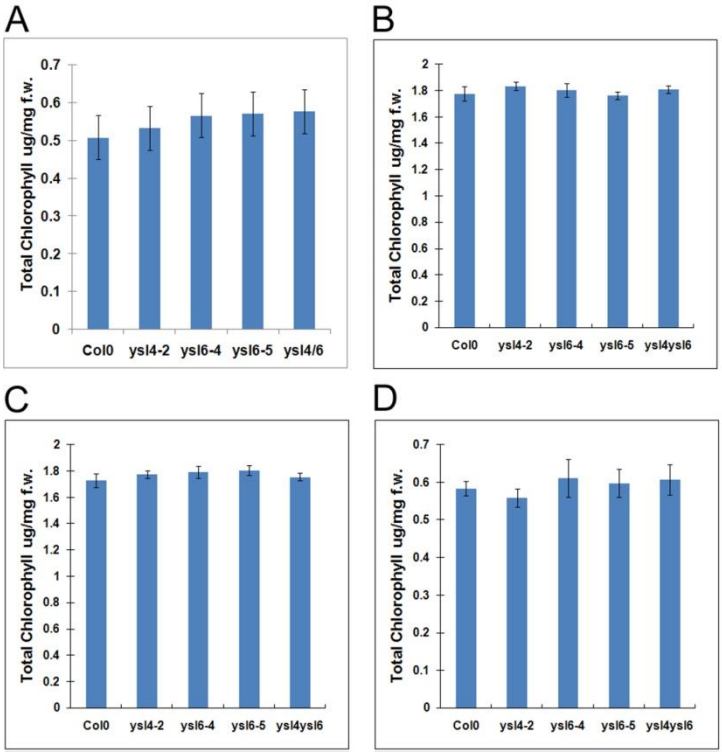
A
Total Chlorophyll ug/mg f.w.
0.7
0.6
0.5
0.4
0.3
0.2
0.1
0
Col0
ysl4-2
ysl6-4
ysl6-5
ysl4/6
B
Total Chlorophyll ug/mg f.w.
2
1.8
1.6
1.4
1.2
1
0.8
0.6
0.4
0.2
0
Col0
ysl4-2
ysl6-4
ysl6-5
ysl4ysl6
C
Total Chlorophyll ug/mg f.w.
2
1.8
1.6
1.4
1.2
1
0.8
0.6
0.4
0.2
0
Col0
ysl4-2
ysl6-4
ysl6-5
ysl4ysl6
D
Total Chlorophyll ug/mg f.w.
0.7
0.6
0.5
0.4
0.3
0.2
0.1
0
Col0
ysl4-2
ysl6-4
ysl6-5
ysl4ysl6

then transferred to MS medium containing 200 uM Fe, 200uM Zn, 100 uM Cu, or 200uM Mn for 21days. No growth difference was observed in comparison to Col0.

5.3.7 Seeds of mutant plants retain correct iron localization:

We have previously shown that the seeds produced by *ysl4* and *ysl6* mutants are low in Fe and high in Cu and/or Zn (Waters et al., 2006). To determine whether iron is localized normally in these seeds, I examined the iron content in *ysl4-2*, *ysl6-4*, and *ysl6-5* mutant seeds by Perl's stain for Fe(III) (Figure 5.12). Using this method, Fe(III) is released from tissue deposits by treatment with dilute hydrochloric acid, and then reacts with potassium ferrocyanide to produce an insoluble blue compound, potassium ferric ferrocyanide (Prussian blue). Ferrous ions do not participate in the reaction, but since measures are not taken to prevent oxidation of Fe(II) to Fe(III) during the staining, both Fe(III) and Fe(II) may ultimately contribute to staining. In Arabidopsis seeds, iron is most concentrated in the vasculature of the embryo's cotyledons (Kim et al., 2006), and Perl's stain reveals this pattern (Figure 5.12). The Perl's stain pattern of all the mutants is similar to that of WT. Thus, all mutants have correct iron localization in seeds. We conclude

Figure 5.12: Perl's stain of seeds for Fe(III). Seeds were cut in half and then stained with Perl's stain solution for 15 min.

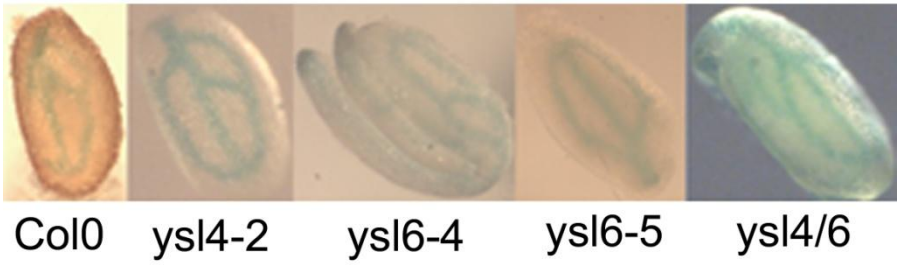
Col0
ysl4-2
ysl6-4
ysl6-5
ysl4/6

that loss of function of YSL4 and/or YSL6 results in low iron levels but do not affect iron localization in seeds.

5.3.8 Over-expression of YSL6:

For a better understanding of the physiological function of the *YSL6* gene, I attempted to increase the expression of *YSL6* to observe the direct impact to plants, *i.e.* whether metal content, seed set, iron deficiency tolerance etc. would be affected. The whole *YSL6* gene was cloned into the pMN20 vector, which contains 4 copies of the CaMV 35S enhancer. This construct is expected to enhance expression of *YSL6* without inducing ectopic expression (Weigel *et al*.,2000; Tian *et al*, 2004; Mora-García et al, 2004). The construct was stably transformed into wild type Arabidopsis plants and homozygous plants were identified in the F2. Three lines of homozygous transformants, YSL6 OX 1.3, 4.7, and 7.10, were generated that have increased mRNA levels (2.1- 1.7- and 1.5- fold, respectively) in the leaves (Figure 5.13A). However, no elevated expression of *YSL6* was observed in reproductive tissues of any of the three transgenic lines (Figure 5.13B-E).

No morphological phenotypes were observed in these lines, so ICP-MS determination of metal content was performed on both leaves and seeds. The results of metal content measurement showed that, except for Zn levels in

Figure 5.13: *YSL6* enhanced expression lines YSL3 OX L1.3, YSL3 OX L4.7, and YSL3 OX L7.10. Each line contains a 4X35S enhancer sequence upstream of a YSL6 genomic clone containing 683 bp of native sequence upstream of the initiating ATG.

(A) Expression of *YSL6* by semi-quantitative RT-PCR. *Actin2* was included as a control for template quantity. Lane1: Col0. Lane2: YSL6 OX L1.3. Lane3: YSL6 OX L4.7. Lane4: YSL6 OX L7.10.

(B) ICP-MS determination of Mn, Fe, Cu, and Zn concentrations of leaves from 20 day old soil-grown plants. Results are given as ppm. Error bars represent standard error. Each sample contains 10 replicates. Asterisks indicate $P < 0.05$ by T-test.

(C) ICP-MS determination of Mn, Fe, Cu, and Zn concentrations of seeds. Results are given as ppm. Error bars represent standard error. Each sample contains 10 replicates. Asterisks indicate $P < 0.05$ by T-test.

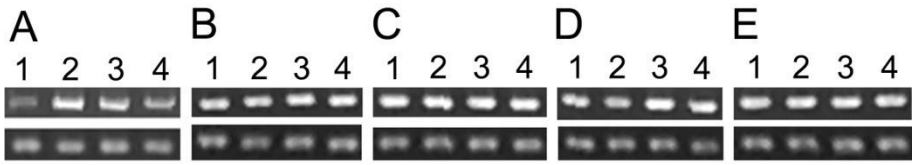
A
B
C
D
E
1 2 3 4 1 2 3 4 1 2 3 4 1 2 3 4 1 2 3 4

F

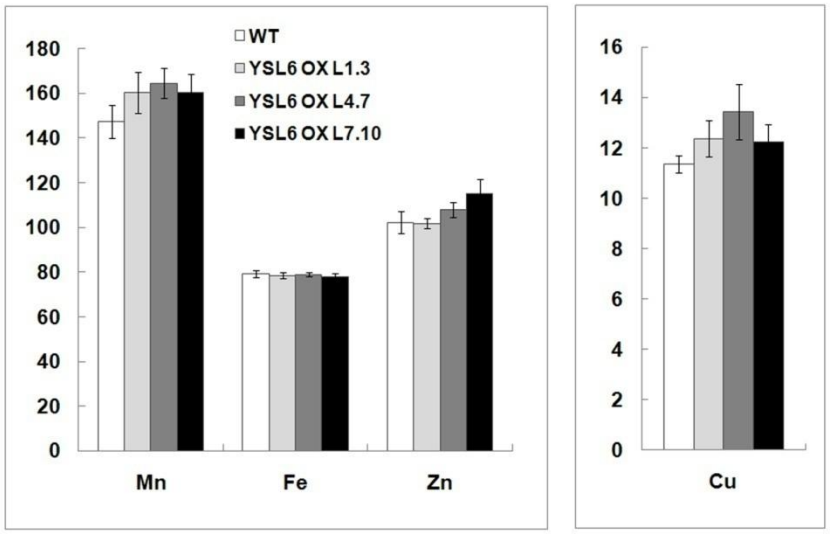
WT
YSL6 OX L1.3
YSL6 OX L4.7
YSL6 OX L7.10
180
160
140
120
100
80
60
40
20
0
Mn
Fe
Zn
16
14
12
10
8
6
4
2
0
Cu

G

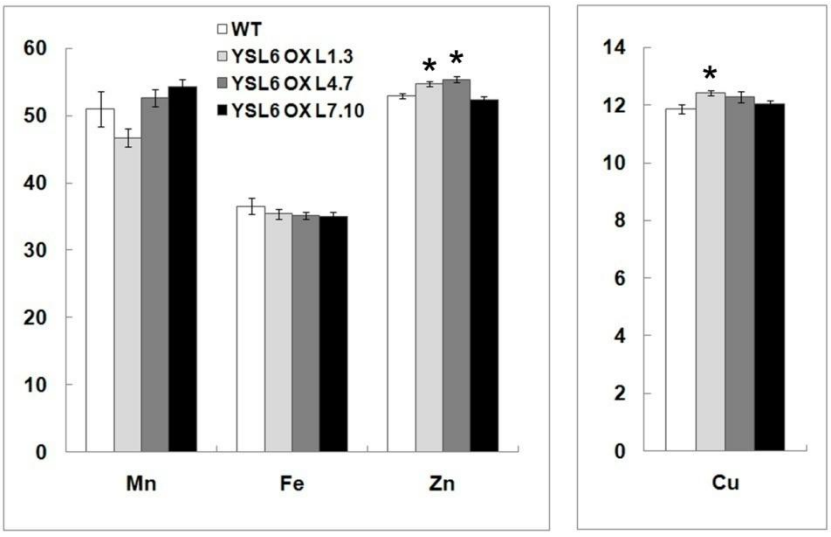
WT
YSL6 OX L1.3
YSL6 OX L4.7
YSL6 OX L7.10
60
50
40
30
20
10
0
* *
Mn
Fe
Zn
14
12
10
8
6
4
2
0
*
Cu

the seeds of YSL6 OX 1.3 and 4.7, metal levels were not changed (Figure 5.13G). The increased Zn phenotype does not correspond to our expectations, since Zn levels are normal in the seeds of *ysl6* mutants. If *YSL6* is strongly involved is seed Zn deposition, I would expect to see decreased levels of Zn in *ysl6* mutant plants.

5.3.9 Examination of YSL6 over-expression lines:

Because overexpression of YSL6 in these lines appears to be strongest in vegetative tissues, we examined whether the lines were resistant or sensitive to metal deficiency stress. In this experiment, seeds were germinated on MS medium for 10 days and then transferred to MS medium lacking Fe, Zn, Cu, or Mn for 28 days. The total chlorophyll level of the seedlings, which reflects the level of iron deficiency chlorosis, was measured at various time points. All three lines (Line 1.3, 4.7, and 7.10) showed no significant differences from wild type Col0 plants (Figure 5.14). Three overexpressing lines were also examined to observe whether they are more sensitive or tolerant to metal excess. Plants were grown on MS medium for 10 days and then transferred to MS medium containing 200 uM Fe, 200uM Zn, 100 uM Cu, or 200uM Mn for 21 days. Again, no growth difference was observed compared to Col0.

Figure 5.14: Metal starvation response in wild-type and *YSL6* over-expression lines YSL6 OX L1.3, YSL3 OX L4.7, and YSL3 OX L7.10. Plants were grown on MS plates for 10 days, and then transferred to MS without Fe, Zn, Cu, or Mn for 28 days. The total chlorophyll content of the shoot system was measured.

(A) Chlorophyll levels of plants grown on MS medium lacking Fe.

(B) Chlorophyll levels of plants grown on MS medium lacking Zn.

(C) Chlorophyll levels of plants grown on MS medium lacking Cu.

(D) Chlorophyll levels of plants grown on MS medium lacking Mn.

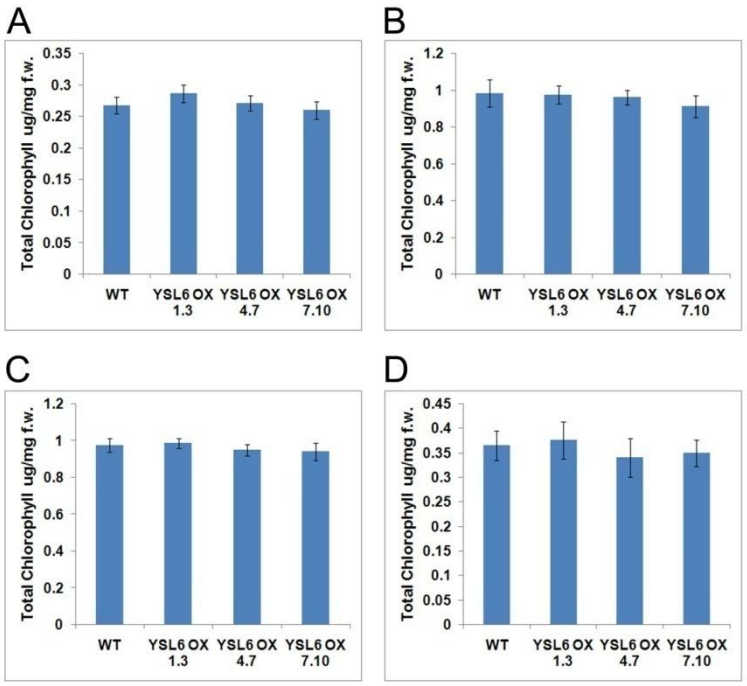
A
Total Chlorophyll ug/mg f.w.
0.35
0.3
0.25
0.2
0.15
0.1
0.05
0
WT
YSL6 OX 1.3
YSL6 OX 4.7
YSL6 OX 7.10
B
Total Chlorophyll ug/mg f.w.
1.2
1
0.8
0.6
0.4
0.2
0
WT
YSL6 OX 1.3
YSL6 OX 4.7
YSL6 OX 7.10
C
Total Chlorophyll ug/mg f.w.
1.2
1
0.8
0.6
0.4
0.2
0
WT
YSL6 OX 1.3
YSL6 OX 4.7
YSL6 OX 7.10
D
Total Chlorophyll ug/mg f.w.
0.45
0.4
0.35
0.3
0.25
0.2
0.15
0.1
0.05
0
WT
YSL6 OX 1.3
YSL6 OX 4.7
YSL6 OX 7.10

5.3.10 Complementation of *ysl1ysl3* double mutants by YSL6:

Both AtGenExpress microarray data and promoter-GUS analysis showed that *YSL3* and *YSL6* are abundantly expressed in leaves and pollen and pollen inviability is a prominent feature of *ysl1ysl3* double mutant phenotype. Thus, I examined whether YSL3 and YSL6 share overlapping biochemical functions using the overt phenotype of the *ysl1ysl3* double mutant as a tool. In the experiment, *YSL6* cDNA was driven by the *YSL3* promoter and stably transformed into *ysl1ysl3* double mutants. If YSL6 has highly similar or identical biochemical functions to YSL3, then the severe phenotypes of double mutant should be alleviated or recovered. *YSL3* whole gene fusion to GFP for localization studies was included as a positive control since this construct contains the same promoter as used in this experiment.

Plants transformed with *YSL3p::YSL6* exhibited only a partially rescued phenotype. Chlorophyll levels of four transgenic lines (YSL3p::YSL6 L3, L5, and L7) were similar to those of *ysl1ysl3* double mutants and significantly lower than those of WT (Figure 5.15A), whereas the positive control, YSL3::GFP, did completely complement the chlorotic double mutant phenotype (Figure 5.15B). The seed number (as an indication of fertility) and seed weight (as an indication of seed development) of the three transgenic

Figure 5.15: Complementation of *ysl1ysl3* double mutants with *YSL6*.

ysl1ysl3 double mutant plants was transformed with *YSL6* cDNA driven by *YSL3* promoter (*YSL3p::YSL6*). Three lines of *YSL3p::YSL6* (L3, L5, and L7) were included. Asterisk indicates $P < 0.05$ by T-test.

(A) Total chlorophyll concentration of leaves of *Col0*, *YSL3p::YSL6*, and *ysl1ysl3* grown on soil for 20 days. Each sample represents 10 replicates.

(B) Total chlorophyll concentration of leaves of Col0, *YSL3-GFP*, and *ysl1ysl3* grown on soil for 20 days. Each sample contains 10 replicates.

(C) Average weight of an individual seed.

(D) Average weight of an individual seed.

(E) Average seed number per plant.

(F) Average seed number per plant.

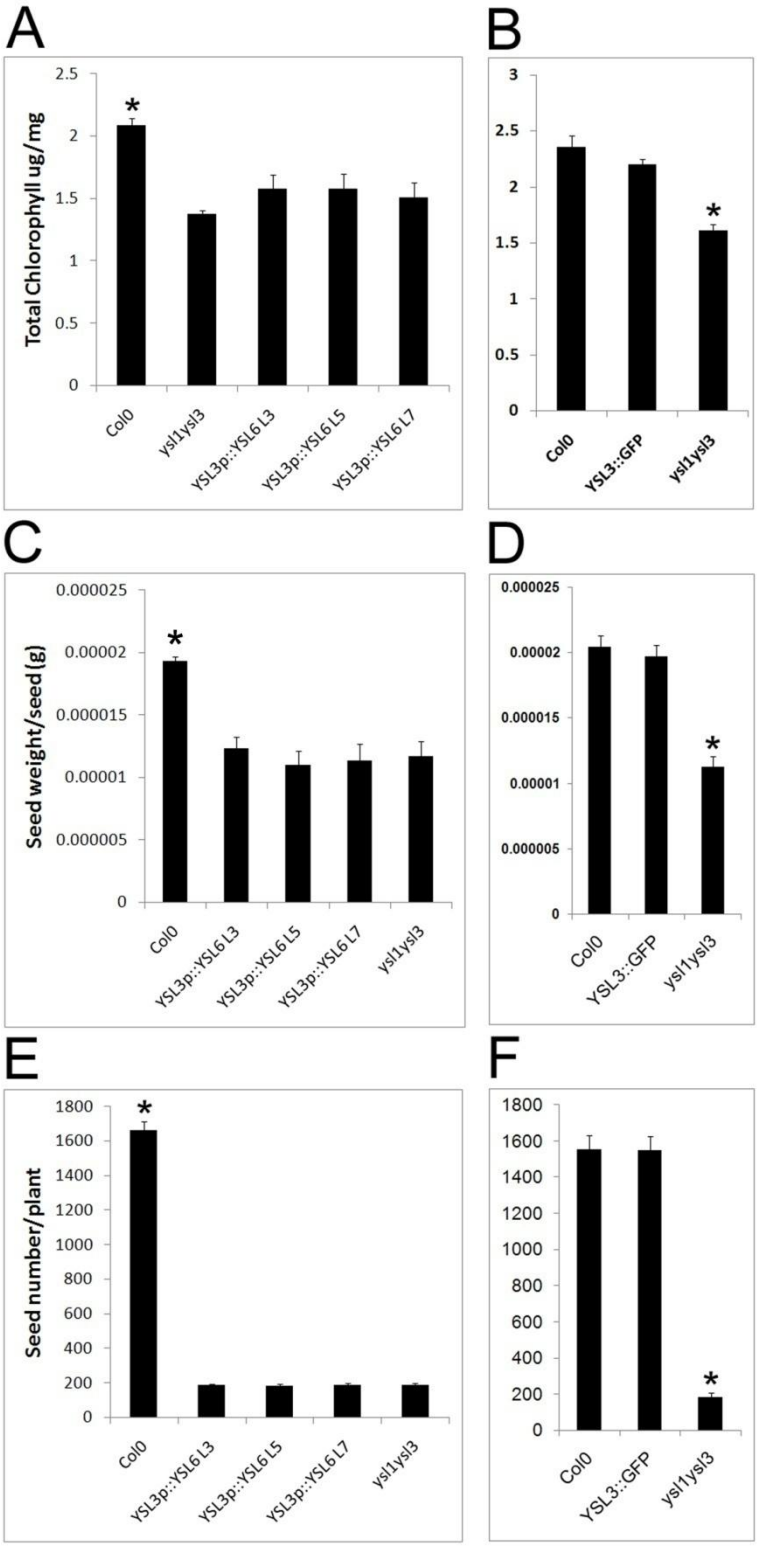
A
Total Chlorophyll ug/mg
2.5
2
1.5
1
0.5
0
*
Col0
ysl1ysl3
YSL3p::YSL6 L3
YSL3p::YSL6 L5
YSL3p::YSL6 L7
B
3
2.5
2
1.5
1
0.5
0
*
Col0
YSL3::GFP
ysl1ysl3
C
Seed weight/seed (g)
0.000025
0.00002
0.000015
0.00001
0.000005
0
*
Col0
YSL3p::YSL6 L3
YSL3p::YSL6 L5
YSL3p::YSL6 L7
ysl1ysl3
D
0.000025
0.00002
0.000015
0.00001
0.000005
0
*
Col0
YSL3::GFP
ysl1ysl3
E
Seed number/plant
1800
1600
1400
1200
1000
800
600
400
200
0
*
Col0
YSL3p::YSL6 L3
YSL3p::YSL6 L5
YSL3p::YSL6 L7
ysl1ysl3
F
1800
1600
1400
1200
1000
800
600
400
200
0
*
Col0
YSL3::GFP
ysl1ysl3

lines were similar to those of *ysl1ysl3* double mutant (Figure 5.15C and E), while both seed number and seed weight are normal in *YSL3::GFP* complemented lines (Figure 5.15D and F). No complementation resulted from expression of the *YSL3p*::*YSL6* construct. RT-PCR was performed to confirm the expression of the transgene. When making the *YSL3p*::*YSL6* construct, an HA tag was added to 3' end of *YSL6*. Primers specific to the HA tag were therefore used to amplify only the *YSL6* mRNA from the *YSL3p*::*YSL6* construct. Expression of *YSL6* controlled by *YSL3* promoter was confirmed (Figure 5.16). Thus, *YSL6* cannot complement *YSL3* transport function *in planta*, suggesting that YSL3 and YSL6 are not redundant at the level of protein function. In conclusion, *YSL3* and *YSL6* appear to have distinct biochemical functions *in planta*.

5.4 Discussion:

An analysis of the tonoplast proteome had suggested that YSL4 and YSL6 were localized to the tonoplast (Jaquinod *et al*, 2007). Localization of YSL4 and YSL6 using whole gene fusion to GFP revealed that YSL4 and YSL6 are actually localized to the plasma membrane (Figure 5.4 and 5.5). This result is in agreement with our yeast functional complementation result, which suggests that YSL4 and YSL6 are plasma membrane bound Fe(II)-NA transporters

Figure 5.16: RT-PCR result showed mRNA level of YSL6 expressed under control of *YSL3* promoter in three lines of *YSL3p::YSL6* (L3, L5, and L7). Primers amplifying only *YSL6* expressed from the construct were used for the PCR. WT cDNA was included as negative control to show that mRNA of *YSL6* under control of native promoter cannot be amplified using this set of primers. Actin2 was included as control.

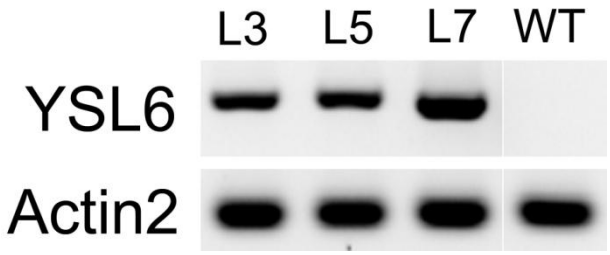
L3
L5
L7
WT
YSL6
Actin2

(Figure 1.4). It is known that tonoplast membrane preparations can easily be contaminated by plasma membrane. Since YSL4 and YSL6 are the most abundantly expressed YSL family members, it is very likely that they would be the YSL most likely to be detected in any proteomic study.

Loss of function of YSL4 or YSL6 resulted in elevated Mn and Zn levels in leaves (Figure 5.8A). This elevated Mn and Zn phenotype is a standard phenotype appearing plants experiencing iron deficiency. This phenotype is seems to be the result of IRT1 transporter activity. In addition to the primary iron uptake transporter, IRT1 also takes up Mn and Zn. During iron limitation, the iron deficiency signal triggers increased expression of IRT1 to maintain iron homeostasis. In this way, increases Mn and Zn levels arise as a by-product of increased IRT1 expression. It has been established that plants under Fe deficiency may not show declined level of iron in leaves, but increased levels of Mn and Zn (Baxter *et al*, 2008). Thus, this could also be happening in *ysl4* and *ysl6* single mutants. To confirm this, IRT1 and ferric reductase activity in the roots need to be checked to observe whether their expression is increased.

I hypothesize that YSL4 and YSL6 may be involved in iron mobilization from roots into shoots, consistent with their expression pattern, revealed by

promoter-GUS analysis, that YSL4 and YSL6 are highly expressed in the vascular tissue of roots. In this model, loss of function of YSL4 or YSL6 results in trapped iron in the roots, which induces iron deficiency responses in the leaves. Metal levels of roots will need to be measured in order to test the hypothesis.

In the seeds, loss of function of YSL4 results in reduced levels of Fe and elevated levels of Zn and Cu (Figure 5.7B). Loss of function of YSL6 results in decreased levels of Fe and increased levels of Cu in seeds (Figure 5.7B). This result implies that YSL4 and YSL6 are involved in iron distribution into seeds, consistent with the high expression levels of YSL4 and YSL6 in flowers and siliques. Interestingly, seeds of double mutants have normal levels of iron. Moreover, seeds of *ysl4ysl6* double mutants have increased levels Mn, Zn, and Cu, which are even significantly higher than those of *ysl4* and *ysl6* single mutant seeds. One explanation is that since loss of ysl4 or ysl6 results in decreased levels of iron in the seeds, and loss of function of both YSL4 and YSL6 may trigger stronger response to iron deficiency. Therefore, in order to compensate the iron levels in seeds of *ysl4ysl6* double mutants, more iron may be remobilized from senescing leaves and be delivered into developing inflorescences and seeds, results in a normal level of iron in seeds.

Furthermore, transporters could transport multiple metals. Our lab has shown that YSL1 and YSL3 are important for Cu and Zn remobilization from senescing leaves (Waters *et al*, 2006). Some other genes may be responsible for moving Fe, Mn, Cu, or Zn out of senescing leaves, distributing these metals to flowers, or loading these metals into seeds. Thus, in order to deliver iron into seeds of *ysl4ysl6* double mutants, Mn, Zn, and Cu may also be moved into seeds causing increased levels of Mn, Zn, and Cu.

Seeds of *ysl4* and *ysl6* single mutants have decreased levels of iron similar to that of *ysl1ysl3* double mutants. I was not able to stain seeds of *ysl1ysl3* mutants using Perl's reagent and even attempting to stain seeds of *ysl1ysl3* mutants with Fe-EDDHA treatment, which have normal iron levels, it took 4 hours to observe staining (Figure 4.6). However, just like seeds of WT, it took only 15 minutes to observe Perl's staining of *ysl4* and *ysl6* single mutant seeds. We know that Perl's stain can only detect Fe(III), which is the typical storage form of iron, but not Fe(II). One possibility is that loss of function of YSL1 and YSL3 somehow prevents the Fe(II) transported to seeds from being oxidized to Fe(III) for storage. This may explain the germination defect of *ysl1ysl3* since iron homeostasis in seeds may be disrupted by the accumulation of an abnormal form of Fe.

Both AtGenExpress microarray data and promoter-GUS analysis showed that *YSL3* and *YSL6* are abundantly expressed in leaves and pollen, implying possible overlapping functions of YSL3 and YSL6. The functional equivalency examination of Arabidopsis YSL3 and YSL6 showed that YSL6 do not share redundant functions *in planta*. *ysl1ysl3* double mutant plants expressing *YSL6* under control of *YSL3* promoter exhibited no complementation in both vegetative tissues and reproductive tissues (Figure 5.15). We cannot make the conclusion at this point because the lack of complementation could be caused by absent or low expression of YSL6 protein. Although the presence of mRNA has been confirmed (Figure 5.16), the presence of mRNA does not guarantee protein expression. I have done western blot for several times to detect the presence and level of YSL6 protein. In this experiment, *ysl1ysl3* double mutant plants transformed with *YSL3p*::*YSL2* were used as a positive control since they showed partial complementation, indicating protein from construct is expressed in this line. However, I was not able to detect HA tag in either line. Thus, optimization of western blots needs to be done to show the presence and level of YSL6 protein.

CHAPTER 6
DISCUSSION

Iron homeostasis in plants requires regulation of many components. Initial work on iron homeostasis was focused on how iron is taken up from soil into roots. As described previously, the key components involved in iron uptake from soil into roots have already been characterized, but little is known about the mechanisms involved in moving iron from root epidermis into xylem, moving iron from xylem into cells or subcellular compartments in leaves, or iron re-distribution from mature leaves into seeds. In order to achieve the goal of biofortification, the mechanisms governing distribution of iron from roots to seeds needs to be understood. At the start of my work, YSL family members, which were putative metal-nicotianamine transporters were candidates for these functions.

We have hypothesized that the Arabidopsis YSL family has roles in lateral movement of metals out of vasculature, and metal movement from mesophyll towards phloem in senescing leaves. Using yeast functional complementation assays, I have shown that Arabidopsis YSL family members are Fe-NA transporters (Figure 3.4), suggesting that they are involved in movement of metals within Arabidopsis. Since NA is the candidate chelator for

iron being distributed from organ to organ within plants, YSLs are implicated in these processes.

Our group has identified a *ysl1ysl3* double mutant that exhibits interveinal chlorosis (Figure 1.5 A to E) and reproductive defects, such as stunting of inflorescence, (Figure 1.5 F) low pollen viability (Figure G), and defective seeds with arrested embryos. We have hypothesized that these phenotype are caused by iron deficiency. From the Fe-EDDHA and ammonium citrate experiments, I conclude that the interveinal chlorosis and reproductive defects of the *ysl1ysl3* double mutants are the result of low iron, and not due to lack of other metals. This is consistent with our hypothesis, suggesting that YSL1 and YSL3 are important for iron homeostasis within Arabidopsis

In the Inflorescence grafting experiment, I showed that *ysl1ysl3* grafts have normal development of pollen and seeds (Figure 4.7A and B) but that seeds have uncorrected metal levels, calling into a question whether the recovery of pollen and seed development is actually caused by normal metal levels. Since *ysl1ysl3* double mutants are chlorotic, they should have less sugar. Less sugar could have two distinct effects. One is that, to drive phloem transport of iron to the seeds, adequate sucrose in the phloem is required. Thus, pollen and seed defects could be the result of poor iron

translocation. Alternatively, sugar is itself needed for pollen and seed development, thus that simple lack of carbohydrate experienced by the chlorotic ysl1ysl3 plants could be the cause of the pollen and seed defects. *ysl1ysl3* grafts to WT rosettes, which have normal sugar content to drive the phloem transport or provide carbohydrate, do correct the pollen and seed weight defects that characterize the double mutant. The ferric ammonium citrate treatment results can be used to address this issue. Ferric ammonium citrate treatment reversed the chlorosis phenotype of *ysl1ysl3* double mutants (Figure 4.3), suggesting normal photosynthesis in treated double mutant leaves. However, ferric ammonium citrate treatment can barely restore seed viability (Figure 4.4A). In this experiment, normal photosynthesis in leaves but loss of function of YSL1 and YSL3 results in poor recovery of pollen and seed development, strongly suggesting that it is metal transport, not sugar production that causes the pollen and seed weight defects of the double mutant. In conclusion, *YSL1* and *YSL3* are required in rosette leaves for normal pollen and seed development, possibly in movement of metals towards phloem for loading of metals into seeds. The uncorrected levels of metals in *ysl1ysl3* grafts suggest that YSL1 and YSL3 are also necessary in the inflorescences for proper accumulation of metals in seeds (Figure 4.7C).

Since YSL1 and YSL3 are poorly expressed in siliques and seeds, the presence of YSL1 and YSL3 in flowers, stems or cauline leaves is likely necessary for proper loading of metals into developing seeds. In conclusion, *YSL1* and *YSL3* not only play a role in moving iron or other metals from leaves directly to seeds but also are needed within the flowers, stems or cauline leaves for correct metal accumulation in seeds.

The initial step towards the goal of biofortification is to characterize “the players” for metal accumulation in different parts of plants. My work described here helps us understand how metal mobilization works and gives a possible way to increase mobilization and thus Fe concentration in seeds.

We have showed that all YSLs are Fe(II)-NA transporters using yeast functional complementation assay. This result raises the question of whether all YSLs identically transport Fe(II)-NA across plasma membrane in Arabidopsis. The substitution experiments I performed suggest distinct biochemical activities for each YSL, indicating that existing biochemical analyses are not enough. This substitution study allows us to test the functional equivalency of YSLs and increases our understanding of the biochemical activities of the whole YSL family. Eventually, these results give us more possible candidate genes to achieve the goal of biofortification.

BIBLIOGRAPHY

Akiyama, K., Nakamura, S., Suzuki, T., Wisniewska, I., Sasaki, N., and Kawasski, S. (1997) Development of a system of rice transformation with long genome inserts for their functional analysis for positional cloning. Plant Cell Physiol. Suppl. **38,** s94.

Aoyama, T., Kobayashi, T., Takahashi, M., Nagasaka, S., Usuda, K., Kakei, Y., Ishimaru, Y., Nakanishi, H., Mori, S. and Nishizawa, N.K. (2009) OsYSL18 is a rice iron(III)–deoxymugineic acid transporter specifically expressed in reproductive organs and phloem of lamina joints, *Plant Mol. Biol.,* DOI 10.1007/s11103-009-9500-3

Brüggemann, W., Maas-Kantel K. and Moog, P.R. (1993) Iron uptake by leaf mesophyll cells: the role of the plasma membrane-bound ferric-chelate reductase, *Planta* **190**, 151–155.

Baxter I, Vitek O, Lahner B, Muthukumar B, Borghi M, Morrissey J, Guerinot ML, and Salt DE. (2008) The leaf ionome as a multivariable system to detect a plant's physiological status. Proc. Natl. Acad. Sci. USA **105**(33):12081-12086.

Chaignon, V., Di Malta, D., and Hinsinger, P. (2001) Fe-deficiency increases Cu acquisition by wheat cropped in a Cu-contaminated vineyard soil. New Phytol. **154,** 121-130.

Cheng, L., Wang, F., Shou, H., Huang, F., Zheng, L., He, F., Li, J., Zhao, F.J., Ueno, D., Ma, J.F. and Wu, P. (2007) Mutation in nicotianamine aminotransferase stimulated the Fe(II) acquisition system and led to iron accumulation in rice, *Plant Physiol.* **145**, 1647–1657

Clemens, S., Palmgren M.G., and Krämer, U. (2002) A long way ahead: understanding and engineering plant metal accumulation. Trends Plant Sci. **7,** 309-315.

Cohen, C.K., Garvin D.F. and Kochian, L.V. (2004) Kinetic properties of a micronutrient transporter from *Pisum sativum* indicate a primary function in Fe uptake from the soil, *Planta* **218**, 784–792.

Cohen, C.K., Fox, T.C., Garvin, D.F., and Kochian, L.V. (1998). The role of iron-deficiency stress responses in stimulating heavy-metal transport in plants. Plant Physiol. **116,** 1063–1072.

Colangelo, E.P. and Guerinot M.L. (2004) The essential basic helix-loop-helix protein FIT1 is required for the iron deficiency response. Plant Cell. **16**:3400-3412.

Connolly, E.L., Campbell, N., Grotz, N., Prichard, C., and Guerinot, M.L. (2003) Overexpression of the FRO2 ferric chelate reductase confers tolerance to growth on low iron and uncovers post-transcriptional control. Plant Physiol. **133,** 1102-1110.

Connolly, E.L., Fett, J., and Guerinot, M.L. (2002) Expression of the IRT1 metal transporter is controlled by metals at the levels of transcript and protein accumulation. Plant Cell **14,** 1347-1357.

Curie,C., Panaviene, Z., Loulergue, C., Dellaporta, S.L., Briat, J.F., and Walker, E.L. (2001) Maize yellow stripe 1 encodes a membrane protein directly involved in Fe(III) uptake. Nature **409,** 346-349.

Dancis, A., Hailw, D., Yuan, D.S., and Klausner, R.D. (1994) The saccharomyces cerevisiae copper transport protein (Ctr1p). Biochemical characterization regulation by copper, and physiologic role in copper uptake. Journal Of Biological Chemistry **269,** 25660-25667.

Dancis, A., Yuan, D.S., Haile, C., Askwith, C., Eide, D., Moehle, C., Kaplan, J., and Klausner, R.D. (1994) Molecular characterization of a copper transport protein in S. cerevisiae: an unexpected role for copper in iron transport. Cell **76,** 393-402.

de la Guardia, M.D. and Alcantara, E. (1996) Ferric chelate reduction by sunflower (*Helianthus annuus* L.) leaves: influence of light, oxygen, iron-deficiency and leaf age, *J. Exp. Bot.* **47,** 669–675.

DiDonato, R.J., Jr, Roberts, L.A., Sanderson, T., Eisley, R.B., and Walker, E.L. (2004) Arabidopsis yellow stripe-like2 (YSL2): a metal-regulated gene encoding a plasma membrane transporter of nicotianamine-metal complexes. Plant Journal **39,** 403-414.

Dinneny, J.R., Long, T.A., Wang, J.Y., Jung, J.W., Mace, D., Pointer, S., Barron, C., Brady, S.M., Schiefelbein, J. and Benfey, P.N. (2008) Cell identity mediates the response of Arabidopsis roots to abiotic stress, *Science* **320,** 942–945.

Durrett, T.P., W. Gassmann and E.E. Rogers, *The FRD3-mediated efflux of citrate into the root vasculature is necessary for efficient iron translocation.* Plant Physiol, 2007. 144(1): p. 197-205

Eckhardt, U., Marques A.M. and Buckhout, T.J. (2001) Two iron-regulated cation transporters from tomato complement metal uptake-deficient yeast mutants, *Plant Mol. Biol.* **45**, 437–448.

Eide, D., Broderius, M., Fett, J., and Guerinot, M.L. (1996) A novel iron-regulated metal transporter from plants identified by functional expression in yeast. Proc. Natl. Acad. Sci. USA **93,** 5624-5628.

Erenoglu, B., Eker, S., Cakmak, I., Derici, R., and Romheld, V. (2000) Effect of iron and zinc deficiency on release of phytosiderophores in barley cultivars differing in zinc efficiency. J Plant Nutr. **23,** 1645-1656.

Gao, CY. and Pinkham, JL. (2000) Tightly regulated, beta-estradiol dose-dependent expression system for yeast. Biotechniques **29**, 1226-1231

Gendre, D., P. Czernic, G. Conejero, K. Pianelli, J.F. Briat, M. Lebrun, and S. Mari, 2006, TcYSL3, a member of the YSL gene family from the hyper-accumulator Thlaspi caerulescens, encodes a nicotianamine-Ni/Fe transporter. Plant J. **49**, 1-15.

Grotz, N. and Guerinot, M.L. (2006) Molecular aspects of Cu, Fe and Zn homeostasis in plants, *Biochim. Biophys. Acta* **1763**, 595–608.

Gries, D., Klatt, S., and Runge, M. (1998) Copper-deficiency-induced phytosiderophore release in the calcicole grass Hordelymus europaeus. New Phytol. **140,** 95-101

Guerinot, M.L. and Y. Yi, *Iron: nutritious, noxious, and not readily available.* Pl. Physiol., 1994. 104: p. 815-820.

Guerinot, M.L. (2001) Improving rice yields—ironing out the details. Nat. Biotechnol. **19,** 417-418.

Guerinot, M.L., and Yi, Y. (1994) Iron : nutritious, Noxious, and nor readily available. Plant Physiol. **104,** 815-820.

Hayama, R., Yokoi, S., Tamaki, S., Yano, M., and Shimoamoto, K. (2003) Adaptation of photoperiodic contro; pathways produces short-day flowering on rice. Nature **422,** 719-722.

Himelblau E, Amasino RM (2001) Nutrients mobilized from leaves of Arabidopsis thaliana during leaf senescence. J. Plant Physiol. **158:** 1317-1323.

Henriques, R., Jasik, J., Klein, M., Martinoia, E., Feller, U., Schell, J., Pais, M.S. and Koncz, C. (2002) Knock-out of Arabidopsis metal transporter gene IRT1 results in iron deficiency accompanied by cell differentiation defects, *Plant Mol. Biol.* **50**, 587–597.

Herbik A, Koch G, Mock HP, Dushkov D, Czihal A, Thielmann J, Stephan UW, Baumlein H (1999) Isolation, characterization and cDNA cloning of nicotianamine synthase from barley: a key enzyme for iron homeostasis in plants. Eur J Biochem **265:** 231–239.

Hiei, Y., Ohta, S., Komari, T., and Kumashiro, T. (1994) Efficient transformation of rice (Oryza sativa L.) mediated by Agrobacterium and sequence analysis of the boundaries of the T-DNA. Plant Journal **6,** 271-282.

Higuchi K, Suzuki K, Nakanishi H, Yamaguchi H, Nishizawa NK, Mori S (1999) Cloning of nicotianamine synthase genes, novel genes involved in the biosynthesis of phytosiderophores. Plant Physiol **119:** 471–479

Higuchi, K., Nishizawa, N., Römheld, V., Marschner, H., and Mori, S. (1996) Absence of nicotianamine synthase activity in the tomato mutant ‘chloronerva’. J. Plant Nutr. **19,** 1235-1239.

Hocking PJ, Pate JS (1977) Mobilization of Minerals to Developing Seeds of Legumes. Annals of Botany **41**: 1259-1278

Hocking PJ, Pate JS (1978) Accumulation and Distribution of Mineral Elements in Annual Lupins Lupinus-Albus L and Lupinus-Angustifolius L. Australian Journal of Agricultural Research **29**: 267-280

Hopkins, B.G., Jolley, V.D., and Brown, J.C. (1992) Plant utilization of iron solubilized by oat phytosiderophore. J Plant Nutr. **15,** 1599-1612.

Inoue, H., Higuchi, K., Takahashi, M., Nakanishi, H., Mori, S., and Nishizawa, N.K. (2003) Three rice nicotianamine synthase genes, OsNAS1, OsNAS2, and OsNAS3 are expressed in cells involved in long-distance transport of iron and differentially regulated by iron. Plant Journal **36,** 366-381.

Inoue, H, Kobayashi, T, Nozoye, T, Takahashi, M, Kakei, Y, Suzuki, K, Nakazono, M, Nakanishi, H, Mori, S, and Nishizawa, N (2009) Rice OsYSL15 Is an Iron-regulated Iron(III)-Deoxymugineic Acid Transporter Expressed in the Roots and Is Essential for Iron Uptake in Early Growth of the Seedlings. J. Biol. Chem. **284, 3470-3479.**

Inskeep WP, Bloom PR (1985) Extinction coefficients of chlorophyll *a* and *b* in *N*, *N*-dimethylformamide and 80% acetone. Plant Physiol **77:** 483–485.

Ishimaru, Y., Suzuki, M., Tsukamoto, T., Suzuki, K., Nakazono, M., Kobayashi, T., Wada, Y., Watanabe, S., Matsuhashi, S., Takahashi, M., Nakanishi, H., Mori, S. and Nishizawa, N.K. (2006) Rice plants take up iron as an Fe^{3+}-phytosiderophore and as Fe^{2+}, *Plant J.* **45**, 335–346.

Jaquinod, M., F. Villiers, S. Kieffer-Jaquinod, V. Hugouvieux, C. Bruley, J. Garin and J. Bourguignon, *A proteomics dissection of Arabidopsis thaliana vacuoles isolated from cell culture.* Mol Cell Proteomics, 2007. 6(3): p. 394-412.

Jolley, V.D., and Brown, J.C. (1991) Differential response of Fe-efficient corn and Fe-inefficient corn and oat to phytosiderophore released by Fe-efficient Coker 227 oat. J plant nutr. **14,** 45-58.

Kandel E.R., Schwartz, J.H., Jessell, T.M. (2000). Principles of Neural Science, 4th ed., pp.152-153. McGraw-Hill, New York.

Kim, S.A., T. Punshon, A. Lanzirotti, L. Li, J.M. Alonso, J.R. Ecker, J. Kaplan and M.L. Guerinot (2006) *Localization of iron in Arabidopsis seed requires the vacuolar membrane transporter VIT1.* Science, **314**(5803): p. 1295-8.

Klatte, M., Schuler, M., Wirtz, M., Fink-Straube, C., Hell, R. and Bauer, P. (2009) The Analysis of Arabidopsis Nicotianamine Synthase Mutants Reveals Functions for Nicotianamine in Seed Iron Loading and Iron Deficiency Responses, Plant Physiol. **150**: 257-271

Koike, S., Inoue, H., Mizuno, D., Takahashi, M., Nakanishi, H., Mori, S., and Nishizawa, N.K. (2004) OsYSL2 is a rice metal-nicotianamine transporter that is regulated by iron and expressed in the phloem. Plant Journal **39,** 415-424.

Korshunova, Y.O., Eide, D., Clark, W.G., Guerinot, M.L., and Pakrasi, H.B. (1999). The IRT1 protein from *Arabidopsis thaliana* is a metal transporter with a broad substrate range. Plant Mol. Biol. **40,** 37–44.

Lanquar, V., Lelievre, F., Bolte, S., Hames, C., Alcon, C., Neumann, D., Vansuyt, G., Curie, C. (2005) A. Schroder, U. Kramer, H. Barbier-Brygoo and S. Thomine, Mobilization of vacuolar iron by AtNRAMP3 and AtNRAMP4 is essential for seed germination on low iron, *EMBO J.* **24**, 4041–4051.

Lahner, B., Gong, J., Mahmoudian, M., Smith, EL., Abid, KB., Rogers, EE., Guerinot, ML., Harper, JF., Ward, JM., McIntyre, L., Schroeder, J., and Salt, D. (2003) Genomic scale profiling of nutrient and trace elements in Arabidopsis thaliana. Nat Biotechnol **21,** 1215–1221

Lasswell, J., Rogg, L.E., Nelson, D.C., Rongey C. and Bartel, B. (2000) Cloning and characterization of IAR1, a gene required for auxin conjugate sensitivity in Arabidopsis, *Plant Cell* **12** (2000), pp. 2395–2408.

Lee, S., Chiecko, J.C., Kim, S.A., Walker, E.L., Lee, Y., Guerinot, M.L. and An, G. (2009) Disruption of *OsYSL15* Leads to Iron Inefficiency in Rice Plants, Plant Physiol. 150: 786-800

Li, L., Cheng X. and Ling, H.-Q. (2004) Isolation and characterization of Fe(III)-chelate reductase gene LeFRO1 in tomato, *Plant Mol. Biol.* **54**, 125–136.

Marschner, H., Romheld, V., and Kissel, M. (1986) Different strategies in higher plants in mobilization and uptake of iron. J. Plant Nutr. **9,** 3-7.

Marschner, H. (1995) Mineral Nutrition of Plants, Academic Press, Boston

Mäser, P., Thomine, S., Schroeder, J.I., Ward, J.M., Hirschi, K., Sze, H., Talke, I.N., Amtmann, A., Matthuis, F.J.M., Sanders, D., Harper, J.F., Tchieu, J., Gribskov, M., Persans, M.W., Salt, D.E., Kim S.A. and Guerinot, M.L. (2001) Phylogenetic relationships within cation transporter families of Arabidopsis, *Plant Physiol.* **126**, 1646–1667.

Miki, D., and Shimamoto, K. (2004) Simple RNAi vectors for stable and transient suppression of gene function in rice. Plant Cell Physiol. **45,** 490-495.

Mori, S., and Nishizawa, N. (1987) Methionine as a dominant precursor of phytosiderophores in graminaceae plants. Plant Cell Physiol. **28,** 1081-1092.

Mori, S. (1999) Iron acquisition by plants. Curr. Opin. Plant Biol. **2**, 250-253

Mora-García, S., Vert, G., Yin, Y., Caño-Delgado, A., Cheong, H., and Chory, J. (2004). Nuclear protein phosphatases with Kelch-repeat domains modulate the response to brassinosteroids in *Arabidopsis*. Genes Dev. **18,** 448–460.

Mukherjee, I, Campbell, N.H., Ash, J.S. and Connolly, E.L. (2006) Expression profiling of the Arabidopsis ferric chelate reductase (*FRO*) gene family reveals differential regulation by iron and copper, *Planta* **223,** 1178–1190.

Murata, Y., Ma, J.F., Yamaji, N., Ueno, D., Nomoto, K., and Iwashita, T. (2006) A specific transporter for iron(III)–phytosiderophore in barley roots. Plant Journal **46,** 563-572.

Oldenburg, KR, Vo KT, Michaelis S, Paddon C (1997) Recombination-mediated PCR-directed plasmid construction in vivo in yeast. Nucleic Acids Res **25**, 451-452.

Olsen, R.A., Clark, R.B., and Bennett, J.H. (1981) The enhancement of soil fertility by plant roots, *Am. Scientist* **69,** 378–384.

Persson, B. and Argos, P. (1994) Prediction of transmembrane segments in proteins utilising multiple sequence alignments. *J. Mol. Biol.* **237**, 182–192.

Persson, B. and Argos, P. (1996) Topology prediction of membrane proteins. *Protein Sci.* **5**, 363–371.

Pich, A., Scholz, G., and Stephan, U.W. (1994) Iron-dependent changes of heavy metals, nicotianamine, and citrate in different plant organs and in the xylem exudate of two tomato genotypes. Nicotianamine as possible copper translocator. Plant soil **165,** 189-196.

Pich, A. and G. Scholz, 1996, Translocation of copper and other micronutrients in tomato plants (Lycopersicon esculentum Mill.): nicotianamine-stimulated copper transport in the xylem. J. Exp. Bot. **47**:41-47.

Rhee, S.Y. and C.R. Somerville, 1995, Flat-surface grafting in *Arabidopsis thaliana.* Pl. Mol. Biol. Reporter. **13**(2):118-123.

Roberts, L.A., Pierson, A.J., Panaviene, Z., and Walker, E.L. (2004) Yellow stripe1. Expanded roles for the maize iron-phytosiderophore transporter. Plant Physiol. **135,** 112-120.

Robinson, N.J., Sadjuga, J.G., and Quentin, J.G. (1997) The froh gene family from Arabidopsis thaliana: putative iron-chelate reductases. Plant Soil **196,** 245-248.

Robinson, N.J., Procter, C.M., Connolly, E.L., and Guerinot, M.L. (1999) A ferric-chelate reductase for iron uptake from soils. Nature **397,** 694-697.

Rogers, E.E., Eide, D.J., and Guerinot, M.L. (2000). Altered selectivity in an Arabidopsis metal transporter. Proc. Natl. Acad. Sci. USA **97,** 12356–12360.

Romheld, V., and Marschner, H. (1986) Evidence for a specific uptake system for iron phytosiderophores in roots of grasses. Plant Physiol. **70,** 175-180.

Rudolph, A., Becker, R., Scholz, G., Procha´ zka, Z., Toman, J., Macek, T., and Herout, V. (1985) The occurrence of the amino acid nicotianamine in plants and microorganisms. A reinvestigation. Biochem. Physiol. Pflanz. **180,** 557–563.

Santi, S., Cesco, S, and Pinton, V.Z.R. (2005) Two plasma membrane H+-ATPase genes are differentially expressed in iron-deficient cucumber plants, *Plant Physiol. Biochem.* **43**, pp. 287–292.

Santi, S. and Schmidt, W. (2008) Laser microdissection-assisted analysis of the functional fate of iron deficiency-induced root hairs in cucumber, *J. Exp. Bot.* **59**, pp. 697–704.

Schaaf, G., Ludewig, B.E., Erenoglu, B.E., Mori, S., Kitahara, T., and Wiren, N.V. (2004) ZmYS1 functions as a proton-coupled symporter for phytosiderophore-and nicotianamine-chelated metals. J. Biol. Chem. **279,** 9091-9096.

Schaaf, G., Schikora, A., Häberle, J., Vert, G., Ludewig, U., Briat, J.F, Curie, C., and von Wíren, N. (2005) A putative function for the Arabidopsis Fe–phytosiderophore transporter homolog AtYSL2 in Fe and Zn homeostasis. Plant Cell Physiol. **46,** 762-744.

Schmidke, I., and Stephan, U.W. (1995) Transport of metal micronutrients in the phloem of castor bean (Ricinus communis) seedlings. Physiol. Plant. **95,** 147-153.

Shirasu, K., Nielsen, K., Piffanelli, P., Oliver, R., and Schulze-Lefert, P. (1999) Cell-autonomous complementation of mlo resistance using a biolistic transient expression system. Plant Journal **17,** 293-299.

Shojima, S., Nishizawa, N.K., Fushiya, S., Nozoe, S., Irifune, T., and Mori, S. (1990) Biosynthesis of phytosiderophores. Plant Physiol. **93,** 1497–1503.

Shojima S, Nishizawa NK, Mori S (1989) Establishment of a cell free system for the biosynthesis of nicotianamine. Plant Cell Physiol **30:** 673–677

Stacey, M.G., Patel, A., McClain, W.E., Mathieu, M., Remley, M., Rogers, E.E., Gassmann, W., Blevins, D.G. and Stacey, G. (2008) The *Arabidopsis* AtOPT3 protein functions in metal homeostasis and movement of iron to developing seeds. *Plant Physiol.* **146**, 589–601

Stephan, U.W., G. Scholz, and A. Rudolph, 1990, Distribution of nicotianamine, a presumed symplast iron transporter, in different organs of sunflower and of a tomato wild type and its mutant *chloronerva*. Biochem. Physiol. Pflanzen. 186:81-88.

Stephan, U.W., and Scholz, G. (1993). Nicotianamine: mediator of transport of iron and heavy metals I the phloem? Physiologia Plantarum **88,** 522-529.

Stephan, U.W., Schmidke, I., Stephan, V.W., and Scholz, G. (1996) The nicotianamine molecule is made-to-measure for complexation of metal micronutrients in plants. Biometals **9,** 84–90.

Supek, F., Supekova, L., Nelson, H., and Nelson, N. (1996) A yeast manganese transporter related to the macrophage protein involved in conferring resistance to mycobacteria. Proc. Natl. Acad. Sci. USA **93,** 5105-5110.

Takagi, S. (1976) Naturally occurring iron-chelating compounds in oat- and rice-root washings. Soil Sci. Plant Nutr. **22,** 423–433.

Takagi, S., Nomoto, K., and Takemoto, T. (1984) Physiological aspect of mugineic acid, a possible phytosiderophore of graminaceous plants. J. Plant Nutr. **7,** 469–477.

Takahashi, M., Nakanishi, H., Kawasaki, S., Nishizawa, N.K., and Mori, S. (2001) Enhanced tolerance of rice to low iron availability in alkaline soils using barley nicotianamine aminotransferase genes. Nat. Biotechnol. **19,** 466–469.

Takahashi, M., Terada, Y., Nakai, I., Nakanishi, H., Yoshimura, E., Mori, S., and Nishizawa, N.K. (2003) Role of nicotianamine in the intracellular delivery of metals and plant reproductive development. Plant Cell **15,** 1263–1280.

Takahashi, M., Yamaguchi, H., Kawasaki, S., Nichizawa, N.K., and Mori, S. (2001) Enhanced tolerance of rice to low iron availability in alkaline soils using barley nicotianamine aminotransferase genes. Nat. Biotechnol. **19,** 466-469.

Takahashi, M., Yamaguchi, H., Nakanishi, H., Shioiri, T., Nishizawa, N.K., and Mori, S. (1999) Cloning two genes for nicotianamine aminotransferase, a critical enzyme in iron acquisition (Strategy II) in graminaceous plants. Plant Physiol. **121,** 947–956.

Tian GW, Mohanty A, Chary SN, Li S, Paap B, Drakakaki G, Kopec CD, Li J, Ehrhardt D, Jackson D, et al (2004) High-throughput fluorescent tagging of full-length Arabidopsis gene products in planta. Plant Physiol. **135:** 25–38

Tiffin LO (1966) Iron translocation I: plant culture, exudate sampling, iron-citrate analysis. Plant Physiol **41:** 510–514

Tiffin LO (1970) Translocation of iron citrate and phosphorus in xylem exudate of soybean. Plant Physiol **45:** 280–283

Tolay, I., Erenoglu, B., Romheld, V., Braun, H.J., and Cakmak, I. (2001) Phytosiderophore release in Aegilops tauschii and Triticum species under zinc and iron deficiencies. J Exp. Bot. **52,** 1093-1099.

Uchimiya, H., Iwata, M., Nojiri, C., Smarajeewa, P.K., Takamatsu, S., Ooba, S., Anzai, H., Christensen, A.H., Quail, P.H., and Toki, S. (1993) Biolophos treatment of transgenic rice plants expressing a bar gene prevents infection by the sheath blight pathogen (Rhizoctonia solani). Bio/Technology **11,** 835-836.

Vacchina, V., Mari, S., Czernic, P., Marques, L., Pilanelli, K., Schaumloffel, D., Lebrun, M., and Lobinski, R. (2003) Speciation of nickel in a hyperaccumulating plant by high-performance liquid chromatography-inductively coupied plasma mass spectrometry and electrospray MS/MS assisted by cloning using yeast complementation. Anal Chem. **75,** 2740- 2745.

Vasconcelos, M, Eckert, H, Arahana, V, Graef, G, Grusak, M.A. and Clemente, T. (2006) Molecular and phenotypic characterization of transgenic soybean expressing the Arabidopsis ferric chelate reductase gene, FRO2, *Planta* **224,** 1116–1128.

Varotto, C., Maiwald, D., Pesaresi, P., Jahns, P., Salamini, F., and Leister, D. (2002) The metal ion transporter IRT1 is necessary for iron homeostasis and efficient photosynthesis in Arabidposis thaliana. Plant Journal **31,** 589-599.

Vert, G., Grotz, N., Dedaldechamp, F., Gaymard, F., Guerinot, M.L., Briat J.-F. and Curie, C. (2002) IRT1, an Arabidopsis transporter essential for iron uptake from the soil and plant growth, *Plant Cell* **14**, 1223–1233.

Vert, G., Briat J.-F., and Curie, C. (2001) Arabidopsis IRT2 gene encodes a root-periphery transporter, *Plant J.* **26**, 181–189.

von Wirén, N., Marschner H., and Romheld, V. (1996) Roots of iron-efficient maize also absorb phytosiderophore-chelated zinc. Plant Physiol. **111,** 1119-1125.

von Wirén, N., Klair, S., Bansal, S., Briat, J.F., Khodr, H., Shioiri, T., Leigh, R.A., and Hider, R.C. (1999) Nicotianamine chelates both FeIII and FeII. Implications for metal transport in plants. Plant Physiol. **119,** 1107-1114.

von Wirén, N., Marchner, H., and Romheld, V. (1995) Uptake kinetics of iron-phytosiderophores in two maize genotypes differing in iron efficiency. Physiol. Planta. **93,** 611-616.

von Wirén, N., Mori, S., Marschner, H., and Romheld, V. (1994) Iron inefficiency in maize mutant ys 1 (Zea mays L. cv Yellow-Stripe) is caused by a defect in uptake of iron phytosiderophores. Plant Physiol. **106,** 71-77.

Waters, BM. and Grusak, MA. (2008) Whole-plant mineral partitioning throughout the life cycle in Arabidopsis thaliana ecotypes Columbia, Landsberg erecta, Cape Verde Islands, and the mutant line ysl1ysl3. New Phytol **177**: 389-405

Waters, B., Chu, H., DiDonato, R., Roberts, L., Eisley, R., Lahner, B., Salt, D., and Walker, E. (2006) Mutations in Arabidopsis Yellow Stripe-Like1 and Yellow Stripe-Like3 Reveal Their Roles in Metal Ion Homeostasis and Loading of Metal Ions in Seeds. Plant Physiol. **141**: 1446-1458.

Waters, B.M., Blevins, D.G. and Eide, D.J. (2002) Characterization of FRO1, a pea ferric-chelate reductase involved in root iron acquisition, *Plant Physiol.* **129**, 85–94.

Weigel, D., Ahn, J.H., Blazquez, M.A., Borevitz, J.O., Christensen, S.K., Fankhauser, C., Ferrandiz, C., Kardailsky, I., Malancharuvil, E.J., Neff, M.M., et al. (2000) Activation tagging in *Arabidopsis*. Plant Physiol*.* **122,** 1003–1013.

Welch, R.M., Norvell, W.A., Schaefer, S.C., Shaff, J.E., and Kochian, L.V. (1993). Induction of iron (III) and copper (II) reduction in pea (*Pisum sativum* L.) roots by Fe and Cu status: Does the root-cell plasmalemma Fe(III)-chelate reductase perform a general role in regulating cation uptake? Planta **190,** 555–561.

Wu, H., Lihua, L., Du, J., Yuan, Y., Cheng X., and Ling, H.Q. (2005) Molecular and biochemical characterization of the Fe(III) chelate reductase gene family in *Arabidopsis thaliana*, *Plant Cell Physiol.* 46**,** 1505–1514

World Health Organization (2003) http://www.who.int/nut/ida.htm.

Yi, Y and Guerinot, M.L (1996) Genetic evidence that induction of root Fe(III)

chelate reductase activity is necessary for iron uptake under iron deficiency, *Plant J.* **10,** 835–844.

Yokosho, K., Yamaji, N., Ueno, D., Mitani, N. and Ma J.F. (2009) OsFRDL1 Is a Citrate Transporter Required for Efficient Translocation of Iron in Rice Plant Physiol. 149: 297-305.

Zhao, H., and Edie, D. (1996) The ZRT2 gene encodes the low affinity zinc transporter in Saccharomyces cerevisiae. J Biol. Chem. **271,** 23203-23210.